THE POSTNATAL REFINEMENT OF INTERAREAL CIRCUITS IN FERRET VISUAL CORTEX

By

REEM KHALIL

A dissertation submitted to the Graduate Faculty in Biology in partial fulfillment of the requirements for the degree in Doctor of Philosophy, The City University of New York

2013

This manuscript has been read and accepted by the
Graduate Faculty in Biology in satisfaction of the
Dissertation requirement for the degree of Doctor of Philosophy

_____	_____
Date	**Chair of Examining Committee** Dr. Jonathan B Levitt, The City College of New York
_____	_____
Date	**Executive Officer** Dr. Laurel Eckhardt

Supervisory Committee

Dr. Tadmiri Venkatesh, The City College of New York

Dr. Adrián Rodríguez-Contreras, The City College of New York

Dr. Joshua Brumberg, Queens College

Dr. Michael J Hawken, New York University

Abstract

THE POSTNATAL REFINEMENT OF INTERAREAL CIRCUITS IN FERRET VISUAL CORTEX

by

Reem Khalil

Advisor: Jonathan B. Levitt

Visual cortical areas are presumed to subserve different perceptual functions as a result of their rich network of interareal anatomical circuits. Interareal circuits have been shown to undergo extensive remodeling in the postnatal period. Revealing the timing of when brain circuits mature may help us assign particular neural substrates to particular visual functions. To illuminate perceptual development, we assessed the postnatal anatomical refinement of interareal feedforward and feedback projections in ferret visual cortex. We also described the developmental trajectory of zinc levels in ferret visual cortex, reflecting a subset of glutamatergic interareal feedforward and feedback processes. We find that the period of major reorganization in feedback circuits, feedforward circuits, as well as the dramatic decline in zinc levels in ferret visual cortex occurs in the month following eye opening.

In chapter 1, we demonstrated that zinc histochemistry can be reliably used to distinguish visual cortical areas in juvenile visual cortex and further reveals circuit refinement. We show that the postnatal decline in levels of synaptic zinc follows a broadly similar timecourse in multiple areas of ferret visual cortex. In chapter 2, we assessed the developmental refinement of feedback projections between primary visual cortex and extrastriate areas in the juvenile ferret brain. We reveal substantial refinement in the spatial organization of feedback projections arising from multiple visual

areas to primary visual cortex of the ferret during the period after eye opening. We find that while certain aspects of feedback circuitry refine with a similar timecourse in all areas, other aspects refine asynchronously. In chapter 3, we investigated the postnatal development of feedforward projections from V1 to different target areas. Before eye opening, at 4 weeks postnatal, synaptic bouton density is very high, and interbouton interval along individual axons is quite short. In all areas examined, both bouton density decreased, and interbouton interval increased substantially from 6 weeks to 8 weeks postnatal. Therefore, feedback and feedforward cortical circuits appear to share a broadly similar developmental trajectory. Our findings are consistent with the notion that visual experience is necessary and crucial in the refinement of these cortical circuits. Furthermore, our findings suggest that at least some aspects of cortical maturation occur largely synchronously in multiple visual areas.

ACKOWLEDGEMENTS

I would like to thank my defense committee, Dr. Tadmiri Venkatesh, Dr. Adrián Rodríguez-Contreras, Dr. Joshua Brumberg, and Dr. Michael J Hawken, for their great insight and valued support. I would like to express my sincere gratitude to my advisor Jonathan B. Levitt. I feel truly privileged and fortunate to have worked with such an amazing scientist; the kind of scientist that I aspire to be. Thank you for all that I have learned from you. Thank you for always succeeding in making me laugh. He has provided me with encouragement, great advice, and challenging questions. It was his lecture on visual cortical anatomy in a neuroscience graduate course, which sparked my interest in visual neuroscience. I am also grateful to have worked with talented lab members, Violeta, Cyndi, Lisa, Syeda, Stephanie, and Moody, who have greatly contributed to this work.

I wish to thank my loving and selfless parents, Ebtesam Jniem and Mazhar Khalil. They provided me with the necessary love, support, and motivation throughout my graduate career. Thanks to the sweetest mom who kept me well fed. Thanks to my light hearted dad who always made an effort to understand my research. I wish to thank my four younger brothers, Munir, Wassim, Mohammad, and Ramy for being a smart, talented, and funny bunch. Thanks to my sister Rasha, who is an amazing poet. A special thanks go to my friends, Rema, Donna, Huda, Hana, Liz, Cindy, and Yan, for being sources of laughter, joy, and support. Thank you for keeping me sane!

Finally, I want to especially thank my brilliant husband Ahmad Farhat for everything. I am very grateful and sincerely appreciate all that you have done. Thank you for encouraging me to pursue a Ph.D in neuroscience. Thank you for believing in me and motivating me from start to finish. Thank you for sacrificing to make this possible. Thank you for your infinite help with data analysis, and writing endless MATLAB code. It would not have been possible without you. Your unyielding support and unwavering optimism has allowed me to finish this difficult journey. Finally, I would like to dedicate this work to my one and only Adam, my son, and the joy of my life. I feel blessed and privileged to have completed this important work, and I want to thank God for making it all possible.

TABLE OF CONTENTS

TABLE OF FIGURES

CHAPTER 1
INTRODUCTION

1.1 Anatomical organization of adult visual cortex

1.1.1 Cortical laminae and cell types

The mammalian visual cortex, located in the occipital lobe of the cerebral cortex is comprised of a number of functionally and anatomically distinct areas. Area 17, also known as primary visual cortex, V1, or striate cortex, has been the most extensively studied area and best understood in a number of species. It is referred to as the primary visual cortex mainly because it is the primary recipient of the input from the retina via the lateral geniculate nucleus (LGN) of the thalamus. However, higher visual areas, or extrastriate areas receive visual information mostly from V1, or from other extrastriate areas. In the monkey, the middle temporal area (MT) also receives a direct projection from the LGN of the thalamus. Furthermore, in carnivores such as cats and ferrets, areas 17 and 18 both receive a direct projection from the LGN of the thalamus.

While each visual cortical area is anatomically unique due to the specificity of its connectional pattern, its cytoarchitecture, and the visual response properties of its neurons, there are basic architectural features common to the entire cortex. Cerebral cortex is comprised of six laminae that contain different cell types, run parallel to the pial surface of the brain, and vary in thickness among the different areas. Each cortical layer consists of a unique distribution of neuronal cell types. Layer 1, also called the molecular layer is closest to the cortical surface and composed mostly of dendrites and axons of cells in deeper layers. Directly below Layer 1 is the external granular layer (layer 2), which is composed of small granule cells and lies above the external pyramidal layer (layer 3), which is primarily made up of pyramidal cells. These layers are generally referred to as the supragranular layers. In V1, the internal granular layer

(layer 4) is composed of small stellate cells and pyramidal cells. The internal pyramidal layer (layer 5) contains large pyramidal cells, while the multiform layer (layer 6) borders the white matter, and contains various types of cells (Lund, 1973). Layers 5 and 6 are referred to as the Infragranular layers.

Cells residing in the different layers of the cortex have unique morphologies that dictate the types of synaptic connections in which they participate. There are three basic types of neurons in the primate visual cortex; spiny pyramidal cells (excitatory), spiny stellate cells (excitatory), and smooth or sparsely spinous interneurons (almost all are GABAergic) neurons. Also, in primates, each cortical layer contains distinct types of GABAergic neurons (Lund, 1987; Lund et al., 1988; Lund and Yoshioka, 1991; Lund and Wu, 1997, reviewed in Buzas et al., 2001), all of which contribute to forming either local or long-range intrinsic inhibitory connections. Hendry et al. (1987) report that many areas of monkey cortex contains a homogeneous number and proportion of GABA neurons, and the main difference between areas is the laminar distribution of GABA neurons which may be related to the varied positions of thalamocortical afferent terminations in these areas. Furthermore, Kritzer et al. (1992) show different patterns of inter- and intralaminar GABAergic connections in V1, V2, and V4 of monkey cortex and offer examples of different organizational principles found in these areas.

Layers 2 and 3 contain pyramidal cells, which are large excitatory neurons, characterized by a single apical dendrite, and basal dendrites near the axon. These pyramidal neurons serve as the major source of output to extrastriate areas. Because of their size, they are well suited in forming longer connections from the upper layers to other cortical areas and layer 5, which has some of the largest pyramidal cells.

Furthermore, in both primates and carnivores, layer 4C is the primary recipient of thalamic input from the lateral geniculate nucleus (LGN). It is comprised of small excitatory spiny stellate cells, and inhibitory smooth stellate cells. Also, layer 4 forms vertical connections with the upper layers 2 and 3. The majority of projections from layer 4 to layer 2 and 3 are excitatory and furnished by the spiny stellate cells, with a small fraction of these inputs arising from smooth stellate cells with an inhibitory influence. A distinction between primates and carnivores is that primate layer 4 is subdivided into 4A, 4B, and 4Calpha and 4Cbeta, while carnivore layer 4 seems to have 2 tiers and is subdivided into 4A and 4B (Lund et al., 1979). Pyramidal cell projections arising from layer 5 make connections to layers 2, 3, and 6 (Gilbert and Wiesel, 1983), corticocortical connections, and connections to the superior colliculus, pulvinar and the pons. Neurons in the deepest layer of the visual cortex (layer 6) are known to vary widely in their morphological as well as physiological characteristics. Therefore, layer 6 is unique because of its large diversity of neuronal cell types; each specialized to participate in distinct neural circuits. This layer is comprised of multiple distinct classes of pyramidal neurons, a broad category of oddly shaped excitatory neurons, and a variety of inhibitory neurons (Lund et al., 1979, 1988; Prieto and Winer, 1999; Callaway, 2004; Douglas and Martin, 2004; Andjelic et al., 2009).

1.1.2 Cortical columns

A striking organizational feature of the mammalian cerebral cortex is the cortical column. The column has recently received more attention primarily questioning whether its functional relevance even exists. In 1955, Mountcastle et al. made a seminal

discovery while recording in cat somatosensory cortex. The term 'column' was initially coined to describe a discrete structure spanning the layers of the somatosensory cortex, comprised of cells responsive to a common sensory modality, such as skin or joint receptor. Over the years the meaning of the term column may have transformed and investigators may have used it to refer to various anatomical entities, a column now refers to cells in any vertical cluster that share the same tuning property for a given receptive field attribute (Horton and Adams, 2005).

Subsequent to Mountcastle's discovery, examples of columns have been revealed in multiple cortical areas. It is now accepted that each cortical column lies perpendicular to the cortical surface and traverses all six layers. The best characterized and most extensively studied, first described in cat primary visual cortex by Hubel and Wiesel (1962, 1968), is the orientation preference column. They observed that by advancing an electrode along a penetration perpendicular to the cortical surface, successively recorded cells shared an identical orientation of their receptive field axis. This is in marked contrast to tangential penetrations that yield systematic changes in the receptive field properties of neurons. In macaque striate cortex, Hubel and Wiesel also found that optimal orientation tuning changes systematically through 180° with an electrode advance of between 0.5 and 1.0 mm. They coined the term 'hypercolumn' to refer to a complete rotation of columns (e.g. 0, 10, 20…180°; Hubel and Wiesel, 1974b). The term hypercolumn now refers to a unit containing a full set of values for any given receptive field parameter. It has subsequently been used to reveal maps for direction preference, spatial frequency (Weliky et al., 1996; Hübener et al., 1997; Everson et al., 1998; Issa et al., 2000) and perhaps color (Ts'o et al., 2001b; Landisman and Ts'o,

2002; Xiao et al., 2003). The hypercolumn appears to be comparable in size for each of these systems.

Another system of columns that has been shown to exist in a number of species is the ocular dominance columns. Axon terminals from LGN cells serving either the right eye or the left eye terminate in a system of alternating stripes called ocular dominance columns (Hubel and Wiesel, 1969). Segregating ocular inputs, these columns represent input from right and left eye at common points in the visual field map. In normal animals, they can be detected using multiple techniques such as single cell recording, silver stains, anterograde transneuronal tracers and optical imaging (LeVay et al., 1975, 1985; Hubel and Wiesel, 1977; Blasdel and Salama, 1986; Blasdel, 1992a). Staining for Cytochrome oxidase (CO), a mitochondrial enzyme, is one of the easiest techniques to apply (Wong-Riley, 1989). Ocular dominance columns can be well labeled by staining striate cortex for cytochrome oxidase (CO) after removal of one eye. As a result, a pattern of dark and light CO stripes emerges in layer 4C. The CO level diminishes in columns formerly served by the affected eye. In normal adult animals, CO activity in layer 4C is homogenous. These stripes are identical to those labeled anatomically by injection into one eye of a transneuronal tracer, such as [3H]proline, proving that they represent ocular dominance columns (Sincich and Horton, 2003a). A popular and effective way to visualize their complete pattern is to unfold the occipital lobe and to flat-mount the cortex prior to sectioning.

Other examples of cortical ‘columns’ have been found in visual, auditory, as well as motor areas. The definition of a cortical column now broadly means either a cluster of cells sharing a common receptive field property, or periodic projection fields arising

from intra or inter cortical axonal connections (Horton and Adams, 2005). In area V3, cells with similar disparity tuning are grouped together (Adams and Zeki 2001). Cells in V3 also make columnar projections to other visual areas (Felleman et al., 1997; Angelucci et al., 2002). Cells in area MT that have the same direction preference are clustered (Albright et al., 1984). Furthermore, tracer injections in MT reveal patch-like clusters of intrinsic projections (Malach et al., 1997). In the inferotemporal cortex, single cell recordings and optical imaging have shown that columns of cells are about 400 μm wide, responsive to similar features of objects (Fujita et al., 1992; Wang et al., 1998). In the auditory cortex, tracer injections in the upper layers yield patches of label from intrinsic horizontal projections, similar to those seen in V1 and MT. These horizontal projections preferentially link regions with similar bandwidth along isofrequency domains (Read et al., 2001). Language cortex in humans contains columnar, horizontal, long-range connections that are spaced 20% more widely in the left hemisphere (Galuske et al., 2000). Although columns have been found most frequently in sensory regions of the cortex, they also occur in motor areas. For example, cells in macaque primary motor cortex with the same preferred direction vector are organized into clusters 200 μm apart, interleaved with clusters of cells preferring the orthogonal direction vector (Amirikian and Georgopoulos, 2003).

Despite the numerous studies dedicated to unraveling the function of the cortical column, Horton and Adams (2005) believe their function remains elusive and much effort is needed to disentangle their true function, if any exist. Although the cortical 'column' has been shown to exist in many regions of the mammalian cortex and in many species, there are caveats that are difficult to reconcile with assumptions about the

functional importance of columns. For instance, some species lack obvious ocular dominance columns (Tigges et al., 1977; Hendrickson et al., 1978). More surprising is the variability found between individuals within the same species. Adams and Horton (2003a) have shown that ocular dominance columns in squirrel monkeys can range from very well defined in some individuals to nearly absent in other individuals. Furthermore, while the existence of orientation columns has been proved in monkeys, cats, ferrets, and other species (LeVay and Nelson, 1991), there is little evidence for orientation columns in mice, rats, and hamsters (Drager, 1975; Shaw et al., 1975; Tiao and Blakemore, 1976). Despite the cortical column's ubiquitous nature in the cerebral cortex, much effort is required to truly understand if this structure indeed underlies an important function.

1.1.3 Organization of intrinsic connections

Corticocortical projections in the mammalian visual cortex can be classified as intrinsic that link cells within an area, or extrinsic, linking cells between two areas. Intrinsic connections, which are often termed, horizontal, tangential, or intraareal connections, have axons that do not travel in the white matter. Long-range horizontal connections formed by excitatory pyramidal cells, link clusters of cells across long distances in cortex. A distinguishing feature of the mammalian cerebral cortex, they form an extensive network of axons running parallel to the cortical surface. The observed laminar pattern of horizontal connections indicates that these projections are prominent in the supragranular layers (1-3), rare in layer 4, but may also be found in layer 5. (Lund, 1973; Gilbert and Wiesel, 1979; Rockland et al., 1982; Rockland and

Lund, 1982; Rockland, 1985). Anatomical tracer studies have shown that intrinsic connections to a single V1 locus form a patchy pattern where the number of monosynaptic connections declines with distance from that locus. Furthermore, a restricted locus in visual cortex was shown to furnish projections spanning several millimeters across the cortical surface and have axons that ramify into terminal clusters at discrete locations across the cortex (Rockland and Lund, 1982, 1983; Gilbert and Wiesel, 1979, 1983). A conspicuous feature common to all intrinsic connections is their anisotropy. These projections usually spread out from the injection site along one axis. Another prominent feature typical of intrinsic connections is their reciprocity. Terminal clusters are usually found to coincide with retrogradely labeled cells indicating that pyramidal cells generally receive inputs to cortical columns to which they project.

It is well known that in primates and carnivores, anatomical circuits serve to connect cells with similar functional properties. For instance horizontal connections interconnect neurons in similar orientation columns within macaque V1 (Gilbert and Wiesel, 1989). Malach et al. (1993) examined the specificity of horizontal projections in layer 2/3 of macaque V1 related to ocular dominance columns. They showed that injections in monocular regions resulted in preferential labeling in other monocular regions corresponding to the same eye. Injections in binocular regions preferentially labeled other binocular regions. Since CO blobs tend to be monocular and interblobs binocular, these observations are in agreement with the earlier observation that blobs are preferentially linked to blobs and interblobs to interblobs (Livingstone and Hubel, 1984b). They further suggest that blobs are connected selectively to other blobs having the same ocular dominance. However, recent findings by Yoshioka et al. (1996) are

somewhat contradictory. By analyzing a large sample of biocytin injections in layer 2/3 of V1 using similar methods, these investigators showed that in some cases biocytin labeling was more prominent in ocular dominance columns corresponding to the opposite eye, and in other cases labeling was not blob specific. Therefore, not all the connections were blob-specific and ocular dominance specific. Although less common, interconnections between neurons with different properties also exist. Some of the apparent lack of ocular dominance specificity can be attributed to differences between the analyses of Yoshioka et al. (1996) and Malach et al. (1993). Lastly, cross correlation studies provide further evidence that intrinsic patchy connections link cells with similar functional properties. Ts'o et al. (1986) used the cross correlation method to demonstrate that cells separated by several millimeters with the same orientation, direction, and eye preference showed correlated firing.

1.1.4 Organization of extrinsic connections

Extrinsic corticocortical connections link neurons located in different cortical areas. When extrinsic connections interconnect neurons located in the same hemisphere, they are termed intrahemispheric connections. When extrinsic connections link neurons in opposite hemispheres, they are classified as interhemispheric connections (Salin and Bullier, 1995). A further classification of extrinsic corticocortical connections as feedforward or feedback has been proposed by (Rockland and Pandya, 1979) to arrange visual cortical areas in a hierarchical fashion, with Area 17 at the lowest level and extrastriate cortical areas located at successively higher levels. This is so because primary visual cortex receives the majority of visual information via the

LGN, and almost all extrastriate areas depend on V1 for their activation (Salin and Bullier, 1995). The hierarchical analysis of visual cortical areas (Rockland and Pandya, 1979; Maunsell and Van Essen, 1983; Felleman and Van Essen, 1991) represents a widely used approach to finding common organizational features in connectional data. This approach examines the patterns of laminar origins and terminations of projections between cortical areas. Figure 1.1 shows a schematic of the organization of the visual cortex in the monkey (Felleman and Van Essen, 1991). This illustration reveals the complexity of the organization of different visual cortical areas (boxes) and the flow of information through feedforward and feedback connections between them (lines).

Visual information is conveyed out of V1 to higher processing levels via feedforward corticocortical connections. Feedforward connections originate mainly from the supragranular layers and terminate most densely in layer 4, and more sparsely in the supragranular and infragranular layers. Therefore, termination of connections in layer 4 is a hallmark of feedforward corticocortical connections. Visual information processed in higher order cortical areas is relayed back to V1 via corticocortical feedback connections. Feedback connections originate mostly from the infragranular layers and terminate outside of layer 4 (Lund et al., 1975; Rockland and Pandya, 1979; Maunsell and Van Essen, 1983; Kennedy and Bullier, 1985). Therefore, one distinguishing feature of feedforward and feedback connections is their axon terminals; the former ramify across all layers, while the latter tend to avoid layer 4.

Figure 1.1. Schematic of visual cortical areas in the macaque monkey

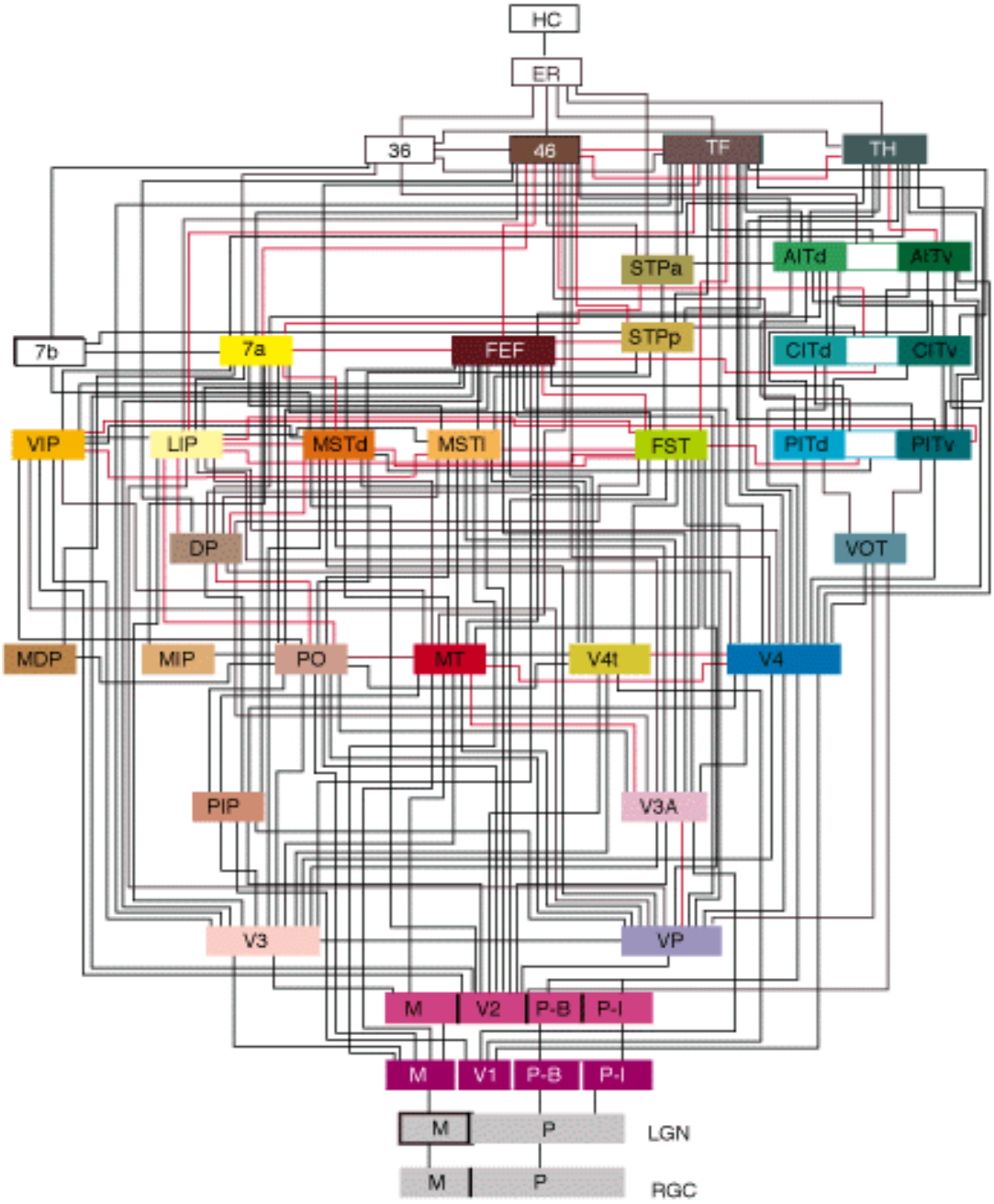

From Felleman and Van Essen (1991)

Hierarchy of visual cortical areas in the macaque brain. Boxes represent visual areas and the lines connecting them represent the neural connections between them.

Individual corticocortical pathways exhibit a precise laminar distribution of the parent neurons characterized by the percentage of labeled supragranular layer neurons-SLN% (Barone et al., 2000). Following injections of tracers in area V4, these authors show that SLN% increases at successive lower hierarchical levels, so the SLN% is 63% in area V3, 93% in V2, and 100% in V1. Conversely, there is a progressive decrease in SLN% at successive higher levels. Consequently, the value of SLN% relates to the number of hierarchical levels separating two cortical areas, which they refer to as hierarchical distance. This makes SLN% values extremely powerful in generating hierarchical models of the visual cortex (Barone et al., 2000).

In comparing corticocortical feedforward and feedback connections, it has been shown that feedforward connections provide converging inputs (convergence) to their target areas while feedback connections provide diverging inputs (divergence) to their target areas. More specifically, convergence refers to the number of neurons sending converging inputs to a given neuron and divergence refers to the number of neurons contacted by a given cortical cell. To understand the functional significance of the convergence and divergence of corticocortical connections in the processing of visual information, it is important to know the extent of visual field represented by neurons converging on a given cortical cell. Because of the visuotopic organization of cortical areas, this is usually possible by measuring the extent of cortex containing the converging neurons (Salin and Bullier, 1995). The convergence region can be defined as the cortical region containing neurons converging on a small column of cells oriented perpendicular to the surface. Likewise, it is possible to define the divergence region as the extent of cortex containing the target neurons of a column of cells. The spatial

extents of the convergence and divergence regions have been measured for extrinsic connections. Using paired injections of retrograde tracers, Salin and colleagues (Salin et al., 1989: Salin et al., 1993) found values of 5-18 mm for the rostrocaudal extents of convergence and divergence values in the cat corticocortical connections of the visual system. Furthermore, data from paired injections in area V1 of macaque monkeys suggest that the divergences of feedback connections to this area from various extrastriate cortical areas also cover 5-7 mm (Perkel et al., 1986).

1.2 Functional aspects of adult visual cortex

1.1.1 Receptive fields

Neurons in the visual system like other sensory neurons are selective filters, allowing only relevant information to be transmitted through the visual pathways and discarding the rest. Neurons in the retina and higher stages of the visual pathways have unique characteristic properties that determine the spatial and temporal attributes of the signals they transmit (Lennie, 2003). The neuron's receptive field (RF) can be thought of as a neuronal filter, the spatial structure and temporal profile of which is largely determined by its functional role and hierarchical level in the visual processing pathways. In visual cortex, receptive fields become increasingly larger and more selective for specific stimulus features as one ascends the visual processing hierarchy. The receptive field of a neuron in the visual system is defined by its synaptic inputs. Each cell's receptive field results from the combination of receptive fields of all of the neurons providing input to it (Levitt, 2009). The receptive field properties of primary

visual cortical (V1) neurons have been extensively studied and are well characterized in a number of species.

The receptive field was originally described in the retina as the region of the visual field from which a stimulus can elicit a response from a neuron (Hartline, 1938; Kuffler, 1953). While the concept of a receptive field may seem straightforward, defining the borders of the receptive field of a neuron in visual cortex has never been a simple issue. This is because the characteristics of a cell's receptive field crucially depend on how one fundamentally measures it. The classical method to determine the location and extent of the receptive field is to present discrete stimuli at different locations in the sensory periphery (i.e. on the retina). The region that causes a change in the spike discharge rate has been variously referred to as the receptive field, the classical receptive field, the receptive field center, the discharge field or discharge center, the minimum discharge field, or the minimum response field (Hubel and Wiesel, 1962; Barlow et al., 1967). A more recent approach is to define the receptive field center as the area of visual space over which increasing the stimulus size elicits a larger response until the response ceases to increase (DeAngelis et al., 1992, 1994: Levitt and Lund, 1997: Sceniak et al., 1999). This is typically assessed using a high contrast sine-wave grating of optimal orientation, spatial and temporal frequencies for the cell. The spatial extent of the receptive field is therefore defined as the smallest stimulus dimensions that produce the maximum discharge rate. This has been defined as the high contrast summation field (hsRF) and corresponds to the region of visual field over which the cell summates stimuli (Angelucci and Bullier, 2003). This method typically provides estimates that are larger than the minimum response field (mRF). Since receptive fields

of cortical neurons have proved to be more complex than their simple definition, the modern definition of the receptive field can now be thought of as the region over which one could influence the firing of a cell, not simply drive it.

It is generally agreed upon that the selectivity of a cortical neuron's receptive field to a particular parameter is a result of the ordered convergence of afferents from lower stages. Moreover, visual cortical neurons sum the input they receive from subcortical structures (i.e LGN) and other cortical neurons in order to shape their receptive fields. Hubel and Wiesel (1962) first proposed that V1 receptive fields of simple cells have distinct and elongated, excitatory (on) and inhibitory (off) subregions that are constructed from the precise alignment of concentric RFs of LGN afferents, which in turn supply excitatory and inhibitory input to be integrated by cortical RFs. In turn, the integration of excitatory and inhibitory input from several simple receptive fields then construct receptive fields of complex cells, which do not themselves have discrete 'on' and 'off' regions. The elongated receptive fields of cortical neurons underlie the orientation selectivity presumed to emerge at the thalamocortical synapse.

V1 is unique in that it is the first place in the mammalian visual pathways where distinctive receptive field properties such as orientation selectivity emerge (Hubel, 1982: Hubel and Wiesel, 1962, 1968, 1977). Simple and complex cells in V1 both respond preferentially to a particular orientation, but simple cells prefer a particular spatial arrangement of oriented light and dark regions, whereas complex cells respond to appropriately oriented patterns at all spatial positions within the RF (Wyeth, 2005). The F1/F0 measure is typically used to classify cells into "simple" or "complex". This measure expresses the amount of temporal modulation at the fundamental frequency

(F1) of a drifting grating relative to the mean evoked response (F0) (Skottun et al., 1991). Simple cells have large F1 values, whereas complex cells, being phase-insensitive, have low F1 values. A distinctive quality of simple cells is their non-overlapping ON and OFF spatial RF subregions (Mata and Ringach, 2005). Overall, simple cells tend to sum linearly the light intensities falling on their receptive fields (Hubel and Wiesel, 1962: Movshon et al., 1978a: Tolhurst and Dean, 1987: Carandini et al,. 1997). By contrast, complex cells exhibit significant non-linearities of spatial summation (Hubel and Wiesel, 1962: Movshon et al., 1978b: Palmer and Davis, 1981: Dean and Tolhurst, 1983). Hubel and Wiesel (1962) proposed that the functional relationship between simple and complex cells is a hierarchical one in which the structure of simple cell CRFs is determined by the excitatory convergence of a number of LGNd neurons and the structure of complex cell CRFs is derived from the excitatory convergence of a number of simple cells (for reviews, Ringach, 2004: Martinez et al., 2005).

1.2.2 Modulatory surround effects

It is widely held that although stimuli presented outside of the cell's receptive field do not by themselves change a neuron's spiking activity, they can however exert robust suppressive or facilitative effects when presented simultaneously with a stimulus in the classical receptive field. Hubel and Wiesel (1965) demonstrated that increasing the stimulus beyond the spike discharge region of the receptive field often caused a decrease in response. Furthermore, there were unresponsive regions that when stimulated alone did not elicit a response from a cell. However, it became apparent that

if a stimulus was presented within these regions simultaneously with a stimulus in the classical receptive field, that often impacted the vigor of the neuron's response (Maffei and Fiorentini, 1976).

It is now appreciated that the response of cells in V1 and extrastriate cortex can be modulated by contextual stimuli lying far outside the neuron's receptive field. Modulatory surround effects change the specificity of responses to stimuli within the classical receptive field and are dependent on the specific sum of input a particular cortical neuron receives (Blakemore and Tobin, 1972; Nelson and Frost, 1978; Gilbert and Wiesel, 1990). For instance, parafoveal receptive fields in macaque V1 only span a degree or less, but the surround modulatory effects or contextual effects were found to span distances up to 10 degrees of visual space (Zipser et al., 1996; Sceniak et al., 2001; Levitt and Lund, 2002). These findings suggest that V1 cells are receiving input from cells that provide information about the visual field at least 10 degrees outside the classical receptive field of these neurons.

These modulatory surround effects can vary substantially and either inhibit or facilitate the cell's response depending on the parameters of the surround relative to those in the receptive field. Mainly, these effects can change the magnitude of the cell's response depending on the spatial relationship and contrast of surround stimuli (Levitt and Lund, 1997; Henry et al., 2013; Sceniak et al., 1999). It is now appreciated that center-surround interactions have a dynamic relationship and are complex in nature. One factor that directly influences the size of the RF center is stimulus contrast (Angelucci and Bullier, 2003). At low contrast, the summation RF is on average twice as large as when it is measured at high contrast (Sceniak et al., 1999). As a result, regions

flanking the mRF along the line of optimal orientation (collinear stimuli) can facilitate the center (mRF) response at low contrast, but suppress it at high contrast (Kapadia et al., 1999: Polat et al., 1998). Thus, it has been possible to identify three overlapping regions in the RF center of a cortical neuron: the mRF, the hsRF and the summation RF at low contrast (lsRF) (Angelucci and Bullier, 2003). Modeling studies have shown that center–surround interactions in macaque V1 neurons can be represented as a center excitatory gaussian overlapping a surround inhibitory gaussian, with the center gaussian corresponding to the lsRF (Sceniak et al., 1999). On the other hand, regions beyond the RF center (mRF or hsRF) that suppress the response of the center to high contrast stimuli have been included in the surround. As a consequence, the regions between the hsRF and the lsRF, that can be suppressive at high contrast, would belong to the surround. Beyond the lsRF lies the remaining portion of the surround. High contrast optimal grating stimuli expanding over the neuron's RF center have been used to determine the surround size and is typically defined as the stimulus diameter at which the cell's response asymptotes (i.e. ceases to decrease). Surround sizes in macaque V1 have been found to be on average about five times larger than V1 cells' hsRF (Angelucci et al., 2002; Levitt and Lund, 2002).

Moreover, stimuli presented in the surround can change the orientation tuning depending on the axis of the surround orientation relative to the neuron's preferred orientation (Gilbert and Wiesel, 1990; Lund et al., 1995; Sengpiel et al., 1997). The strongest suppressive modulatory effects occur when the orientation of the surround stimulus matches the orientation of the center stimulus (Gilbert and Wiesel, 1990). However, when the orientation of the surround stimuli is significantly different or

orthogonal to the center orientation, it facilitates the neuron's responses to stimuli within the receptive field. Evidence for contrast-dependent collinear facilitation comes from a study conducted by Mizobe et al. (2001). They showed that facilitation with collinear flankers occurred most frequently at target contrasts just above the cell's firing threshold and suppression prevailed at high contrasts. Furthermore, both facilitation and suppression occurred often in the same cells, when orientations of the target and flankers matched the receptive-field's optimal orientation. Lastly, in addition to stimulus orientation and contrast, Li and Li (1993) showed in cat that the inhibitory or facilitory effects of surround depend on the spatial frequency and speed of the surround stimulus. More recently, Shushruth et al. (2013) demonstrated that surround suppression in the near surround (subserved by horizontal connections) is more sharply orientation tuned than far surround suppression (subserved by feedback connections) in macaque V1 and human perception.

Taken together, these findings suggest that, like the receptive fields, the surrounds are also tuned for specific stimuli. In addition, these studies emphasize the dynamic nature of the relationship between V1 neurons' RF and the surrounding region of visual space, and further show that V1 RFs have dynamic spatial properties, changing in size depending on stimulus contrast.

1.2.3 Retinotopic maps

The mammalian cerebral cortex can be divided into multiple functionally and anatomically unique regions, for example, motor cortex, auditory cortex, somatosensory cortex, and visual cortex. All cortical sensory areas contain a topographically ordered

map based on the spatial order of the sensory receptors and the environment to which they respond (Mountcastle, 1957). It is generally accepted that visual cortex in carnivores and primates contains a map of visual space unique to each area. This retinotopic (visuotopic) map is a map of visual space and based directly on its projections from the retina (Daniel and Whitteridge, 1961; Allman and Kaas, 1971, 1971a,b, 1975, 1976; Palmer et al., 1978; Tusa et al., 1978, 1979; Van Essen and Zeki 1978; Tusa and Palmer, 1980; Gattass et al., 1981, 1988; Manger et al., 2002). The retinotopic maps found in visual cortex are typically described as degrees of elevation (i.e lines of constant elevation span horizontally across the visual field), and degrees of azimuth (i.e lines of constant azimuth scan vertically across the visual field). Furthermore, these maps are produced by adjacent neurons having adjacent or overlapping receptive fields. The topographically organized representation of the visual field is faithfully relayed through multiple stages of processing in the mammalian visual pathways.

While each cortical area contains a map of visual space, the representation of visual space can vary in spatial extent and selective emphasis on certain parts of the visual field. The extent to which the central or peripheral portions of the visual field are emphasized in each area can vary greatly. However, in general, there seems to be an overemphasis on the central visual field. Additionally, primary visual cortex (Area 17) has the most complete representation of the visual field. Allman and Kaas (1974) have classified the transformation of the visual field onto cortex into first order and second order transformations, both of which represent the contralateral half of the visual field. A first order transformation is when adjacent points in the cortex respond to adjacent

points in the contralateral half of the visual field. A second order transformation is when the representation of the contralateral half of the visual field is more complex. Primary visual cortex contains a first order transformation of the visual field, and has a point-to-point representation on visual cortex. Second order transformations are found in extrastriate areas, where there is often more than one representation of the visual field within an area, and the representation of the horizontal meridian is usually split (Palmer et al., 1978). There can be a point-to-point representation, or a point-to-line representation. In the latter case a single point in visual space, such as the center of the visual field, is represented as a line on visual cortex (Palmer et al., 1978). Both representations of the visual field are advantageous in visual perception. The point-to-point representation preserves the order of visual space in the cortex. However, the point-to-line transformation of, say, the horizontal meridian is useful for functions that require extensive cellular interactions within central locations in the visual field such as stereopsis and control of vergent eye movements (Tusa et al., 1981).

It is now widely recognized that there is an increased number of cellular interactions within the center of the visual field, which is projected on the fovea in primates and area centralis in carnivores. This in turn has lead to a marked increase in the amount of cortex dedicated to the central portion of the visual field relative to the periphery. Numerous studies across a number of species have shown that the cortical magnification factor, defined as millimeters of cortex corresponding to 1° of visual field (Talbot and Marshall, 1941; Daniel and Whitteridge, 1961), in V1 and extrastriate areas decreases with eccentricity, which is the distance from the fovea or area centralis in degrees (Hubel and Wiesel, 1974b; Gattass et al., 1981; Van Essen et al., 1984; Law et

al., 1988; Pinon et al., 1998). In addition, the central visual field, horizontal, and vertical meridians have multiple representations across cortex because they are represented in each cortical area, and often have multiple representations within a given area. They also form the borders between some visual areas (Allman and Kaas, 1971a, 1971b; Van Essen and Zeki, 1978; Tusa et al., 1978; Gattas et al., 1981, 1988; Manger et al., 2002). While the unequal allocation of cortex results in distortions in the maps of visual space, even in point-to-point and first order transformations, it does emphasize the sensory information coming from the center of the visual field. Furthermore, receptive fields located in the foveal region or area centralis tend to be smaller than receptive fields located in the periphery (Daniel and Whitteridge, 1961). This in turn provides better spatial resolution in the center of the visual field.

Visual cortical areas each have a distinct representation of the visual field that's largely dictated by the physiological role of each area. For example, by comparison with V1, the map in monkey MT overemphasizes the peripheral visual field (Albright and Desimone, 1987) and hugely overemphasizes its lower temporal quadrant (Maunsell and Van Essen, 1983). In contrast, in areas V3 and V4, the representation of the central visual field is magnified relative to that of the periphery. Furthermore, in cat visual cortex, the four caudal areas within the suprasylvian sulcus (PMLS, PLLS, VLS, and DLS) have a limited representation of the vertical meridian and an extentive representation of the horizontal meridian (Tusa et al., 1981). Presumably, each cortical area has adequate visual field representation for the particular functions it performs.

1.2.4 Functional maps

Visual cortical neurons are differentially tuned to specific stimulus features, such as their position in visual space, orientation, direction of motion, spatial frequency, color, and temporal frequency (Hubel and Wiesel, 1962, 1968; Maffei and Fiorentini, 1973; Movshon, 1974). In carnivores and primates, neurons with similar stimulus preferences are clustered into radial columns, which are arranged in a systematic fashion across the cortical surface. This unique arrangement of response preference in primary visual cortex forming functional maps was first recognized by Hubel and Wiesel nearly fifty years ago.

One of the most striking functional properties of neurons in the adult primary visual cortex is their orientation selectivity. The majority of neurons in primary visual cortex of primates and carnivores are exceptionally sensitive to the orientation of a stimulus. Furthermore, neurons with similar preferred orientations are clustered together into radial columns running perpendicular to the cortical surface, as was first shown by Hubel and Wiesel (1962) in cat visual cortex. In contrast, parallel to the cortex, the preferred orientation changes continuously in most locations, forming orientation preference maps (Hubel and Wiesel, 1962, 1963, 1965). Orientation preference maps in V1 of carnivores and primates are characterized by numerous iterations of pinwheel motifs and linear zones that represent orientation preference in a smooth and continuous fashion across the surface of V1 (Bonhoeffer and Grinvald, 1991; Bosking et al., 1997; Blasdel, 1992). Moreover, orientation columns span 180 degrees, and as one moves tangentially across cortex they are mainly ordered sequentially but sometimes form a nonsequential pinwheel pattern (Hubel and Wiesel, 1963; Blasdel, 1992).

Interestingly, Coppola et al. (1998) have demonstrated that more circuitry in the ferret visual cortex is devoted to processing contours oriented in the cardinal axes than to oblique contours. There is also evidence that in several other species there are fewer neurons tuned to oblique orientations than horizontal or vertical orientations (De Valois et al., 1982; Maffei and Campbell, 1970; Mansfield, 1974; Zemon et al., 1983). This anisotropy in the visual system favoring the representation of cardinal orientation may reflect the real world prevalence of contours in the cardinal axes and possibly explain the greater sensitivity of many animals to vertical and horizontal stimuli.

The ocular dominance map, established in layer 4 of primary visual cortex is organized to accommodate the two sets of monocular inputs that arise from the principal layers of the LGN. Cells within an ocular dominance column receive their major input from the same eye and therefore respond preferentially to one eye or the other (Hubel and Wiesel, 1962). Although all these columns are independent of each other (Hubel and Wiesel, 1968), they are formed by the same principle; functionally related cells are associated with each other, and create a functionally based architecture in cortex (reviewed in Gilbert, 1992; White et al., 2001). Unlike the ocular dominance maps in primates and cat, ferrets have a fairly complex ocular dominance map (White et al., 1999). Ocular dominance domains in the more peripheral parts of the binocular region are of the familiar stripe or patch type. However, the central region of area 17 often consists of a single elongated region of contralateral eye dominance and the entire representation in area 18 is exclusively monocular. The authors further reveal significant discontinuities in the mapping of visual space along the V1–V2 border, which correspond to the boundary between these monocular representations.

Neurons in visual cortex are also tuned to a preferred spatial frequency. The organization of spatial frequency preference in cats was shown to be laminar in origin by Maffei and Fiorentini (1977). The authors demonstrated that cells in a column running perpendicular to the cortex have different preferred spatial frequencies while cells of the same layer maintain the same preferred spatial frequency and visual acuity. Tootell et al. (1981) on the other hand demonstrated in cat that the spatial frequency map was columnar in nature. Their results indicate that striate neurons tuned to particular spatial frequencies are anatomically arranged in columns, perpendicular to the cortical surface. It seems that high spatial frequency columns are confined to the foveal region of striate cortex while low spatial frequency columns extend more peripherally. Furthermore, using optical imaging of intrinsic signals, Issa et al. (2000) showed that grating stimuli of different spatial frequencies drifting at various speeds produce distinct activity patterns. Rather than observing a map of continuously changing spatial frequency preference across the cortical surface, they found only two distinct sets of domains, one preferring low spatial frequency and high speed, and the other high spatial frequency and low speed. Collectively, these studies suggest that, like ocular dominance, the spatial frequency preference of cortical cells in cats and monkeys varies both tangentially across the cortical surface and radially throughout cortical laminae.

Neurons in primary visual cortex of monkeys and cats also form direction preference maps. Payne et al. (1981) and Tolhurst et al. (1981) have provided evidence for direction preference maps in area 17 of cats. They also showed that there were frequent 180” reversals in direction preference, as well as of a local clustering extending

over lateral distances of up to about 300 μm. Tolhurst et al. (1981) also present evidence that direction preference, like orientation preference remains constant with depth in the cortex, i.e., has a columnar organization. Weliky et al. (1996) reveal that the map of direction preference in ferret primary visual cortex consists of many regions within which direction preference changes in a slow and continuous fashion. These regions are separated by discontinuities (fractures) across which direction preference shifts abruptly.

1.2.5 Functional relationship to the underling connectivity

1.2.5.1 Contribution of feedforward input to the classical receptive field

The functional distinction between the receptive field center that produces spike discharge and a surrounding region that modulates the response to stimuli in the center naturally led to the question of the underlying cortical circuitry that mediate these effects. It is now appreciated that the receptive field center and surround of a V1 neuron are mediated by fundamentally different cortical circuits. Feedforward connections provide much of the excitatory drive that shapes the classical receptive field center (Schiller and Malpeli, 1977). In addition, feedforward connections relay a message by defining the patterns of activity at each stage in the visual processing hierarchy. The selectivity of a neuron in a higher order area is presumably constructed by the ordered arrangement of feedforward inputs from lower order areas. It is thought that these inputs contribute to the construction of progressively larger and more complex receptive fields at successive levels of the hierarchy (Felleman and Van Essen, 1991). Sherman and Guillery (1998) have made the distinction between ‘drivers’ and ‘modulators’ in the

retinogeniculate and geniculocortical pathway based on a set of criteria. They define a driver as the transmitter of receptive field properties and the modulator as altering the probability of certain aspects of that transmission. Driver inputs presumably have large, powerful synapses, while modulator inputs are small and weak. In addition, driver synapses activate only ionotropic receptors, while modulator synapses activate metabotropic receptors as well. Based on these descriptions by Sherman and Guillery (1998), feedforward connections in the visual cortex can be thought of as drivers, while feedback connections can be thought of as modulators.

Results from inactivation experiments of feedforward connections also confirm that the ordered arrangement of feedforward connections is important in establishing the receptive field selectivities in higher order areas (Bullier et al., 1994; Bullier, 2001). In addition to these functions, feedforward inputs channel inputs into the ventral and dorsal processing streams that are specialized for the representation of visual objects and spatial relationships (Maunsell and Newsome, 1987).

1.2.5.2 Contribution of feedback and horizontal connections to the non-classical receptive field

Candidate circuits mediating the surround effects in V1 are presumed to be feedback connections from extrastriate cortex, intrinsic connections within V1, and feedforward input from LGN. At present, the issue of the relative contribution of each circuit or whether intrinsic connections in V1 or feedback connections from extrastriate cortex are more important in the modulation of the RF center by the surround remains unresolved. Elucidating the neural circuits that mediate these contrast and orientation dependent center-surround interactions has been the subject of intense focus for over

two decades. The notion that long range intrinsic connections play a role in establishing receptive field surround effects rests heavily on their extent. Since, horizontal connections extend for distances across the cortical surface that allows them to link neurons with non-overlapping receptive fields.

Axons of intrinsic neurons within V1 appear not to drive their target neurons, but only elicit subthreshold responses (Hirsh et al., 1991: Yoshimura et al., 2000), thus exerting a modulatory influence on their target neurons. Accordingly, horizontal connections are thought to be the underlying anatomical substrate accountable for some of the modulatory effects exerted on the responses of V1 neurons. Neurons linked by horizontal connections in V1 can respond only to a limited spatial extent in visual space, and can therefore only summate information from a restricted area. Horizontal connections arising from pyramidal cells are recruited in the facilitatory surround effects since they link cells along a collinear axis in the map of visual space and link neurons with similar orientation preferences (Gilbert and Wiesel, 1989; Malach et al., 1993; Fitzpatrick, 1996). Facilitation is frequently seen when the surround stimulus is presented along the collinear axis in space in a similar orientation to the cell's preferred orientation (Maffei and Fiorentini, 1976; Nelson and Frost, 1985; reviewed in Fitzpatrick, 2000). However, recruiting appropriate groups of horizontal fibers can also have a suppressive effect (Hirsh et al., 1991).

Similar to horizontal connections, feedback connections are presumed to have a modulatory influence on the responses of lower order neurons, i.e. information already processed (Zeki and Shipp, 1988). Therefore, these connections may produce modulatory effects that enable objects to be perceived in context (Lamme et al., 1988).

Input from feedback connections can supposedly elicit changes in the response to stimuli within the receptive field. In primates, Angelucci et al. (2002) found that feedback connections link cells that respond to non-overlapping areas of visual space that are still centered on the same retinotopic location. Therefore, they provide for the convergence of larger visuotopic areas onto smaller visuotopic areas in V1, and integrate information across large distances in the visual field (Bullier et al., 1998; Salin et al., 1992). The physiological role of feedback connections has been most effectively studied by reversible cooling of higher cortical areas and recording of the effects of neuronal responses in lower cortical areas. Experiments in monkeys have shown that feedback inputs from both V3 and V2 to V1 facilitate responses to stimuli moving within the classical receptive field (Sandell and Schiller, 1982) and enhance suppression from outside the receptive field (Sherk, 1978; Girard et al., 1991; Hupe at al., 1998; Huang et al., 2007). These effects suggest that feedback connections are involved in the discrimination of objects relative to the background.

Studies have shown that there is an early suppressive modulatory component (Alitto and Usrey 2008; Xing et al., 2005) that likely arises through fast feedforward lateral geniculate nucleus (LGN) afferents. It seems that LGN neurons already exhibit extraclassical surround suppression (Alitto and Usrey 2008; Ozeki et al. 2004; Sceniak et al. 2006; Solomon et al. 2002; Webb et al. 2005a) and therefore make a substantial contribution to contrast dependent spatial summation in V1.

1.3 The postnatal development of visual circuits

1.3.1 Developmental sequence of visual cortical areas

It is widely held that the differentiation and specification of neocortical areas is controlled by an interplay between intrinsic mechanisms, i.e. genetic mechanisms that operate within the cortex, and extrinsic mechanisms such as the sensory periphery and thalamic input. However, there is less agreement about the order in which cortical areas reach functional and structural maturity. While some studies support concurrent maturation in all cortical areas, others provide evidence for a hierarchical sequence of maturation. Nonetheless, the notion that the postnatal maturation of cortical areas indeed proceeds in a hierarchical fashion with lower order areas maturing first, followed by the maturation of higher order association areas seems to be functionally adaptive. Evidence in support of the concurrent maturation view is provided from studies conducted by Bourgeois et al. (1989,1994). They show that the rapid proliferation phase of cortical synaptogenesis occurs simultaneously in multiple and diverse regions of the cerebral cortex. The earliest accounts supporting the concept of hierarchical maturation of cortical areas come from classic studies by Flechsig (1920). He showed that during the first years of postnatal life, pathways to the primary motor, somatosensory, visual, and auditory cortical areas are the first to be myelinated. More recently, in vivo imaging studies have confirmed Flechsig's finding and similarly showed regional differences in the rate of cortical maturation (Girard, 1991; Paus, 2001; Sowell, 2002). Chiron (1992) showed that blood flow in human cerebral cortex reaches adult levels first in primary sensory regions and last in association cortices.

Conde et al. (1996) examined the postnatal maturation of visually related areas in the macaque cortex to determine if their maturation progress proceeds from posterior primary visual cortex to anterior prefrontal regions. They followed the timing and patterns parvalbumin expressions in two major classes of local circuit neurons, basket chandelier cells, in areas V1, V2, TE, 7a, and 46 in two series of macaque monkeys ranging in age from embryonic day 132 to adult. Their findings suggest that the number of laminar distribution of parvalbumin labeled neurons reached adult levels first in area V1, followed by the adjacent visual association area V2, then by higher order visual area TE, 7a, and area 46. Bourne and Rosa (2006) provided further evidence in support of the concept of hierarchical maturation of cortical areas. They labeled the cortex of New World marmoset monkeys of late fetal and early postnatal ages with an antibody to a neurofilament protein (a marker of structural maturation of a subset of pyramidal cells) and found labeled cells at birth in V1, S1, A1, and not most other cortical areas.

An unanswered question is whether the functional connectivity between visual cortical areas ensues in a sequential fashion from posterior to anterior regions, reflecting the proposed functional hierarchy of these regions, or if they exhibit similar developmental trajectories. It is plausible that lower order visual areas would mature first, establishing functionally stable connections and relaying information to higher order areas. Higher cortical areas would thereby rely on lower cortical areas for their input, so that the relatively mature corticocortical connections established in lower areas can provide a stable input on which the higher areas can then build. Burkhalter (1993) determined the sequence in which feedforward and feedback connections

develop between V1 and V2 of infants and concluded that while the laminar distribution of labeled fibers and cell bodies in V1 and V2 indicate that feedforward and feedback connections emerge shortly before birth, the laminar termination pattern of feedforward connections appears relatively mature before feedback connections reach their mature form.

1.3.2 Regressive events and the pruning of inappropriate connections

A major developmental strategy commonly used by many developing corticocortical pathways is the initial overproduction of projections followed by the selective removal of a subset to yield the mature adult pattern of connections. While the phenomenon seems to be widespread, the magnitude of exuberance and time course of selective elimination might differ among species. Despite any observed differences, it seems like this common event of cortical development is critical in the construction of neural circuits, thus ensuring the proper formation of functional circuitry. Studies in primates have indicated that elimination of immature projections is not a major mechanism in the development of feedforward pathways, although it seems to be a common feature of feedback pathways.

The laminar refinement of interareal feedback connections in monkey visual cortex has been investigated in the monkey (Barone et al., 1995). The authors established that each visual cortical area in the adult monkey has a characteristic laminar distribution of feedback cells. Moreover, although a greater proportion of feedback cells were found in supragranular layers of a number of extrastriate visual areas, there appears to be an area specific reduction in that proportion. Furthermore,

their findings also reveal that the developmental decline in the proportion of labeled supragranular neurons is complete by the one to two months after birth, thus establishing the adult configuration. Similarly, Batardiere et al. (2002) investigated the development of cortical connectivity of area V4 to illustrate a major difference in strategy in the formation of feedforward and feedback pathways. The development of area V2 to V4 seems to be complete early in prenatal life and does not involve a large scale elimination of transitory axons. However, there seems to be a prolonged remodeling of feedback projections involving massive pruning of early formed connections. Remarkably, despite the massive reorganization, there is a clear specification of hierarchy in the prenatal monkey cortex as well as throughout development.

In kittens, the immature cortex lacks a hierarchical organization of feedback projections present in the young monkey. Batardiere et al. (1998) established that the laminar distribution of feedback neurons to area 17 in kittens is uniform across individual extrastriate areas and the selective reduction of the supragranular neurons generates the laminar distribution characteristic of each area in the adult. The authors also found a relative decrease in the number of feedback neurons in the periphery of the labeled cell clusters in the supragranular layers. By contrast, they observed little or no refinement of the extent of feedback connections in the infragranular layers.

A number of studies have demonstrated the presence of ipsilateral and contralateral transient auditory projections to kitten visual cortex as well as exuberant connections between adjacent visual cortical areas. Innocenti and Clark (1984) found transitory connections from primary and secondary auditory areas to ipsilateral and

contralateral area 17 and 18 in newborn kittens. These auditory to visual projections disappear by postnatal day 38 through axon elimination rather than neuron death. Similarly, Dehay et al. (1988) used tracer injections to demonstrate the existence of ipsilateral transient cortical projections to areas 17, 18, and 19 from frontal, parietal, and temporal cortices in the kitten. Transiently projecting neurons were found to be mostly in the supragranular layers. Furthermore, anterograde tracer injections at the site of origin of transient projections showed only a few retrogradely labeled cells in areas 17,18, and 19, demonstrating that transient projections to these areas are not reciprocal.

Area 17 in the neonate of numerous species receives exuberant projections from cortical areas that are subsequently pruned in the adult. The adult laminar distribution of feedback neurons to area 17 is characteristic for each cortical area. It seems that this distribution emerges during development from an immature state in which labeled neurons are more numerous in supragranular. This developmental elimination of neurons may well be related to the maturation of retinotopic maps and their spatial precision.

The elimination of transitory projections seems to be a general feature of cortical development leading to the adult pattern of interareal connections thus establishing which areas will be connected in the adult. The overproduction of exuberant projections and what can be achieved through their selective elimination seems unclear. Electrophysiological evidence indicates that exuberant inhibitory connections in the ferret visual cortex undergo remodeling, which might relate to the emergence of selective response properties (Chen et al., 2005). Indeed, an important function of

exuberant connections could be to endow the system with a high degree of flexibility and developmental plasticity.

1.3.3 Development of long-range horizontal connections

The highly specific and clustered pattern of horizontal connections in adult V1 is the end product of developmental processes that extensively remodel this circuit during development. Horizontal connections that span over distances of several millimeters within individual cortical layers have been variously termed as tangential, intralaminar, or intrinsic, and are especially prominent in layers 2/3 and 5 of the visual cortex in primates and carnivores. Similar to other cortical circuits, horizontal connection in V1 require a period of substantial postnatal refinement ultimately leading to an adult-like pattern of connections. The maturational processes that yield the adult pattern of intrinsic circuits in V1 are common to a variety of species.

In the primary visual cortex of kittens, intrinsic connections largely furnished by pyramidal cells in layers 2/3 initially extend long collaterals in a diffuse, unclustered pattern. Clustered intrinsic connections arise from an initially diffuse network extending an average distance of 2–3.5 mm from an injection site (Luhmann et al., 1986; Callaway and Katz, 1990; Lubke and Albus, 1992). Limited clustering of retrogradely labeled cells is first discernible by postnatal day 8 (Callaway and Katz, 1990). By PND 12–15, crude clusters of retrogradely labeled cells then emerge, with an adult-like periodicity of 1 mm (center-to-center). During this period, the intercluster areas contain a large number of retrogradely labeled cells (Callaway and Katz, 1990). Cluster refinement takes place over the next 3–4 weeks leading to an adult-like

topography with distinct clusters and few labeled cells in intercluster areas (Callaway and Katz, 1990).

Similarly, the development of horizontal projections in ferret visual cortex was studied by Durack and Katz (1996). The authors demonstrated that axon collaterals of layers 2/3 pyramidal cells first appear around P22 and require several weeks of refinement until distinct adult-like clusters are observed at P45. Interestingly, since ferrets open their eyes around P30, these presumably orientation specific patches begin to develop in the absence of patterned visual input and when cortical neurons are not yet tuned for orientation. While these results suggest that spontaneous activity plays a critical role in initiating cluster formation, Krug et al. (2001) believes some patterned input is necessary. Indeed, the refinement of clustered connections has been shown to coincide with the maturation of orientation selective responses (Chapman and Stryker, 1993). Given that these connections link iso-orientation columns in the mature cortex, it is not surprising that the refinement of clusters would coincide with the refinement of orientation tuning (Ruthazer and Stryker, 1996). For ease of comparison, (Fig. 1.2) illustrates the relative timing of major events in the development of the visual cortex in the ferret and its connections with the thalamus (Sur and Leamey, 2001). Looking at this timeline, one can appreciate the remarkable precision in the timing of some of these developmental events.

It is well known that the final adult-like topography of clustered connections may be affected by visual experience. Manipulation studies whereby pattered visual input was altered have revealed how critical experience is in the precise refinement of these connections. Callaway and Katz (1991) demonstrated that depriving kittens of

patterned visual experience by binocular lid suture prior to eye opening had minimal effect on the formation of crude clusters. By contrast, visual deprivation had a major impact on the subsequent maturation and refinement of clusters. Lowel and Singer (1992) reared kittens with an artificially induced strabismus to eliminate correlation between signals from the two eyes. The resulting pattern of local connections in V1 was altered such that intracortical projections preferentially connect cell groups driven by the same eye. Taken together, the findings suggest that experience plays a critical role in sculpting the final pattern of intrinsic connections and the precision of connections.

Figure 1.2. Comparison of the relative timing of visual developmental events in the ferret

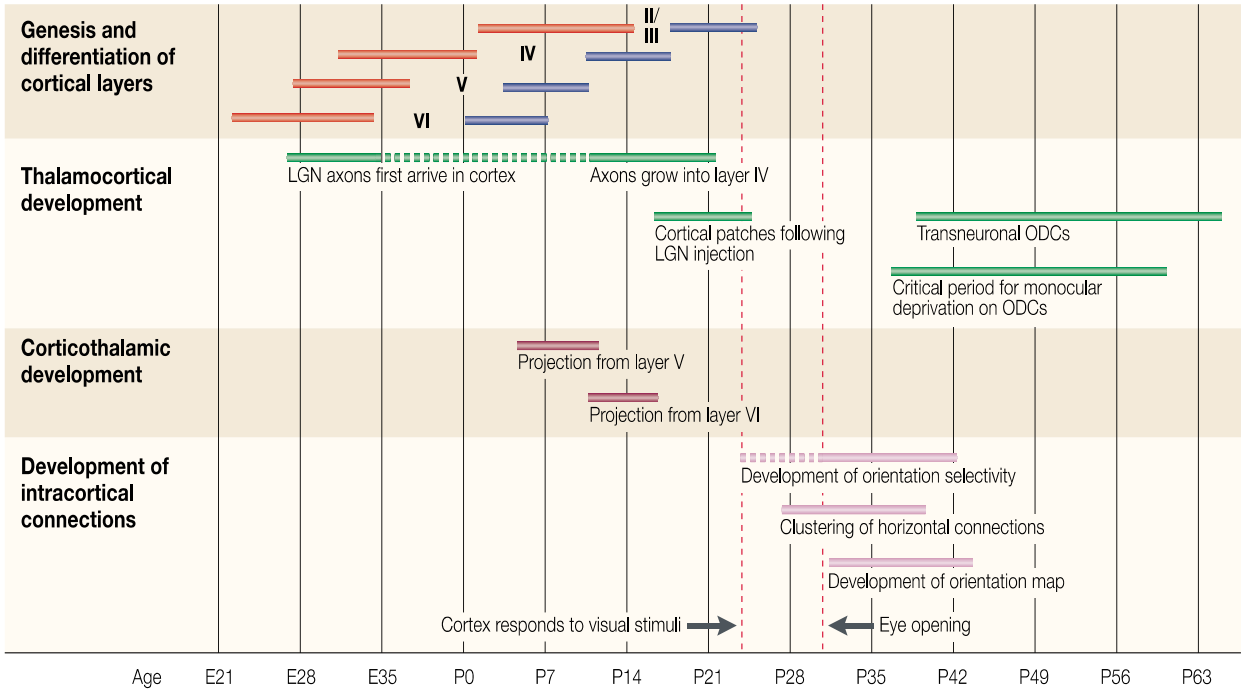

From Sur and Leamey (2001)

Timeline illustrating the development of major anatomical and functional events in the visual thalamus and cortex of the ferret.

The development of local axonal connections within the visual cortex of human infants was first studied by (Burkhalter et al., 1993). Using the fluorescent dye DiI to trace axonal projections in postmortem human brains, the investigators showed that local circuits within primary visual cortex are assembled in a sequence in which vertical connections between layers develop at the beginning of the third trimester of gestation. Long horizontal connections within layers do not emerge until shortly before birth and continue to develop throughout the first postnatal year and possibly beyond. Furthermore, the authors show that unlike the patchy horizontal projections within layers 4B and 5, which seem to develop through a process of collateral elimination, long-range projections within layer 2/3 are patchy from the outset and seem to develop with greater topographical precision.

1.3.4 Development of interareal feedforward and feedback connections

Despite the ubiquitous nature and functional importance of feedforward and feedback connections in the mammalian visual cortex, the literature regarding the anatomical emergence of each circuit during development remains sparse. Nevertheless, interareal feedforward and feedback circuits in the visual cortex of a few species have been shown to refine and reorganize early in postnatal life. A major developmental strategy commonly used by many developing corticocortical pathways is the initial overproduction of projections, followed by the selective removal of a subset to yield the mature adult pattern (Changeux and Danchin, 1976; Innocenti and Price, 2005; Rakic et al., 1986). It is important to mention that cortical immaturities are undoubtedly

limited by or partly due to subcortical immaturities, as the response properties of V1 neurons are inherited from LGN neurons (Hawken et al., 1997)

Developmental studies in the cat and monkey have demonstrated a reduction in the proportion of feedback arising from the supragranular layers of extrastriate areas (Kennedy et al., 1989; Kato et al., 1991; Barone et al., 1995), while little refinement was observed in the infragranular layers. Specifically, Batardiere et al. (1998) showed that in newborn kittens, the tangential spread of labeled supragranular neurons was coextensive with that of the infragranular layers. However, during the course of development there is a relative decrease in the number of labeled neurons in the periphery of supragranular cell clusters but not in the infragranular cell clusters. Furthermore, it has been demonstrated in kittens that the laminar distribution of feedback projections to area 17 is uniform across individual extrastriate areas and the selective reduction in the proportion of supragranular layer neurons leads to the stereotyped distribution characteristic of each area (Batardiere et al., 2002). However, this does not seem to be the case with feedback connections in primate visual cortex. In primates, there appears to be a rudimentary stereotypical laminar proportion of feedback projections reflecting the hierarchy of visual areas right at the start of corticocortical pathway formation (Barone et al.,1995).

The postnatal development of feedforward connections from V1 to extrastriate cortex has been examined in the cat by Price and Blakemore (1989). By injecting an anterograde tracer into V1, the authors showed that dense orthograde label at topographically appropriate regions was present only in area 18 of P4 kittens. At P4 and P8, area 19, 21a, and suprasylvian contained only sparse label. Furthermore, dense

orthograde label in area 19, 21a, and suprasylvian was observed only in animals aged 12 days or older. Consistent with the concept of hierarchical maturation, the authors provide further evidence that lower order areas form basic anatomical connections before higher order areas. Using retrograde and anterograde tracers targeted at areas 17 in newborn kittens, Carić and Price (1996) demonstrated that innervation of the superficial layers of extrastriate cortex from area 17 is much more spatially precise from the outset, while innervation of the deep layers from area 17 occurs with much less specificity. To date, there has been no detailed analysis of developmental changes in the distribution of feedforward terminals from area 17 to other extrastriate visual areas in the ferret.

The development of feedforward and feedback connections between V1 and V2 of human visual cortex was investigated by Burkhalter et al. (1993). The fluorescent dye DiI was injected into V1 and V2 of postmortem human brains of different pre and postnatal ages, the author demonstrates asynchronous refinement of each pathway. By 4 months of age feedforward connections from V1 to V2 have assumed the laminar features of mature connections. They arise from layers 2/3, 4B, 5, and 6 of V1, and terminate in layers 3 and 4 of V2. In contrast, at 4 months of age feedback connections to V1 are still relatively immature, showing terminations in layers 4B, 5, 6, but no input to layers 2/3. The findings suggest that feedforward connections from V1 to V2 attain their mature termination pattern before feedback connections from V2 to V1.

Recent work in mouse visual cortex by Berezovskii et al. (2011) provides evidence for dissociation in the timing of axonal outgrowth of feedforward and feedback

connections. Using retrograde tracers targeted at primary visual cortex, the authors convincingly demonstrate that feedforward axon terminals from primary visual cortex to extrastriate cortex were present at the earliest age studied (P2). In contrast, feedback neurons were first observed in the lateral medial area (LM) of extrastriate cortex nearly ten days later (P11). Feedback neurons remained relatively few in number through P14 and adult levels of feedback neurons was reached by (P18). The results are in agreement with previous study in monkeys and humans (Batardiere et al., 2002; Burkhalter, 1993) suggesting that feedforward connections from primary visual cortex develop relatively early in postnatal development and feedback connections are delayed in their timing of axonal outgrowth.

1.4 The postnatal development of functional properties of V1 neurons

1.4.1 Development of cortical orientation selectivity

Electrophysiological and optical imaging studies have revealed the timing of the development of orientation selectivity at the single-cell level. Moreover, pharmacological manipulations and visual deprivation studies have investigated the roles of spontaneous and visually driven neuronal activity. These studies have shown that orientation selectivity and its orderly representation in orientation preference maps appear early in development. In addition, they demonstrate that normal neuronal activity patterns are essential for the development of proper orientation selectivity. However, visually driven activity is not needed for the initial development of orientation selectivity or orientation maps. The basic structure of orientation maps is therefore innate, but experience is necessary for specific features of these maps, as well as for maintaining the

responsiveness and selectivity of cortical neurons (Chapman et al., 1996; Godecke et al., 2006)

The critical question of how orientation selectivity or selectivity to any stimulus feature develops during early postnatal life and the role of visual experience in this process is of great interest. The question becomes particularly perplexing in light of the observation that orientation selectivity develops in the absence of patterned visual input, e.g. before kittens and ferrets open their eyes (Hubel and Wiesel, 1970, Movshon and Van Sluyters, 1981; Fregnac and Imbert, 1984; Crair et al., 1998). Interestingly, Krug et al. (2001) showed weak orientation selective responses from V1 neurons in juvenile ferrets through the closed eyelids.

Some of the earlier developmental studies on orientation selectivity were carried out in monkey primary visual cortex by Hubel and Wiesel (1974a). Remarkably, it was observed that orientation tuning is adult-like at or soon after birth. In kittens, orientation selective responses were found in the deep layers of primary visual cortex at postnatal day 6 (P6) (Albus and Wolf, 1984; Fregnac and Imbert, 1984). The maturation of orientation tuning proceeds for the next several weeks to an adult-like state. This development appears to be mostly independent of the presence or absence of visual experience until after P18 (Crair et al., 1997a). However, young ferrets have proven to be more useful in studying the development of orientation selectivity as they provide a robust electrophysiological preparation during chronic optical imaging. They have a visual system which is quite similar to cats (Law et al., 1988), but they are born developmentally 3 weeks younger (Linden et al., 1981). The first to investigate the normal development of orientation selectivity in young ferrets were Chapman and

Stryker (1993). They demonstrated that visual cortical responses can be recorded as young as P23, with 25% of cells in all layers showing some orientation selectivity. These immature responses continue unchanged till roughly postnatal week 5, the time at which a major development in orientation selectivity occurs in layer 2/3.

Although it is well known that visual experience is not required for the initial development of orientation selectivity, it is indeed necessary for the maintenance and maturation of both orientation selectivity at the single cell level (Chapman and Stryker, 1993) and orientation preference maps (Crair et al., 1998). Manipulating the pattern of spontaneous or visually driven neuronal activity has proven useful in understanding how orientation selectivity develops in visual cortex. Chapman and Stryker (1996) showed that blocking all activity in ferret cortex with tetrodotoxin (TTX) prevents the development of orientation selectivity beyond the initial state observed at P23. Godecke and Chapman (1998) demonstrated that blocking the visual responses of ON-center retinal ganglion cells with DL-2-amino-4-phosphonobutyric acid (APB), leaving OFF responses intact, also prevents the development of orientation selectivity beyond the state observed at P23. Furthermore, Chapman and Stryker (1993) showed that even during binocular visual deprivation some degree of single cell orientation selectivity does develop in ferret visual cortex. Early maps are seen in ferret visual cortex before the time of natural eye opening (Chapman et al., 1996). The findings suggest that the proper maintenance and normal maturation of both individual cell orientation selectivity and orientation preference maps occurs only if patterned visual input is present (Chapman el al., 1996). Furthermore, their findings indicate that appreciably more circuitry in the ferret visual cortex is devoted to processing contours oriented in the

cardinal axes than to oblique contours, a bias in the mature visual cortex that accords with the early emergence of orientation domains that respond preferentially to cardinal stimuli (Chapman el al., 1996).

1.4.2 Development of direction selectivity

Neurons in primary visual cortex are also selective for the direction of motion of a stimulus across their receptive field. Direction selectivity is distinct from other neuronal response properties in the visual cortex in that it relies on detecting the temporal order of stimulus presentation. Similar to orientation selectivity, direction selectivity is first observed at the level of cortical circuits and, like both ocular dominance and orientation preference, neurons that are tuned for the same direction of motion are clustered into columns that are further organized into a map of direction preference (Weliky et al., 1996). However, unlike orientation selectivity, which has been shown to be present at eye opening in kittens and juvenile ferrets (Hubel and Wiesel, 1970, Movshon and Van Sluyters, 1981; Fregnac and Imbert, 1984; Crair et al., 1998; Chapman and Stryker, 1993; Chapman et al., 1996; White et al., 2001), neurons in primary visual cortex lack selectivity to a particular direction of motion at eye opening.

The development of direction selectivity in primary visual cortex of juvenile ferrets was examined in a study conducted by Li et al. (2006). Using optical imaging techniques and electrophysiological recordings of single cells in primary visual cortex, the authors convincingly show that direction selectivity first emerged after eye opening and then rapidly achieved mature levels of tuning over the following 2 weeks. Furthermore, the authors revealed that ferrets reared in absolute darkness immediately after eye opening did not develop normal direction selectivity tuning and required visual

experience during this formative period for the development of direction selectivity. Additionally, the development of direction selectivity lagged behind the establishment of ocular dominance and orientation preference, both of which were present and organized into functional maps at the time of eye opening in these same individual. Remarkably, a few hours of experience with a moving stimulus, but not a flashing stimulus, is sufficient to produce the rapid emergence of direction-selective neurons and direction columns in visually naïve ferrets (Li et al., 2008). Clemens et al. (2012) examined the laminar chronology of the development of direction selectivity in ferret visual cortex around the time of eye opening. Not surprisingly, the authors found that direction selectivity in all cortical layers was weak just before natural eye opening. Layer 4 neurons exhibited increases in direction selectivity that occurred earlier than layer 2/3 neurons, and both of these layers showed robust increases in direction selectivity several days after eye opening. Moreover, just after the time of eye opening, increases in direction selectivity were primarily due to increases in spiking responses to the preferred direction, while in subsequent days, increases were mainly due to decreases in spiking responses to the null direction.

Hubel and Wiesel (1963) recorded direction selective responses in very young visually inexperienced kittens. The authors noted that in the 8 day old kitten, some neurons in striate cortex responded well to two opposing direction of motion, while some responded well to one direction and not at all to the other. Furthermore, the authors noted that all receptive field properties in the adult cortex such as orientation specificity, direction selectivity, and binocularity can also be found in the naïve cortex (Movshon and Van Sluyters, 1981). In contrast, Pettigrew (1974) found no cell in the early

postnatal period having orientation selectivity and only some cells possessed selectivity for the direction of stimulus motion. Furthermore, Pettigrew noted that the proportion of neurons selective for a particular direction of motion approached the adult values after the fifth postnatal week. Albus and Wolf (1984) obtained similar results when they examined the development of direction selectivity in striate cortex of young kittens. The authors revealed a significant increase in the proportion of cells selective for a particular direction of motion during the first postnatal month. This proportion increases from about 50 in the second postnatal week to 28% at the beginning of the fourth week, which is approximately equal to the number of directionally selective cells found in the adult cat (Albus, 1980). Most subsequent studies investigating receptive field properties in young kittens have provided evidence that suggest a maturity level of cells somewhere between Hubel and Wiesel (1963) and Pettigrew (1974)'s claim.

Hatta et al. (1998) used single unit recordings in monkey V1 to show that direction selective responses can be elicited in very young monkeys. However, overall directional sensitivity and the peak monocular response amplitudes of units in the juvenile were significantly lower during the first 4 weeks of life than in adults. Furthermore, Chino et al. (1997) also observed direction selectivity in nearly all simple and complex cells in monkeys younger than 4 weeks postnatal. However, the abnormally broad tuning of V1 cells shortly after birth suggests the presence of cortical immaturities.

1.4.3 Development of spatial and temporal frequency tuning

Neurons in primary visual cortex of adult monkeys and cats show sharp spatial frequency tuning to a stimulus (Maffei and Fiorentini, 1973; De Valois et al., 1982; Schiller et al., 1976c; Movshon et al., 1978c). Using sinusoidal gratings of varying spatial frequencies one can obtain a tuning curve of a V1 neuron to reveal its preferred spatial frequency. Derrington and Fuchs (1981) were the first to study the normal development of this neuronal property in kittens. The authors revealed that neurons in area 17 of young kittens had low sensitivities and responded only to low spatial frequencies. Selectivity for spatial frequency defined as the proportion of selective cells and the narrowness of their tuning curves improved rapidly and reached adult values within the first 6 weeks. Derrington (1984) has also investigated the effects of visual experience on the development of spatial frequency tuning in young kittens. The results indicate that kittens up to 3 weeks of age show an initial improvement in spatial frequency tuning. However after 3 weeks of age, visual experience is necessary for further maturation of this neuronal response property. Chino et al. (1997) has shown that in 1 week old monkeys, cells in V1 have a very low optimal spatial frequency. The peak response amplitude for these cells was substantially lower than that for the adult cells. The authors also demonstrate that both the optimal spatial frequency and the spatial resolution quickly increase in the next 3–4 weeks with a steady but slow improvement over the following several months.

The development of temporal frequency tuning and contrast sensitivity of V1 and V2 neurons in macaque monkeys was investigated by Zheng et al. (2007). Using microelectrode recordings, the authors demonstrate that temporal response properties

and contrast sensitivity of V1 and V2 neurons were immature during the first 4 weeks of life but become mostly adultlike by 8 weeks of age. However, optimal temporal frequency and temporal resolving power of V2 neurons did not reach adult levels even at 8 weeks of age. DeAngelis et al. (1993) investigated the spatiotemporal organization of simple-cell receptive fields in the cat's striate cortex during development using reverse correlation methods at 4 and 8 weeks postnatal as well as adults. Their results indicate that spatial and temporal aspects of receptive-field structure mature with a different time course. The spatial extent of simple-cell receptive fields is adult-like by 8 wk postnatal, although the response latency and time duration of spatiotemporal receptive fields do not mature until well beyond 8 wk postnatal. By 8 wk postnatal, spatial frequency tuning appears to have reached adult values. On the contrary, temporal frequency selectivity remains noticeably immature at 8 wk. Moreover, they authors also examined the distribution of optimal spatial and temporal frequencies. From 4 wk postnatal until 8 wk postnatal, the range of optimal spatial frequencies increases substantially, whereas the range of optimal temporal frequencies remains largely unchanged. From 8 wk postnatal until adulthood, there is a large increase in optimal temporal frequencies for cells tuned to low spatial frequencies. However, for cells tuned to high spatial frequencies, the distribution of optimal temporal frequencies does not change much beyond 8 wk postnatal.

1.4.4 Development of spatial and temporal contrast sensitivity

Cortical neurons are sensitive not only to the orientation and direction of motion of a visual stimulus but also to other stimulus properties including spatial and temporal

contrast sensitivity. The spatial and temporal contrast sensitivity of human and monkey infants are reduced compared to that of adults. Zheng et al. (2007) investigated how neurons in the primary visual cortex (V1) and visual area 2 (V2) of infant monkeys respond to temporal modulation of spatially optimized grating stimuli and a range of stimulus contrasts. Their results suggest that temporal response properties and contrast sensitivity of V1 and V2 neurons were immature during the first 4 weeks of life and become mostly adultlike by 8 weeks of age. However, the optimal temporal frequency and temporal resolving power of V2 neurons did not reach the adult level even at 8 weeks of age. Their findings are in accord with the hierarchical model of cortical maturation whereby lower order visual areas reach functional maturity before higher visual areas.

Gary-Bobo et al. (1995) investigated the development of contrast sensitivity to spatial and temporal frequencies in the visual cortex of 6 week old kittens reared from birth with 3 different conditions: normal, dark-reared (DR) and dark-reared after 6 h of visual experience. The authors demonstrate that compared to the low values found in the DR kittens, animals dark reared after 6 hours of visual experience possess cells with higher spatial frequencies that are comparable to those found in adults. Moreover, an increase of contrast sensitivity at low temporal frequencies was observed as well as a shift of the cell optimum towards 3 Hz, all values close to the normal ones. Contrast sensitivity and detection of higher temporal frequencies continue to develop with age and visual experience.

1.4.5 Development of cortical binocularity

Behavioral studies suggest that some aspects of basic binocular connections are functionally immature at birth because newborn humans and macaque monkeys are unable to detect objects embedded in random dot stereograms. Stereopsis appears to emerge suddenly at 4 weeks in monkeys (O'Dell et al., 1997) and 4 month of age in humans (Birch et al., 1982). However, physiological data on a single cell level indicates this is not attributable to the absence of disparity-sensitive neurons in V1, but rather it could be either the behavioral methods are not sensitive enough to detect their stereoscopic vision or the presence of immaturities in higher level visual areas. Chino et al. (1997) investigated the physiological basis for the absence of stereoscopic vision in monkey neonates by measuring the disparity sensitivity of individual V1 neurons in infant rhesus monkeys ranging in age from 6 d to 16 weeks. The authors concluded that the binocular connections for encoding binocular disparity information are operating in a qualitatively normal manner in primate V1 only a few days after birth. Furthermore, they found an adultlike proportion of cells sensitive to interocular image disparity as early as postnatal day 6. However, the monocular spatial-frequency response properties of these disparity sensitive cells were immature in that their responsiveness was far lower than that in adults. By the forth postnatal week, the spatial frequency response properties and peak response amplitude rapidly improve to adult levels. Binocularity in striate cortex of kittens was studies by Pettigrew (1974). As early as 2 weeks postnatal, monocular responses could not be elicited, nevertheless a strong binocular response was present. Although he found some neurons selective for binocular disparity in animals younger than 4 weeks postnatal, the degree of binocular specificity found in the

adults was not achieved until the fifth postnatal week. The development of binocular vision in kittens was later investigated by Freeman and Ohzawa (1992) with the aim of understanding when binocular vision becomes adultlike. The authors recorded from single units in striate cortex of 2, 3, and 4 week old cats to compare with adult values. Binocular interactions such as phase specific and non-phase specific suppression or facilitation of cells in 3 and 4 week old kittens were comparable to those found in the adult. Moreover, monocular and binocular tuning characteristics were also similar between kittens and adult cats. However, the author report distinct changes that occur with age such as optimal spatial frequency and peak responses. Their results suggest that the functional connections required for binocular vision are present in early postnatal development, but require normal visual experience for the fine tuning of response properties present in the adult.

The maturation of cortical binocularity during postnatal development is known to be adversely affected by early abnormal visual experience. The maturation and refinement of neural connections that subserve binocular vision can be readily perturbed by the presence of conflicting visual images between the two eyes. This may arise early in development from unilateral form deprivation, optical defocus (anisometropia), or an interocular misalignment of the visual axes (strabismus) (Movshon and Van Sluyters, 1981). Hubel and Wiesel (1965) were the first to study the effects of rearing kittens with an interocular misalignment (strabismus) and showed a dramatic loss of binocularly activated cortical neurons and, in some cases, a shift in ocular dominance toward one eye. Moreover, Crawford et al. (1975) found that nearly half the cells studied in a monkey that had been binocularly deprived early in life were

unresponsive to visual stimulation. A more recent study conducted by Chino et al. (1994) investigated the binocularity of neurons in striate cortex of cats at 4 weeks of age reared with different durations of discordant binocular visual experience. The authors measured the sensitivity of cells to binocular image disparity and concluded that a short period (2 wks) of optically induced strabismus in young kittens initiated strong suppressive interactions in the cortex, which continued even after the removal of optical dissociation and recovery period. However, extended periods of interocular misalignment, either optically or surgically induced, drastically reduced binocular interactions, including interocular suppression. This caused the majority of cortical neurons to become monocular, and often exhibited a spatial-frequency-dependent contrast sensitivity loss. Collectively, the results suggest that the normal development of binocularity in the visual cortex of young animals is highly dependent on normal visual experience.

1.5 The postnatal maturation of visual perceptual abilities

1.5.1 Development of orientation sensitivity

Vision is relatively poor in infant monkeys and humans and matures in the following months or years. There is an extensive literature assessing the behavioral development of visual functions in humans and to a lesser extent in non-human primates (for reviews see Teller, 1997; Braddick and Atkinson, 2011). A common behavioral method used to investigate infant vision by researchers is the forced choice preferential looking (FPL) test. The preferential looking technique was originally conceived by Fantz (1961), as a means of revealing infants' visual discriminative

abilities. In the mid 70's, Teller et al. (1974) invented the combination of preferential looking with forced choice by a 'blind' observer (forced-choice preferential looking = FPL). Since then, various research groups have used FPL. This method takes advantage of infants' preference to look at something patterned over something plain. For example, to test an infant's grating acuity, black-and-white stripes paired with a gray stimulus of the same mean luminance is shown, and the size of the stripes is varied across trials. A tester watches the baby's eye movements, and the measure of grating acuity is the smallest size of stripe for which the tester can judge correctly from the baby's eye movements where the stripes are located (Lewis and Maurer, 2005).

Orientation sensitivity is one of the first visual functions to appear after birth. To reveal orientation-selective responses, Braddick et al. (1986) isolated infants' VEPs to reversals of grating orientation between opposite obliques by embedding them in a series of random shifts in the gratings' spatial phase. The VEP is an electrical signal elicited by a visual stimulus, which reflects the summed activity of many neurons, measured non-invasively from the surface of the head. This reliable signal can be identified as a repetitive signal at a frequency related to alternations between stimuli of 2 different orientation (Atkinson and Braddick, 2003). Therefore, with a suitable stimulus sequence this signal provides evidence for orientation selective mechanisms. Braddick et al. (1986) showed that orientation-selective responses first appeared around 6 weeks of age. However, subsequent research revealed that at lower reversal frequencies (i.e the frequency at which the orientation was reversed), the response could be recorded at 3 weeks (Braddick, 1993).

Behavioral experiments subsequently conducted by Atkinson et al. (1988) revealed broadly similar results with VEP data obtained from Braddick et al. (1986) with one exception. Orientation discrimination was measured behaviorally in two infant control habituation procedures, with both dynamic and static patterns. When dynamic patterns identical to those in previous VEP studies were used, the first sign of orientation discrimination was found at around 6 weeks postnatally. Therefore, the time course of both the VEP and the behavioral measures was similar. Nevertheless, with static patterns, evidence of orientation discrimination by newborns was found only when the infants were allowed to compare the habituated and novel orientations in a paired simultaneous comparison after habituation, but was not found when the habituated and novel stimulus were presented sequentially. Their results suggest that some orientation discrimination in newborns is present and can be used for discrimination of static patterns. However, some maturation over the next few weeks is required before a positive electrophysiological VEP response can be measured for dynamic patterns changing in orientation. The results from Atkinson's group (1988) were later corroborated by Slater et al's. (1988) study using similar behavioral experiments. The authors concluded that even in newborn infants, some orientation discrimination capabilities are present at birth. It appears that even though orientation selective responses emerge early in postnatal life, mature orientation discrimination abilities require several months before becoming adult like in nature.

1.5.2 Development of motion perception

Direction selective responses to motion have been shown to emerge early postnatal development, but lag behind orientation selectivity. Wattam-Bell (1991)

isolated VEPs for reversals of motion direction, which are embedded in a series of non-directional transitions to study the development of visual motion mechanism in infants. This response was not seen in infants under 10-12 weeks of age. Furthermore, the author concluded that the development of direction selectivity starts at low velocities and extends to higher velocities with age.

Using forced-choice preferential looking (FPL), Wattam-Bell (1992) found that infants aged 8 weeks and above were able to discriminate between opposite directions of motion. The author used random-dot patterns in which a target region moved in the opposite direction to the background; for adult observers the opposite directions resulted in perceptual segregation of the patterns. Between 8 and 15 weeks, dmax (maximum displacement limits) for discrimination of coherent from incoherent motion, and for discrimination of opposite directions of coherent motion, increased with age. These results suggest that while directional mechanisms are present in the visual system by 8 weeks, infants' sensitivity to direction is confined to a limited range of velocities. Later research by Wattam-Bell (1996) using preferential looking experiments in 1 month old infants showed that direction discrimination at any of the test velocities used was not present. The author also measured velocity thresholds (V_{min} and V_{max}) for direction discrimination and showed between 10-13 weeks of age V_{min} decreased while at the same time V_{max} increased. The results suggest that 1 month old infants appear to be insensitive to the direction of visual motion.

1.5.3 Development of contrast sensitivity

The function relating an observer's contrast sensitivity to the spatial frequency of a sinusoidal grating test target is the spatial contrast sensitivity function (Movshon and Kiorpes, 1988). Young monkeys and humans have poor spatial contrast sensitivity; both the peak contrast sensitivity and the spatial resolution of the visual system are significantly lower young humans and monkeys than they are in adults. Boothe et al. (1988) assessed the development of spatial contrast sensitivity longitudinally in monkeys using operant conditioning methods. The authors report several changes that occur in the contrast response function during development, including an overall increase in sensitivity to contrast, a shift in the peak of the function toward higher spatial frequencies, and an increase in the cutoff spatial frequency. Furthermore, they show that the timecourse for the changes in the contrast sensitivity function were characterized by rapid development during the first 10-20 weeks, followed by a gradual more protracted development to adult levels over the remainder of the year. Interestingly, sensitivity to contrast for different spatial frequencies was also found to develop with a different timecourse; sensitivity to low spatial frequencies reached adult levels much earlier than sensitivity to high spatial frequencies.

Atkinson et al. (1977) assessed contrast sensitivity in infants aged 5-12 weeks by measuring fixation preference for static or drifting sinusoidal gratings over a uniform field assessed by two-alternative forced choice by a "blind" observer. The investigators found that there was a rapid improvement in the contrast sensitivity between 5 weeks and 8-12 weeks. Both contrast sensitivity and visual acuity improve substantially, and the older groups showed evidence of a low spatial-frequency cutoff, which the younger

group did not have. Acuity and contrast sensitivity was similarly measured in 1,2, and 3 month old infants by Banks and Salapatek (1978). The results are broadly consistent with Aktinkon's group (1977) in that the spatial frequency cut off (reflecting visual acuity) increased with age. Furthermore, evidence for the presence of a low-frequency fall-off at 2 and 3 months, but not at 1 month further suggest an improvement in contrast sensitivity and visual acuity.

While most studies of visual development have focused on visual development of infants, the number of studies that have extended this to children and revealed the point at which visual function is adultlike are sparse. Benedek et al. (2003) investigated the development of visual contrast sensitivity (CS) in children between 5 and 14 years of age. The authors revealed significant maturation of CS, which reached the adult-like values by 11 – 12 years of age. Moreover, the development was more pronounced at low spatial frequencies (<2 cycles/degree) and in the dynamic condition. Leat et al. (2009) found that visual acuity was fully mature between the ages of 5 and the mid teenage years, while contrast sensitivity was reported to be fully mature between the ages of 8 to 19 years.

Temporal vision is known to develop comparatively quickly. Stavros and Kiorpes (2008) described the time course of temporal contrast sensitivity development in monkeys and found that adult levels are reached by about 6 months after birth, substantially earlier than spatial contrast sensitivity. Similarly, Ellemberg et al. (1999) reported that temporal contrast sensitivity in human children reaches adult levels before spatial contrast sensitivity. The authors take the difference in the time course of

development between spatial and temporal contrast sensitivity as evidence to suggest that the two functions are mediated by different underlying mechanisms.

1.5.4 Development of grating acuity

Visual acuity of newborn infants is poor at birth and improves rapidly during the first 6 months. For infants, acuity is measured with stripes of decreasing size, and the measure of acuity can be revealed by determining the finest stripes that the infant can resolve—a measure known as grating acuity (Lewis and Maurer, 2005). Generally, there are two methods that can be used to measure the visual acuity in children. The first is psychophysical/ behavioral methods, which require some response from the child. The second is an objective method, such as pattern VEP (pVEP) (Leat et al., 2009). When tested behaviorally with preferential looking, newborns' grating acuity is typically about 40 times worse than that of visually normal adults tested under the same conditions (Brown and Yamamoto, 1986; Courage and Adams, 1990; Dobson et al., 1987; Mayer and Dobson, 1982): Newborns preferentially look at stripes only if they are 30 to 60 min wide whereas adults can resolve stripes less than 1 min wide (One minute is 1/60 of a degree of visual angle). It has been shown that by 6 months of age, grating acuity improves from being about 40 times worse than that of normal adults to being only 8 times worse. Thereafter, grating acuity improves more gradually and reaches adult values at 4 to 6 years of age (Courage and Adams, 1990; Ellemberg et al., 1999; Mayer and Dobson, 1982). Norcia and Teller (1985) used the VEP method to study infants' visual acuity and concluded that during the first year of life VEP acuity increased from 4.5 c/deg in the first month to 20 c/deg by the end of the first year. Moreover, mean

acuities of 17-22 c/deg found for the 8-13 month old infants do not quite reach the adult mean of 24.3 c/deg.

Poor visual acuity of newborns is largely attributable to immaturities in the morphology and arrangement of retinal cones, optics of the eye, as well as immaturities in the central visual pathways (LGN and primary visual cortex). Although a great deal of retinal maturation takes place between birth and early childhood, the 45-month old's retina is not completely adultlike (Yuodelis and Hendrickson, 1986). These authors have shown that the morphology of the photoreceptor's outer segment undergoes great changes during development. The marked improvement in visual acuity during the first 6 months reflects, in part, the maturation of foveal cones in their ability to filter out less information and allow finer and finer detail through to tune cells in the visual cortex (Banks and Bennett, 1988; Wilson, 1988, 1993). The more gradual changes observed through age 4 to 6 years likely reflect further refinement of the retinal and cortical connectivity (Garey and De Courten, 1983; Huttenlocher, 1984; Huttenlocher et al., 1982; Kiorpes and Movshon, 1998). Therefore, it seems that poor vision at birth is due to both optical as well as neural immaturities.

1.5.5 Development of vernier acuity

Similar to grating acuity, vernier acuity, which is the smallest detectable misalignment reflecting the spatial position sensitivity of the visual system has also been shown to be impoverished in human infants, but matures to adult levels during the course of development. Using a preferential looking procedure, Shimojo et al. (1984) assessed the development of grating acuity and vernier acuity in human infants aged 2-

9 months. The authors found that vernier acuity was found to be superior to grating acuity only after 3 months of age. These two visual functions were similar in terms of their developmental time-courses up to three four months of age. However, vernier acuity continues to improve up to the oldest age tested, while grating acuity asymptotes around five months of age. Manny and Klein (1984) used a similar experimental paradigm and found that vernier acuity, like grating acuity, improved about 3 octaves over the first 6 months of life. Furthermore, the authors found that vernier resolution of infants, as in adults, was better than grating resolution. Shimojo and Held (1987) used similar methods and reported that vernier acuity is less than grating acuity at 11-12 weeks of age or younger. However, they revealed that the developmental rate of vernier acuity is greater than that of grating acuity in the first 6 months of life.

Skoczenki and Norcia (1999) assessed the development of vernier and grating acuity in infants aged 8-80 weeks postnatal using the VEP method. The investigators found that VEP vernier acuity and grating acuity develop at different rates, with grating acuity approaching adult levels earlier than vernier acuity. Furthermore, VEP vernier acuity remains rather immature throughout the first year of life, similar to behavioral vernier acuity. The authors also report that vernier thresholds at 50 weeks were approximately 10 times lower than adult values; this marked immaturity of the displacement thresholds contrasts with grating acuity, which is within a factor of two of adult values at 50 weeks of age.

Kiorpes (1992a) assessed the developmental timecourse of vernier acuity and grating acuity in normally reared monkeys. Behavioral measurements of vernier acuity

and grating acuity reflect the positional sensitivity and spatial resolution of the visual system. Near birth, grating acuity was found to be relatively more mature than vernier acuity. The author found that the two measured visual functions develop at different proportional rates, but approach adult levels at about the same postnatal age. During the course of development, grating acuity improved 15-fold whereas vernier acuity improved about 60-fold. Furthermore, both visual functions appeared to approach adult levels by about 40 weeks of age. The author attributes poor grating and vernier acuity early in development largely to retinal limitations and credits the improvement in both visual functions to the maturation in the morphology and topography of photoreceptors. The time course of development for both vernier acuity and grating acuity were similarly assessed in experimentally induced strabismic monkeys by Kiorpes (1992b). The findings suggest that similar to human strabismic amblyobes, monkey strabismic amblyobes have greater deficits in vernier acuity than in grating acuity. However, the developmental time course for vernier acuity and grating acuity seem to be disrupted in parallel. The author proposes that these deficits seem to result from a slowing of the development of spatial vision for the deviated eye.

1.5.6 Development of Stereopsis

Binocular interactions and the development of stereopsis in human infants have shown that the onset of stereopsis in the human visual cortex is between 10 and 16 weeks of age (for reviews see Braddick and Atkinson, 1983; Braddick et al., 1983). A number of groups have focused on studying the development of stereopsis in human infants (Birch et al., 1982; Braddick et al., 1980; Fox et al., 1980; Held et al., 1980; Julesz et al., 1980). Braddick et al. (1980) and Julesz et al. (1980) both have measured

VEPs while infants watched a dynamic random-dot correlogram. A periodic VEP response, which corresponds to alternations between a correlated and anticorrelated display can be tracked longitudinally in individual infants. Smith et al. (1988) used a similar random dot correlogram in a forced choice preferential looking test and found broadly consistent results. The same infants were tested both with the VEP and FPL technique and a strong correlation was found between the ages at which a reliable response of each kind was detected. However, the average age of onset using the FPL technique was two weeks later compared with the VEP method. Birch et al. (1982) made measurements using the FPL method with line stereograms rather than random dots. The authors find that infants show a preference for a display of three vertical bars in which the central bar has a crossed disparity relative to the others, compared with a set of bars which line in a single stereo plane. Despite the difference in stimuli used, both Birch et al. (1982) and Braddick at al. (1980) find that the onset age for disparity sensitivity is typically 12-16 weeks. Furthermore, Birch's group also tested the minimum disparity for which infants show a preference. The authors find that after the initial onset of sensitivity, stereoacuity shows a rapid increase, typically going from 80 min arc to 1 min arc in a period of 4-5 weeks.

O'Dell and Boothe (1997) assessed stereoacuity in infant monkeys using a force choice preferential looking technique. The authors show that by 8 weeks of age all of the monkeys were responding to at least coarse levels of disparity, and by 13 weeks of age all were responding to fine levels of disparity. Although electrophysiological evidence (Chino et al., 1997) suggests the presence of units with binocular receptive fields that were disparity sensitive within the first week after birth, there are still some

receptive field properties such as overall responsiveness and spatial frequency tuning that are immature. Chino et al. (1997) implicates the maturation of receptive fields in the behavioral onset of sensitivity to disparity.

1.5.7 Development of contour integration

While the more basic visual functions mature early in development, more complex visual functions that presumably depend on the maturation of extrastriate visual areas have a more extended developmental timecourse. The maturation of extrastriate visual areas in turn allows for the efficient integration of signals received from V1, which only encodes local stimulus properties. Moreover, it is now accepted that contour integration requires the ability to process local orientation cues and subsequently organize coherent elements into a global texture or shape. For instance, contour integration (the ability to integrate information over space) abilities develop comparatively late. Kovács et al. (1999) reported that children younger than 3 years of age were unable to identify a coherent contour defined by a circular ring of Gabor patches imbedded in noise, and their ability to perform the task improved into their teenage years. The authors attribute this early inability not to the lack of long-range spatial interactions, but rather to functional immaturities in terms of their spatial range.

In monkeys, the ability to perform a contour integration task develops late as well. Kiorpes and Bassin (2003) studied the development of contour integration, a global perceptual task, in comparison to that of grating acuity in macaque monkeys. The task required the detection of a specific feature (a circular contour) in the presence of background noise. Presumably, detection of the contour requires perceptual linking of

the elements in the ring in the presence of noise elements. This is considered to be a "global" task, as the feature linking cannot be solved on the basis of detection of the local features alone (Kiorpes and Bassin, 2003). The authors reveal that contour integration develops substantially later than acuity. Monkeys were first able to perform contour integration reliably at 5–6 months, around the time that acuity development is complete and continues to mature well into the second postnatal year. El-Shamayleh et al. (2010) assessed the development of second-order form sensitivity by training monkeys to discriminate the orientation of pattern modulation in a two-alternative forced choice paradigm. The authors showed that infant monkeys were able to discriminate the orientation of texture-defined form as early as 6 weeks postnatal, and their behavioral sensitivity was essentially adultlike around 40 weeks of age. Furthermore, sensitivity to both texture- and contrast-defined form was found to be mature earlier than sensitivity to luminance-defined form. Wilkinson and Crotogino (1995) studied the development of texture segmentation in kittens by using a two-alternative forced choice-jumping paradigm. Their results show that kittens younger than 80 days are unable to perform an orientation based texture segmentation task. However, kittens older than 90 days were able to perform this task quite easily.

Atkinson and Braddick (1992) investigated visual segmentation of oriented textures by infants and concluded that the segmentation of textures based on orientation differences emerges between 10 and 16 weeks of age, and is slower to develop than segmentation based on luminance differences. By recording visual-evoked potentials, Norcia et al. (2005) tested whether young infants can detect orientation-defined textures and contours. They measured responses to an organized texture

comprised of many Gabor patches of the same orientation, alternated with images containing the same number of patches, but all of random orientation. Their results reveal differential responsiveness to organized versus random textures emerges no later than 2–5 months of age. Moreover, responsiveness to orientation-defined contours emerges no later than 6–13 months.

A more recent study conducted by Palomares et al. (2010) investigated whether 4- to 5.5-month-old infants are sensitive to the global structure of Glass patterns by measuring visual-evoked potentials. Glass patterns are moirés created from a sparse random-dot field paired with its spatially shifted copy (Palomares et al., 2010). The authors found that sensitivity to the global structure of the Glass patterns in the infants spanned a very limited range of spatial separation. However, they observed robust responses in the infants when the dot pairs of the Glass pattern were connected with lines. Their results suggest that infants' insensitivity to structure in conventional Glass patterns is due to their inability to extract local orientation cues generated by the dot pairs. Once the local orientations are made unambiguous, infants can integrate these signals over the image. A similar study was conducted by Lewis et al. (2004) studying the development of sensitivity to global form in 6-year-olds, 9-year-olds, and adults using Glass patterns with varying ratios of paired signal dots to noise dots. The authors concluded that thresholds were equally immature for both types of pattern (concentric or parallel) at 6 years of age (about twice the adult value) but were adult-like at 9 years of age. Taken together, the studies suggest that while sensitivity to glass patterns may be found in infants, the processes underlying Glass pattern recognition have a protracted developmental period.

1.5.8 Development of global motion perception

Another visual function that also depends on extrastriate cortical processing is global motion sensitivity. It is important to distinguish between low-level mechanisms that provide local motion signals from higher-level mechanisms that integrate motion information across space and time. Kiorpes and Movshon (2004) studied global motion sensitivity in monkeys ranging in age from birth to 3 years. The authors show that unlike contour integration tasks, monkeys could perform the motion direction discrimination task at the earliest ages studied (3–5 weeks). However, the maturation of this visual function continued up to 3 years. These data suggest a long developmental timecourse for complex visual functions that depend on extrastriate cortical areas. A recent study of Kiorpes and Movshon (2012) aimed at exploring the relative development of the dorsal and ventral extrastriate processing streams by studying the development of sensitivity to form and motion in macaque monkeys between the ages of 5 weeks and 3 years. By using Glass patterns and random dot kinematograms (RDK) to reveal global form and motion sensitivity, the authors measured coherence threshold for discrimination of the global form or motion pattern from an incoherent control stimulus. The authors concluded that sensitivity to coherent motion in RDKs was measurable earlier than sensitivity to Glass patterns and was higher at all ages, but adult performance on both tasks was reached at a similar age, 2–3 years. The findings suggest that the development of global form and motion sensitivity for the particular stimuli used in their study proceeds at a similar timecourse.

Bucher et al. (2006) investigated the development of the visual motion system to reveal potential maturational changes in adolescents (15 – 17 years) and adults (20 –

30 years) by measuring brain activity with event-related EEG potentials (ERPs) and functional magnetic resonance imaging (fMRI) in these two groups. Subjects had to perform a visual form discrimination task—with forms being either defined by motion or luminance contrast. The authors concluded that the spatial organization of the basic visual network for processing motion- and luminance-defined shape is established by the age of 15 – 17. However, the authors argue that visual motion processing in area MT continues to become faster and more efficient during late development. Parrish et al. (2005) studied the development of global motion and texture-defined form sensitivity in children ranging in age from 3 to 12 years to reveal any maturational difference in their developmental time course. The investigators found no significant improvement in global motion sensitivity, as measured by coherence threshold, between age 3 years and adult. However, other metrics of motion sensitivity continued to mature up to age 7. Furthermore, their results for texture-defined form sensitivity showed continued maturation up to age 10–11 years. The results suggest that certain aspects of both global motion and texture-defined form develop at different times in school aged children.

Ellemberg et al. (2003) compared sensitivity to first- versus second-order motion in 5-year-olds and adults tested with stimuli moving at slower (1.5° s-1) and faster (6 ° s-1) velocities. The authors measured thresholds for the discrimination of direction using patterns of random noise that were either added to (first-order stimulus) or multiplied by (second-order stimulus) a sinusoidal grating modulated in luminance. The authors concluded that sensitivity to second order motion develops more slowly than sensitivity to first-order motion. Their findings are consistent with notion that first-order and

second-order motion are represented by different mechanisms and that they mature at different rates. A study conducted by Wattam-Bell et al. (2010) using high high-density VERP study in human infants found global motion responses to be more prevalent in 4 month olds than global form responses, although the activation patterns were different in infants compared to adults (Wattam-Bell et al., 2010). Therefore, their findings are in line with previous studies suggesting that dorsal stream function matures earlier than ventral stream. Collectively, behavioral data on the development of sensitivity to form and motion suggests that motion sensitivity may appear and mature earlier in humans and non-human primates than form sensitivity. In addition, behavioral data revealing earlier maturation of motion sensitivity, presumably reflecting dorsal stream functioning, is consistent with anatomical data (Bourne and Rosa, 2006; Condé et al., 1996).

Therefore, it seems that vision is rather poor at birth in infant monkeys and humans and requires some postnatal visual experience to mature to adult levels. Visual acuity and contrast sensitivity develop similarly in human and non-human primates, becoming adultlike between 3 and 7 years in humans, and between 9 and 12 months in monkeys (Boothe et al., 1988; Ellemberg et al., 1999; Kiorpes, 1992, 2008; Teller, 1997). In human infants orientation discrimination abilities first appear around 6 weeks postnatal and require several months of postnatal experience to become adultlike in nature (Braddick et al., 1986). This ability is followed by the discrimination of direction of motion, which appears at 8 weeks of age and similarly requires several months of postnatal experience (Wattam-Bell, 1991). Recent evidence suggests that at least some aspects of intermediate level form vision mature simultaneously with basic spatial vision and not necessarily follow sequentially (El-Shamayleh et al., 2010). More complex

visual functions seem to appear relatively late in development and require even more postnatal visual experience for full maturation. For instance, Kovács and colleagues (Kovács et al., 1999; 2000) demonstrated that children under the age of 3 could not identify a contour defined by a circular ring of Gabor patches imbedded in noise, and the ability to perform the task improved well into the teenage years. Similarly, this integrative task develops late in monkeys as well, with the ability to perform contour integration appearing around 16 weeks and full maturation requiring at least one year (Kiorpes and Bassin, 2003).

In summary, the onset, duration, and time at which particular visual functions attain their adult like state differs substantially; this differs among species. The developmental timecourse and duration of refinement varies significantly as more basic visual functions mature earlier and require less time than more complex ones, which require considerable postnatal time to refine. To compare the developmental timing of different visual functions discussed above, we constructed a timeline reflecting the relative onset and duration of maturation in humans, monkeys, and ferrets from physiological as well as behavioral data in the literature (Fig. 1.3).

This thesis consists of three chapters on the postnatal refinement of interareal circuits in ferret visual cortex. In chapter 1, I describe the use of zinc histochemistry in delineating areal boundaries between different visual areas and more importantly how the zinc expression reveals circuit refinement of feedforward and feedback projections in ferret visual cortex. In chapter 2, I describe developmental refinement of feedback projections between primary visual cortex and extrastriate areas in the juvenile ferret brain. In the third chapter, I describe the postnatal development of feedforward

projections from V1 to different target areas. The overarching goal of this thesis is to reveal potential differences in the rate at which distinct feedforward and feedback pathways refine postnatally. This is relevant as the refinement of cortical circuits underlies the maturation of neuronal physiological properties and more broadly distinct visual functions. Therefore, by understanding the timing of when distinct feedforward and feedback are qualitatively adultlike, we can attribute particular neural substrates to particular visual functions.

Figure 1.3. Developmental timeline of different visual functions

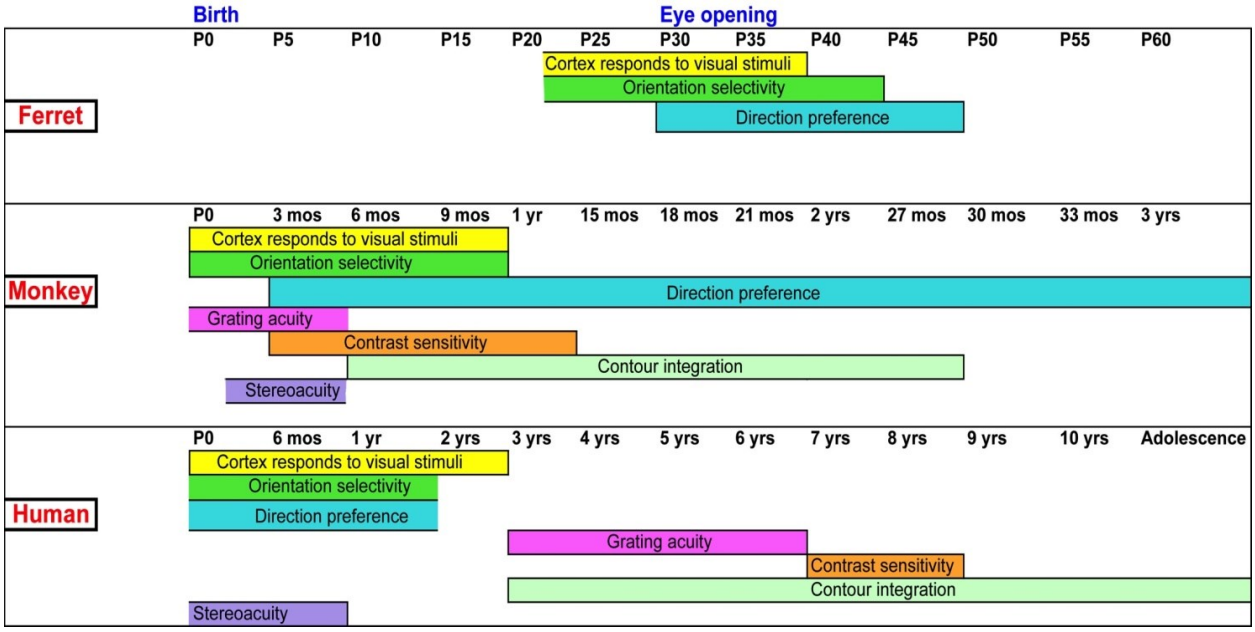

From Khalil and Levitt (2012a)

Timeline reflecting the relative onset and duration of maturation of different visual functions in ferrets, monkeys, and humans from physiological as well as behavioral data.

CHAPTER 2
Zinc histochemistry reveals circuit refinement and distinguishes visual areas in the developing ferret cerebral cortex

(published in Brain Struct Funct. 2013 Sep;218(5):1293-306. [Epub 2012 Sep 30.])

2.1 Abstract

A critical question in brain development is whether different brain circuits mature concurrently or with different timescales. To characterize the anatomical and functional development of different visual cortical areas, one must be able to distinguish these areas. Here, we show that zinc histochemistry, which reveals a subset of glutamatergic processes, can be used to reliably distinguish visual areas in juvenile and adult ferret cerebral cortex, and that the postnatal decline in levels of synaptic zinc follows a broadly similar developmental trajectory in multiple areas of ferret visual cortex. Zinc staining in all areas examined (17, 18, 19, 21, and Suprasylvian) is greater in the 5-week-old than in the adult. Furthermore, there is less laminar variation in zinc staining in the 5-week-old visual cortex than in the adult. Despite differences in staining intensity, areal boundaries can be discerned in the juvenile as in the adult. By 6 weeks of age, we observe a significant decline in visual cortical synaptic zinc; this decline was most pronounced in layer IV of areas 17 and 18, with much less change in higher-order extrastriate areas during the important period in visual cortical development following eye opening. By 10 weeks of age, the laminar pattern of zinc staining in all visual areas is essentially adultlike. The decline in synaptic zinc in the supra- and infragranular layers in all areas proceeds at the same rate, though the decline in layer IV does not. These results suggest that the timecourse of synaptic zinc decline is lamina specific, and further confirm and extend the notion that at least some aspects of cortical maturation follow a similar develop- mental timecourse in multiple areas. The postnatal decline in synaptic zinc we observe during the second postnatal month begins after eye opening, consistent with evidence that synaptic zinc is regulated by sensory experience.

2.2 Introduction

Interareal corticocortical projections are largely furnished by pyramidal neurons that utilize glutamate as their primary neurotransmitter. A subpopulation of glutamatergic neurons sequesters zinc into synaptic vesicles of their terminal boutons (Beaulieu et al. 1992; Martinez-Guijarro et al. 1991). This subpopulation could constitute an anatomically and functionally distinct subset of interareal projections, with distinct physiological properties. Furthermore, the cerebral cortex is characterized by a highly specific regional and laminar pattern of zinc staining (Dyck et al. 1993; Garrett et al. 1991, 1994). The supragranular and infragranular layers of cortical areas exhibit high zinc levels, while layer IV has the lowest levels. This pattern is especially obvious in primary sensory areas such as S1 and V1, and results because the thalamocortical recipient layer IV of primary sensory areas is nearly devoid of zinc-positive synapses (Casanovas-Aguilar et al. 1998; Garrett et al. 1992). Furthermore, zinc-rich corticocortical projections in the rat appear to be organized in a highly specific manner, forming two segregated systems, one arising from the supragranular layers and the other from the infragranular layers (Casanovas-Aguilar and Miro-Bernie 2002).

Synaptic zinc is known to be developmentally regulated in cat primary visual cortex (Dyck et al. 1993), rat and mouse forebrain (Garrett and Slomianka 1992; Valente et al. 2002) as well as mouse somatosensory cortex (Czupryn and Skangiel-Kramska 1997). Our aim in this study was to examine the change with age of the distribution of synaptic zinc in five visual cortical areas of the juvenile ferret from 5 to 10 weeks postnatal (as well as in adults) to establish the age at which synaptic zinc density is adultlike. Ferrets (Mustela putorius furo) are ideal for use in developmental

connectional studies because of their protracted postnatal period of brain development, and their relatively smooth cerebral cortex that facilitates access to all visual cortical areas. These ages were chosen to span the period just after eye opening, during which emergent visual responses undergo much of their refinement to the adultlike state. We wished to determine if the change in zinc staining proceeds at the same rate in different visual areas. Of course accurate anatomical identification of these cortical areas is essential to the characterization of their anatomical and physiological development. In the course of these studies, we discovered that synaptic zinc histochemistry can be used to reliably distinguish visual areas in juvenile ferret visual cortex as early as 5 weeks postnatal. This is important since the myelination of juvenile ferret cortex is not complete until the end of the second postnatal month (Barnette et al. 2009); thus, the commonly used myelin stain to distinguish cortical areas in the adult is not a suitable anatomical marker of visual cortical areas in early postnatal development.

Here, we describe the developmental trajectory of zinc staining in five visual cortical areas of the ferret brain. We provide evidence for a decline in zinc staining in layer IV of several visual cortical areas in the period after eye opening; this change was most prominent in areas 17 and 18 (which unlike higher-order areas receive a prominent thalamic input from the lateral geniculate nucleus). We observed less of a decrease in staining in the supragranular and infragranular layers in all areas over this same period. Our measurements suggest that synaptic zinc levels in visual cortex are essentially adultlike by 6 weeks postnatal, and suggest that this aspect of cortical maturation follows a similar developmental timecourse in all visual cortical areas.

2.3 Materials and Methods

Animal treatment

We studied twenty-four female ferrets (Mustela putorius furo) at five postnatal ages: 5 weeks (n = 3), 6 weeks (n = 5), 8weeks (n=4), 9weeks (n=4), and 10weeks (n=3), plus adults (n = 5). Adult ferrets were sexually mature and at least 1 year old. Animals were obtained from Marshall Farms (North Rose, NY); kits were housed with the jill under a 12 h light/dark cycle. The ages of ferret kits were determined by their recorded birthdates. Some of these animals underwent anatomical injection experiments yielding data for a separate study; anatomical tracer injections were performed as described in Cantone et al. (2005). Histochemical markers are routinely used in conjunction with anatomical tracer injections, and typically do not affect tissue quality or staining. All procedures conformed to National Institutes of Health guidelines. Animals were lightly anesthetized with an intra- muscular injection of ketamine (25 mg/kg) and xylazine (2 mg/kg), and then received an intraperitoneal injection of the zinc chelator sodium selenite (15 mg/kg). Following the injection, selenium salts travel to the brain and react with endogenous zinc, rendering precipitates that can be enhanced by silver development (Danscher 1982).

Tissue preparation

At 40–60 min after receiving the selenite injection, animals were euthanized with an overdose of sodium pentobarbital (100 mg/kg, i.p) and perfused transcardially with 0.9 % NaCl for 10 min, followed by 4 % paraformaldehyde for 20 min. A final 10 % sucrose in 4 % paraformaldehyde solution was used with a total fixation time of roughly

1 h. The brains were quickly removed from the skull, hemi- spheres were separated, and the posterior part of the brain was blocked and postfixed in 4 % paraformaldehyde in 0.1 M phosphate buffer (PB) for several hours. Blocks were then placed into a 30 % sucrose solution in 0.1 M PB. Once the brains were sunk, 40 µm thick sections were cut through visual cortex on a freezing, sliding microtome. The sections were separated into numbered series. For both juvenile and adult animals, one series was immediately mounted on eggwhite subbed slides, dried overnight at room temperature, and processed histochemically for synaptic zinc. For juveniles, another full series was processed for cytochrome oxidase using the modified protocol of Wong-Riley (1979): incubation for 2–8 h at 40 °C with 3 % sucrose, 0.015 % Cytochrome C, 0.015 % catalase and 0.02 % diaminobenzidine in 0.1 M PB, The remaining series for the adult animals was divided so that alternate sections were stained for myelin (Gallyas 1979) or cytochrome oxidase. Myelin-stained sections are not shown here.

Synaptic zinc histochemistry

Histochemical localization of synaptic zinc was revealed using a modification of the method described by Danscher (1982). This selenium-based histochemical method is specific for zinc in the brain that is localized to presynaptic vesicles of neurons that use zinc (Danscher et al. 1985; Frederickson 1989; Frederickson and Danscher 1988). The coincidence of the zinc distribution shown by silver amplification with that shown by specific zinc fluoroprobes con- firms that the labeled metal in the vesicles is zinc (TSQ, zincquin: Frederickson et al. 1992); this TSQ fluorescent method produces bright fluorescence when complexed with zinc, but not when complexed with other transition

metals such as iron or copper (Frederickson 2003). Briefly, slides were fixed in absolute alcohol for 15 min and allowed to dry at room temperature. Sections were then immersed briefly in a 1 % gelatin solution and allowed to dry at room temperature. The sections were then reacted in the dark in a freshly prepared silver developing solution containing the following: 60 ml of 30% gum Arabic in dH2O,10 ml of 2.52g citric acid plus 2.35 g sodium citrate in dH2O at pH 4.0, 15 ml of 0.85 g hydroquinone in dH2O, and 15 ml of 0.11 g silver lactate in dH2O. Solutions were mixed in the order in which they were described. The sections were allowed to develop at room temperature in total darkness, and generally required 120–180 min for complete development. The development of the reaction was visually inspected every 30 min. Once the desired intensity was achieved, the reaction was terminated by rinsing the slides in warm water for 10 min to remove the gelatin coat and the outer silver deposit. Slides were allowed to dry at room temperature, and were then dehydrated in 100 % EtOH, cleared in xylene, and cover slipped with Permount. Sections from three animals without previous selenite treatment (negative controls) underwent silver amplification but showed no staining; the lack of staining was independent of age.

Areal and laminar boundaries

The architecturally defined features of visual cortical areas in the adult ferret (Innocenti et al. 2002) were utilized to aid in the identification of different areas. The borders of cor- tical areas in the adult were determined by comparing the pattern of staining in myelin, cytochrome oxidase (CO), and synaptic zinc stain. Areal boundaries in the juveniles were similarly determined by comparison of the CO and synaptic zinc

stain. Sections were examined and photographed with bright field illumination using a Nikon Eclipse Ti inverted scope at low power (49) lens. Contrast and brightness of photomicrographs were enhanced in image processing software (Adobe Photoshop CS5, v.12) for display purposes, but were otherwise unaltered. Images used for optical density measurements were not altered in any way.

Densitometric analysis

To quantitatively assess the developmental change in zinc staining, we measured the optical density of selected zinc- stained sections in areas 17, 18, 19, 21, and Suprasylvian (Ssy) at 5, 6, 8, 9, and 10 weeks postnatal, and in the adult. This was accomplished by randomly choosing a cortical column 300–500 μm wide from photomicrographs spanning all cortical layers from the pial surface to the white matter. At least one sample column was chosen from each of at least three sections in each area, at each age. Column images were imported into ImageJ (NIH, v.1.44) and contrast inverted. Optical density profiles were generated from these images; each value in these profiles represents the average gray scale value at each depth across the width of the column. Because of variation in overall staining intensity across animals due to different reaction times, tissue stainability, and other variables, we use the relative density of synaptic zinc to make quantitative comparisons. To calculate relative zinc density, plot profile values were smoothed with a boxcar average of every successive 20 pixels (1 pixel = 2.5 μm) in depth, and normalized to maximum intensity for each sample. We also used a second normalization whereby density values were produced by dividing each value by the mean white matter value for each section. White

matter optical density values were obtained from sample cortical columns (300–500 μm wide) that included the underlying white matter (approximately 150 μm below layer 6) in areas 17, 18, and Ssy. The white matter values obtained at each age below each area were similar, and were averaged together. We then calculated the mean minimum pixel value in the lightly stained region of layers IV and VI, and the mean maximum pixel value in layer V. Mean values were determined in the depth range encompassing the minimum or maximum value by ±5 pixels. The mean pixel intensity of the supragranular and infragranular layers was also calculated. The limits of layer IV, supragranular, and infragranular layers in the contrast-inverted images were judged by comparison with the original photomicrographs as well as the adjacent CO section. This allowed us to be confident of the identity of each layer examined, and precluded the possibility of intruding on adjacent layers.

All statistical analyses were performed in MATLAB (The Mathworks, Natick, MA). We used the Kruskal– Wallis test to assess statistical differences in mean optical density values among age groups and areas with a significance level of $p < 0.05$. Post hoc pair-wise comparisons between ages (in each area) and areas (at each age) were then computed using a Bonferroni correction.

2.4 Results

Synaptic zinc staining distinguishes visual cortical areas in adult and juvenile ferret brain.

Visual cortical areas in the adult ferret are readily distinguishable with the aid of several histochemical markers, such as those for myelin and cytochrome oxidase (CO).

The cytoarchitecture and myelination patterns of different visual areas in the adult ferret cortex have been well characterized (Innocenti et al. 2002; Cantone et al. 2005). Here, we demonstrate that synaptic zinc staining similarly differs among visual cortical areas, even in the juvenile cortex.

Areal boundaries and laminar features of zinc staining in adult and juvenile ferret visual cortex

Adult and 5-week-old

Areas 17 and 18 The distribution of synaptic zinc staining in the adult ferret visual cortex is illustrated in a representative semi-tangential section in Fig. 2.1a. The arrows mark areal boundaries. In general, intense synaptic zinc staining is observed in layers I, II, III, and V (though we note that layer 1 stains more intensely in areas 17 and 18 than in areas 19, 21, and Ssy); layer VI is only moderately stained, while layer IV is nearly devoid of zinc. The adjacent section stained for cytochrome oxidase (CO) (Fig. 2.1b) reveals similar locations of areal boundaries and illustrates the reciprocal nature of CO and synaptic zinc in layer IV; in areas 17 and 18 regions of low zinc staining generally correspond to those of high CO staining. A high power view of the laminar features of zinc staining in the adult is illustrated in Fig. 2.2a. Representative photomicrographs of columns

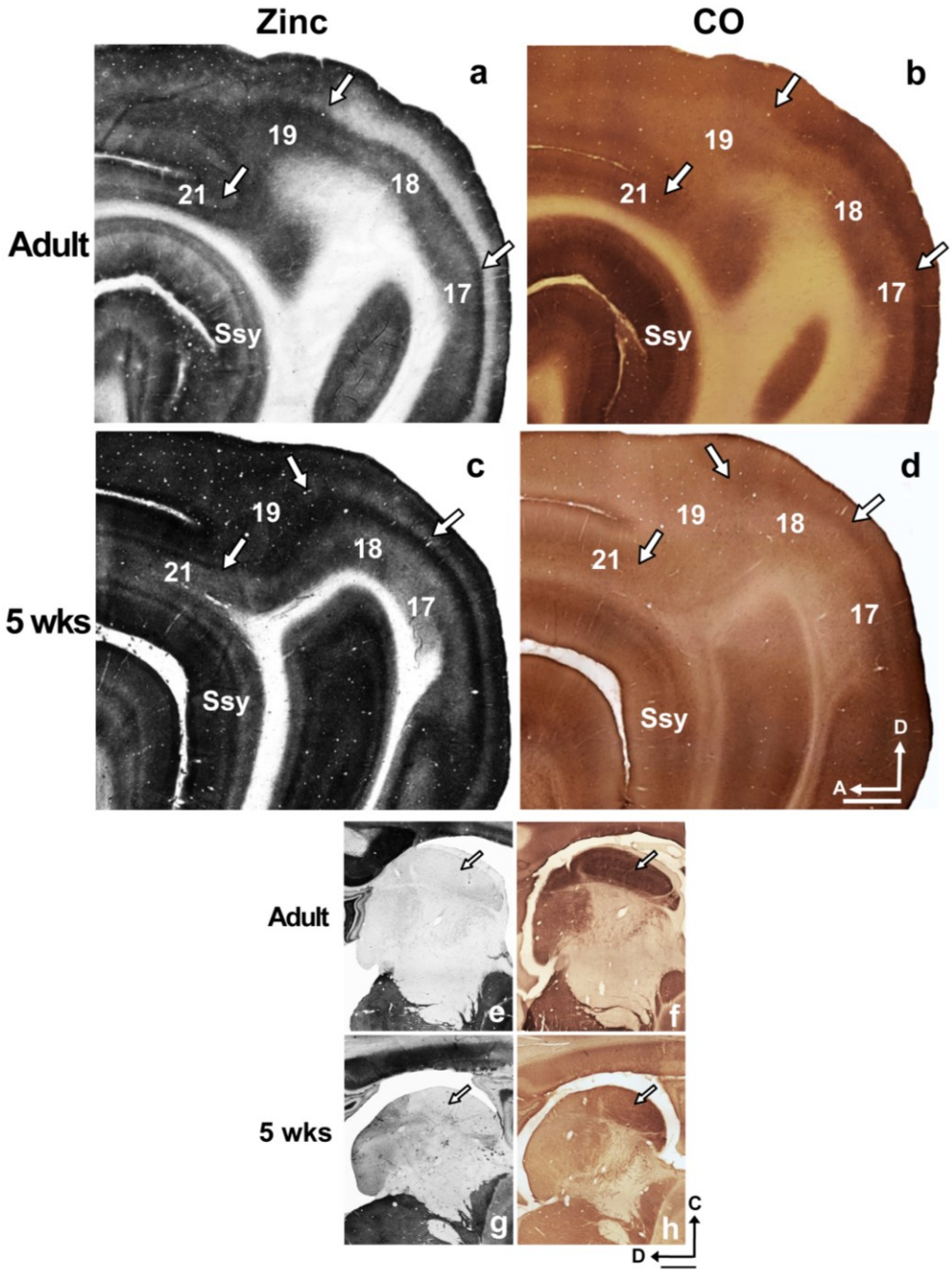

Figure 2.1. Synaptic zinc staining in the adult and juvenile ferret brain distinguishes different visual cortical areas. Photomicrographs of adjacent semi-tangential sections stained for a synaptic zinc or b cytochrome oxidase (CO) in the adult, and c synaptic zinc or d CO in the 5-week-old juvenile. Arrows mark areal boundaries. Photomicrographs of adjacent semi-tangential sections of thalamus stained for e synaptic zinc or f CO in the adult, and g synaptic zinc or h CO in the 5-week-old juvenile. Arrows indicate lateral geniculate nucleus. Ssy Suprasylvian cortex, A anterior, D dorsal. Scale bar 1 mm

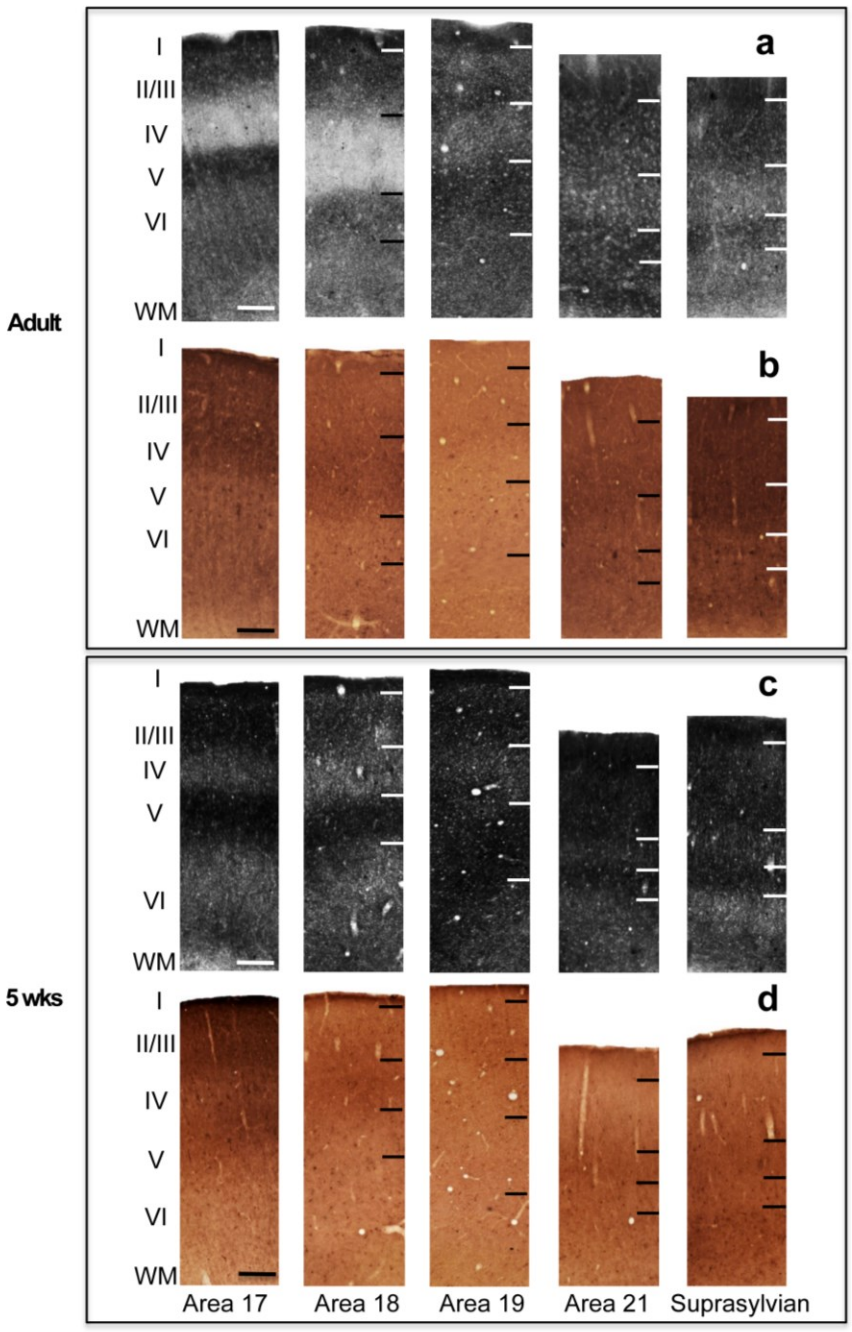

Figure 2.2. Variation of zinc and CO staining in different visual cortical areas in the adult and juvenile ferret. Photomicrographs of columns taken from adjacent sections in adult cortex stained for a synaptic zinc or b CO, and juvenile cortex stained for c synaptic zinc or d CO. Roman numerals indicate cortical layers (I–VI). Scale bar 200 μm.

from pia to white matter were taken from each visual cortical area. Area 17 is to the left with successively more rostral areas to the right. The cortical layers are indicated by the roman numerals. Primary visual cortex (area 17) and area 18 are unique in that layer IV stain very lightly (Figs. 2.1a, 2.2a). The lack of zinc staining in layer IV of area 17 contrasts with the intensely labeled layer IV band found in CO-stained material (Fig. 2.1b); the darkly stained layer IV in area 17 maintains a sharp border with layers III and V. The high power columnar photomicrographs of adjacent sections better illustrate the laminar CO reactivity pattern in each area in Fig. 2.2b.

Synaptic zinc staining in area 18 is qualitatively similar to area 17 with subtle laminar differences. Layers IV and V of area 18 stain even lighter than in area 17 (Figs. 2.1a, 2.2a). Layer VI is characterized by its bipartite staining with a moderately stained sublamina just below layer V, and a thin darkly stained sublamina just above the white matter. This is more clearly seen in the low power view in Fig. 2.1a. In CO preparations (Figs. 2.1b, 2.2b), the intense layer IV band characteristic of primary visual cortex is maintained in area 18 with a slight decrease in intensity. Moreover, the upper boundary of this band blurs with layer III, but maintains a sharp border with layer V (Fig. 2.2b). The distribution of synaptic zinc in a semi-tangential section at 5 weeks of age is depicted in Fig. 2.1c. The most striking difference in zinc staining between the 5-week-old and the adult is that the overall staining intensity is greater in the juvenile. Similar to the adult, the supragranular layers, and layer V of areas 17 and 18 stain very intensely, while layer VI is of moderate intensity. Layer I in all areas of the 5-week-old stains very intensely. Also similar to the adult is the subtle decrease in zinc intensity in area 18 relative to area 17 (Figs. 2.1c, 2.2c). Unlike the adult, however, layer IV of areas 17 and

18 is of moderate intensity. Similar to the adult, the intense CO band occupying layer IV characteristic of area 17 is maintained in area 18 with a slight decrease in intensity (Fig. 2.2d). Moreover, the upper boundary of this band blurs with layer III, but maintains a sharp border with layer V (Fig. 2.2d).

Area 19 The distribution of synaptic zinc in adult area 19 is different than in areas 17 and 18 in that there is less laminar variation (Figs. 2.1a, 2.2a), as well as a thinner and moderately stained layer IV that fills in. Layers IV and VI of area 19 are of similar intensity, while the supragranular layers and layer V stain intensely. In the complementary CO section (Figs. 2.1b, 2.2b), there is little CO staining in area 19, with a weak and inconsistent CO band in layers III and IV. Area 19 in the 5-week-old also has less laminar variation in zinc staining, but greater staining intensity than area 19 of the adult (Fig. 2.1c). As in the adult, area 19 of the 5-week-old is characterized by very low CO reactivity (Figs. 2.1d, 2.2d).

Area 21 Area 21 has a qualitatively similar synaptic zinc distribution as area 19 (Figs. 2.1a, 2.2a), with a very subtle increase in intensity in layer IV. However, the bottom of layer VI stains more intensely in area 21 than in area 19. In CO-stained material (Figs. 2.1b, 2.2b), area 21 is characterized by the reappearance of the layer III/IV band present in area 18. Area 21 of the 5-week-old shows a slight increase in laminar variation with a thinner layer IV that is comparable in zinc intensity to layer VI (Fig. 2.2c). In CO-stained material (Figs. 2.1d, 2.2d), area 21 is characterized by the reappearance of the layer III/IV band present in area 18.

Suprasylvian cortex (Ssy): Ssy lies immediately rostral and ventral to area 21, and lies along the posterior bank of the Suprasylvian sulcus (SsyS). In zinc-stained

sections, Ssy is characterized by a pale and thin layer IV, and pale layer VI. Layer V stains intensely and the supragranular layers are of variable intensity (Fig. 2.1a). In CO-stained material, it can be distinguished from adjoining areas mainly in the supragranular layers (Fig. 2.1b). The supra- granular layers are more intensely stained than the adjoining caudal posterior parietal (PPc) and lateral temporal visual areas.

The laminar variation in zinc staining characteristic of Ssy in the 5-week-old is comparable to that in area 21, with a slight decrease in zinc intensity in layer VI (Figs. 2.1c, 2.2c). The dark CO band reappears in layer IV of area 21 and Ssy. However, layer VI of Ssy shows more CO reactivity relative to that in area 21 (Fig. 2.2d). Although there is less laminar variation across areas and an overall greater staining intensity in the 5-week-old than in the adult, areal boundaries in the 5-week-old correlate well with boundaries observed in the adult (Fig. 2.1c).

As further confirmation of the observed staining pat- terns, Fig. 2.1e–h shows adjacent semi-tangential sections of the thalamus in the adult and 5-week-old stained for zinc or CO. The lack of zinc staining in the lateral geniculate nucleus of the thalamus, indicated by the arrow, is consistent with previous reports (Dyck et al. 1993; Valente et al. 2002). Taken together, the lack of staining in the LGN and white matter, and the observed areal and laminar differentiation of zinc staining, suggests that the dark zinc staining in visual cortex of younger animals is genuine.

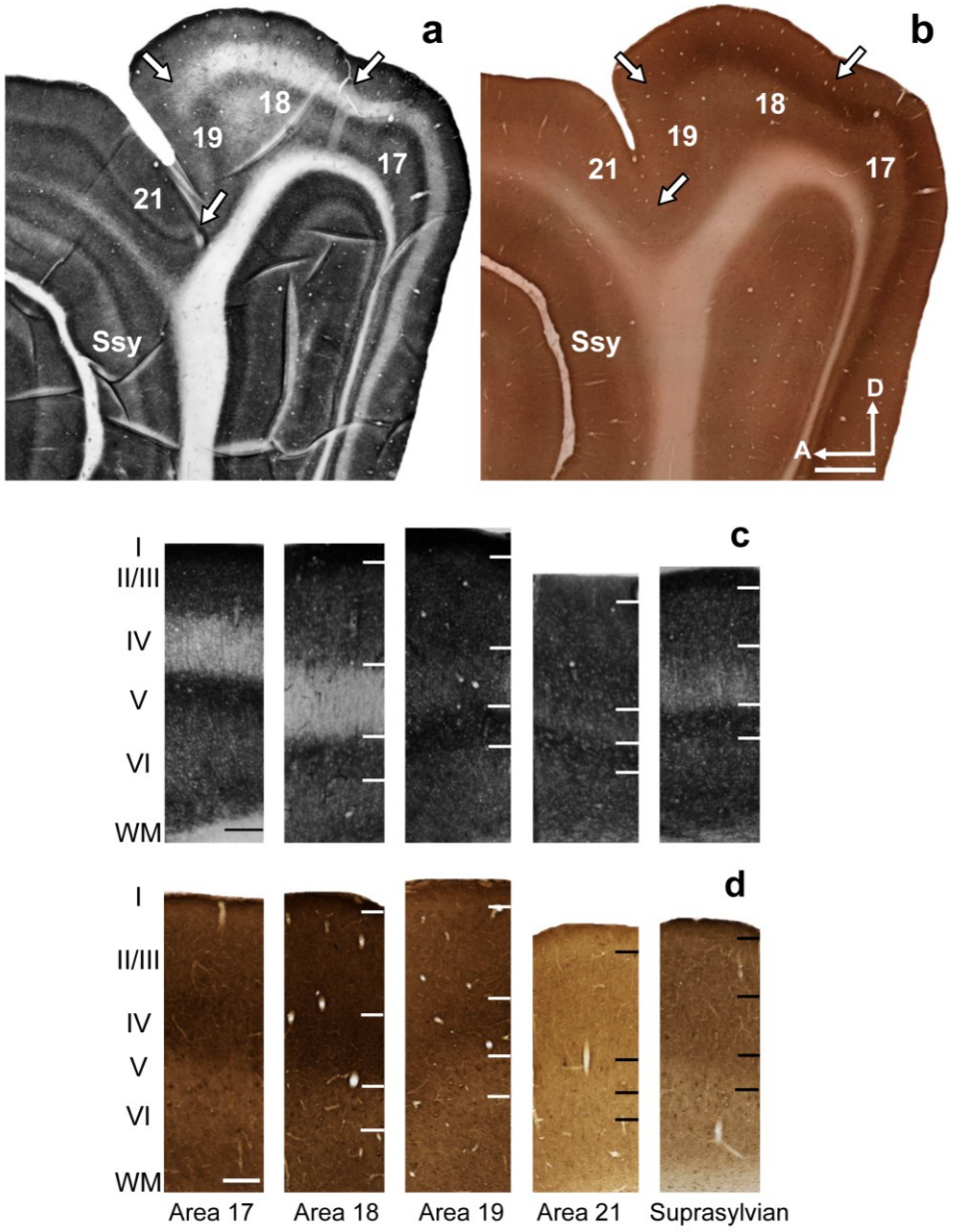

Figure 2.3. Synaptic zinc staining and laminar variation in the 9-week-old juvenile ferret brain distinguishes different visual cortical areas. Photomicrographs of adjacent semi-tangential sections stained for a synaptic zinc or b (CO). Photomicrographs of columns taken from adjacent sections stained for c synaptic zinc or d CO. Ssy Suprasylvian cortex, A anterior, D dorsal. Scale bar 1 mm

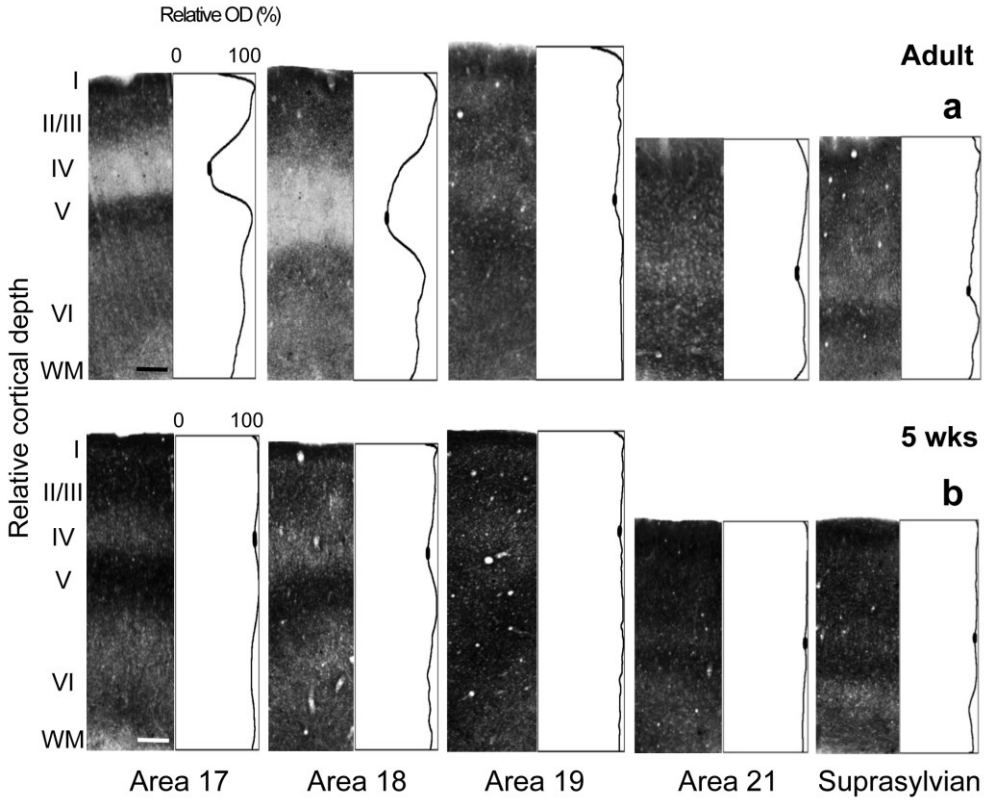

Figure 2.4. Laminar distribution of synaptic zinc in different visual cortical areas in the adult and juvenile ferret. Representative photomicrographs of columns through all cortical layers wit corresponding normalized optical density profiles in a adult and b 5-week-old. Low synaptic zinc density in layer IV of adult areas 17 and 18 is indicated by the trough in the profile plot. In each plot profile, filled ovals in the trough of layer IV indicate the values used to determine average minimum pixel intensity value. Scale bar 200 µm

Nine-week-old

Areas 17 and 18 The zinc staining and CO reactivity in the visual cortex of the 9-week-old are shown in Fig. 2.3a and b respectively. The semi-tangential zinc and CO sections in Fig. 2.3a were taken at a similar cortical depth to the representative sections from the 5-week-old and adult. By 9 weeks of age, the areal and laminar pattern of synaptic zinc across areas is nearly identical to that found in the adult. Columnar photomicrographs

taken from a section in a 9-week-old stained for synaptic zinc are shown in Fig. 2.3c. Similar to the adult (and unlike the 5-week-old), layer IV of areas 17 and 18 in the 9-week-old is only lightly stained. Further, layer IV of area 18 is slightly paler than layer IV of area 17. Areas 17 and 18 show stereotypical high intensity staining in the supragranular layers as well as in layer V, layer VI is of moderate intensity, while layer IV is of very low intensity.

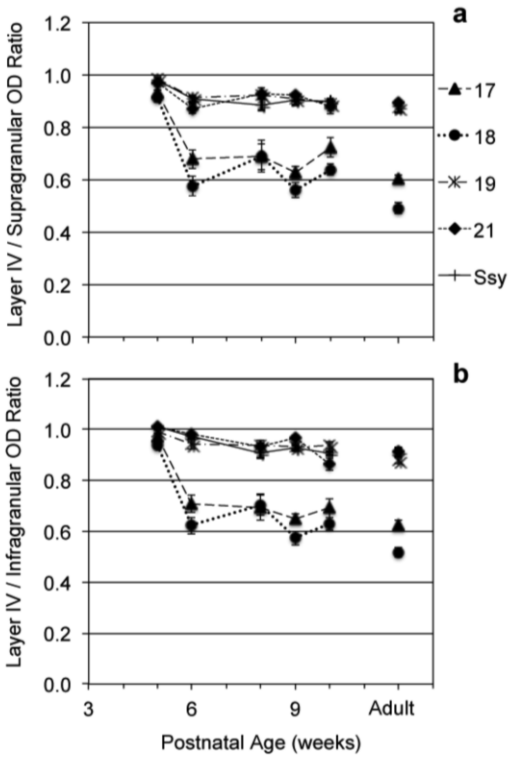

Figure 2.5. Ratio of synaptic zinc optical density in layer IV relative to that in the supragranular (a) and infragranular (b) layers in different visual cortical areas at different postnatal ages. Adult mean values are plotted on the right for comparison. Error bars represent ±SEM

Area 19 Similar to the adult, the distribution of synaptic zinc in area 19 of the 9-week-old is clearly different than in areas 17 and 18. There is less laminar variation (Fig. 2.3a, c) in area 19, and the most obvious difference is the thinner and moderately stained layer IV that fills in. In the complementary CO section (Fig. 2.3b, d), there is little CO staining in area 19, with a weak and inconsistent CO band in layers III and IV.

Area 21 The subtle laminar variation in zinc staining found in area 21 of the adult is also seen in area 21 of the 9-week-old (Fig. 2.3a, c). The complementary adjacent CO section shown in Fig. 2.3b similarly reveals a staining pattern shared between the 9-week-old and adult. The laminar pattern of CO reactivity unique to each area shared in the 9-week-old is better illustrated in Fig. 2.3d.

Suprasylvian cortex (Ssy) Both the laminar distribution of zinc staining and pattern of CO reactivity observed in the adult are also seen in the 9-week-old. The laminar variation in zinc staining characteristic of Ssy in the 9-week-old is comparable to that in area 21, with a slight decrease in zinc intensity in layer IV (Fig. 2.3a, c). The dark CO band reappears in layer IV of area 21 and Ssy. How- ever, layer VI of Ssy shows more CO reactivity relative to that in area 21 (Fig. 2.3d).

At all postnatal ages, areal transitions in zinc staining correlate well with those seen in CO staining. Furthermore, areal transitions seen in zinc staining and CO staining in the juvenile are consistent with those observed in the adult.

Quantitative changes in synaptic zinc density during development

We quantitatively assessed the distribution of synaptic zinc in all visual cortical areas at several postnatal ages; comparisons between the 5-week-old and adult revealed a significant decline in zinc density in layer IV. Optical density values were normalized to the maximum intensity value in that section. Plots of normalized optical density values were then constructed as a function of cortical depth. Each value in these profiles represents the average gray scale value at successive cortical depths. Columnar photomicrographs of representative adult zinc-stained sections and their

complementary normalized optical density plot profiles are shown in Fig. 2.4a. The most striking feature is the trough in the plot profile of areas 17 and 18 that corresponds to the low zinc density in layer IV. The filled-in ovals represent the mean minimum pixel intensity value. This significant drop in zinc density in layer IV of areas 17 and 18 is less obvious in areas 19, 21, and Ssy, and is demonstrated by the subtle dip within layer IV. Typically, the supragranular layers and layer V of areas 17 and 18 stain more intensely than layer VI.

In contrast, we find a significantly different pattern in the 5-week-old (Fig. 2.4b). Optical density measures reveal more intense zinc staining in layer IV of areas 17 and 18 (indicated by the subtle dip in the plot profile) relative to that found in the adult. However, zinc staining density in layer IV of areas 19, 21, and Ssy is only slightly greater in the juvenile relative to that in the adult. Both the supragranular and infragranular layers appear to have greater synaptic zinc density in the 5-week-old relative to the adult.

The greater dip in relative zinc staining density in adult layer IV might reflect different changes with age in absolute zinc staining in different cortical layers. We therefore compared the synaptic zinc optical density in layer IV of each area to the mean values in the supragranular and infragranular layers. We calculated ratios of zinc optical density in layer IV to the mean of that in both supra- and infragranular layers, and plotted values as a function of age (Fig. 2.5). The mean ratio of optical density in layer IV compared to the upper layers (LIV/supra) in all areas of the 5-week-old was 0.95, indicating nearly equal zinc staining in layers II/III and IV of these areas (Fig. 2.5a). By 6 weeks of age, the mean ratios in areas 17 and 18 (dashed and dotted lines,

respectively) decrease markedly to 0.62 ($p < 0.05$). However, there is a modest decline from 10 weeks until adulthood, suggesting a more protracted developmental process. The LIV/supra ratios in areas 19, 21, and Ssy (long dashed and dotted, short dashed, and solid lines, respectively) show a less prominent decline from 0.95 to 0.90 from 5 to 6 weeks of age. From 6 weeks until adulthood, the ratios in all areas remained essentially unchanged with no significant differences among ages.

Similar to LIV/Supra ratios, ratios of optical density between those in layer IV and infragranular layers (LIV/ Infra) are initially high (mean 0.98) in all areas of the 5-week-old (Fig. 2.5b). By 6 weeks of age, the ratios in areas 17 and 18 (dashed and dotted lines, respectively) show a marked decrease to 0.66 ($p < 0.05$). From 6 to 10 weeks of age LIV/infra ratios in areas 17 and 18 are relatively stable, with a gradual decline from 10 weeks until adulthood. Areas 19, 21 and Ssy (long dashed and dotted, short dashed, and solid lines, respectively) show a subtle decrease to 0.96 from 5 to 6 weeks of age, with ratios remaining unchanged thereafter, with no significant differences among ages. From 6 weeks of age, the LIV/infra ratios in areas 17 and 18 remain significantly different than the LIV/infra ratios in areas 19, 21, and Ssy ($p < 0.05$).

We further separately quantified the relative mean optical density of synaptic zinc in layer IV, supra- and infragranular layers to reveal whether the postnatal declines in (LIV/supra) and (LIV/infra) ratios were due to a decrease in optical density in specific layers. The decline in the (LIV/supra) and the (LIV/infra) ratios may be due to a decrease in zinc density in layer IV and an increase in zinc density in the supra- or infragranular layers. However, our findings show that the zinc density decreases with age in all layers, though most in layer IV.

Unlike the values obtained previously from the LIV/ Supra and LIV/Infra ratios whereby each normalized plot profile value was divided by the mean value in the supra-granular or infragranular layers, the relative mean optical density in LIV, supragranular, and infragranular layers is simply normalized to the highest pixel value in each sample. The mean relative optical density of synaptic zinc in layer IV of all visual areas is plotted as a function of age in Fig. 2.6a. Typically, the mean relative layer IV optical density in all areas of the 5-week-old was high (94 %). By 6 weeks of age, mean relative optical density in layer IV of areas 17 and 18 (dashed and dotted lines, respectively) decreased to 60% ($p < 0.05$). From 10 weeks until adulthood we observe a gradual decrease in mean relative optical density in layer IV of areas 17 and 18, suggesting a longer maturation phase. Areas 19, 21, and Ssy (long dashed and dotted, short dashed, and solid lines, respectively) showed a less prominent yet statistically significant ($p < 0.05$) drop in mean relative optical density in layer IV from 5 to 6 weeks, as well as a slow decrease from six weeks until adulthood. Therefore, it appears that zinc staining in layer IV of areas 17 and 18 decreases more than in layer IV of areas 19, 21, and Ssy. From 6 weeks until adulthood, mean relative optical density in layer IV remains unchanged in areas 19, 21, and Ssy. At all ages examined, the mean relative optical densities in layer IV of areas 17 and 18 are significantly lower ($p < 0.05$) than in layer IV of areas 19, 21, and Ssy.

The relative optical density in the supragranular layers initially averages 97 % in all areas of the 5-week-old (Fig. 2.6b). All areas show a subtle insignificant decrease in relative optical density from 5 to 6 weeks of age (to a value of 94 %). From 6 weeks to adulthood, relative supragranular optical density values appear essentially unchanged.

Similarly, relative zinc optical densities in the infragranular layers in all areas of the 5-week-old are high (95 %) (Fig. 2.6c). By 6 weeks of age, areas 17 and 18 exhibit a similarly modest, yet significant decrease in relative optical density in their infragranular layers ($p < 0.05$), while areas 19, 21, and Ssy show a subtle and insignificant decrease in relative optical density in their infragranular layers. It therefore appears that the developmental decline in the LIV/supra and LIV/infra ratios is largely due to the decrease in the relative optical density of zinc in layer IV, with a minor contribution from the decline in relative optical density of zinc in the supragranular and infragranular layers.

We sought to confirm the major decline in relative zinc density in layer IV as well as the minor decline in the supra- and infragranular layers of all areas by normalizing optical density values of synaptic zinc to the mean white matter (WM) value in each sample. The mean white matter value serves as a baseline measure against which gray matter values could be compared. The relative optical density values reflect the proportion of zinc density relative to the maximum pixel value in each section. Maximum pixel intensity may be the same for some ages; revealing the WM-normalized values with age, thus seems more informative as it allows us to unequivocally assert that overall staining intensity is greater in the juvenile, and that the decline in zinc density in layer IV is most pronounced in areas 17 and 18. We therefore calculated WM-normalized optical density values by dividing each plot profile value by mean white matter (WM) value in each section. We did not observe a developmental change in the white matter values. In fact, white matter values were very similar across all examined

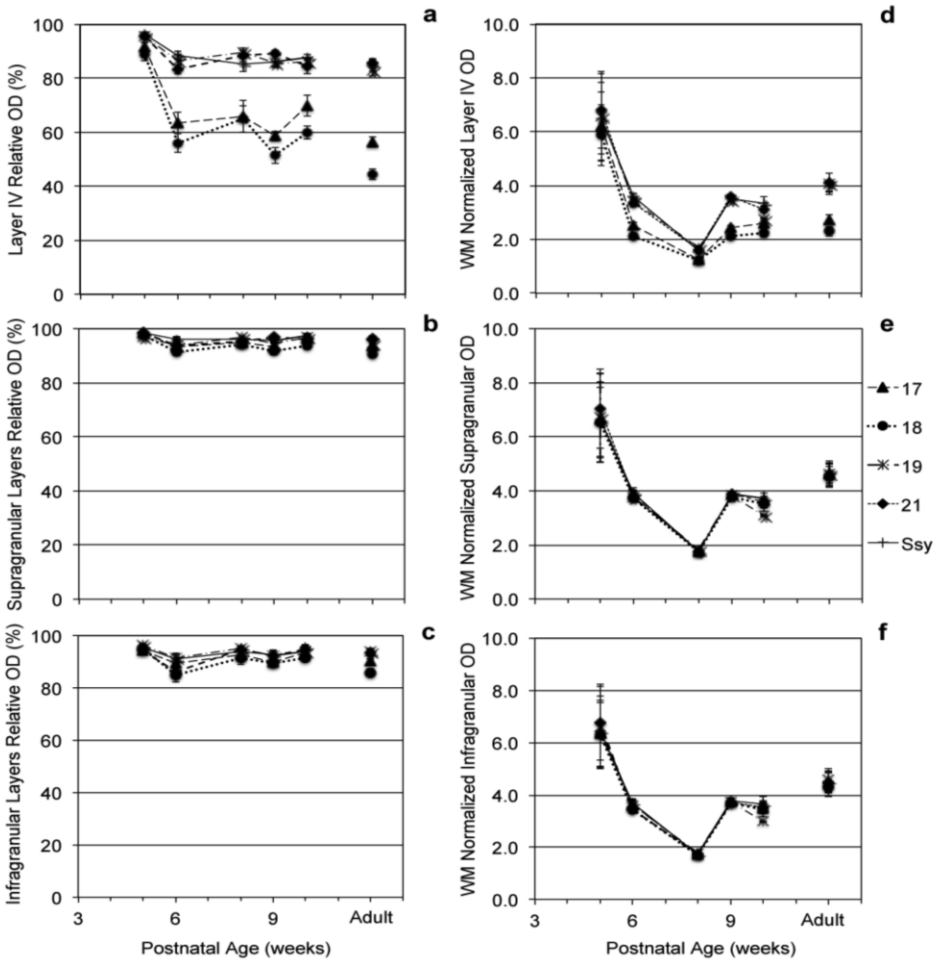

Figure 2.6. Average normalized synaptic zinc optical density (OD) in layer IV, supragranular II/III, and infragranular V/VI (a–c), and average white matter (WM) normalized synaptic zinc (OD) in layer IV, supragranular II/III, and infragranular V/VI (d–f) in different visual cortical areas at different postnatal ages. Adult mean values are plotted on the right for comparison. Error bars represent ±SEM

ages, except at 8 weeks of age. This is why we observe a dip in optical density in the gray matter from 6 to 8 weeks of age. Figure 2.6d shows the WM-normalized optical density values in layer IV as a function of age. Like the relative optical density values in Fig. 2.6a, the WM-normalized values in layer IV of all areas in the 5-week-old were relatively high (mean 6.4). By 6 weeks of age, WM-normalized mean optical density values in areas 17 and 18 (dashed and dotted lines, respectively) drop significantly to 2.3, while areas 19, 21, and Ssy (long dashed and dotted, short dashed, and solid lines, respectively) showed a less prominent, yet still, significant drop in mean optical density in layer IV (mean 3.4).

The WM-normalized mean optical density value in the supragranular layers of all areas of the 5-week-old is 6.7 (Fig. 2.6e). All areas show a similarly significant decrease in optical density at 6 weeks of age (mean 3.8). Similarly, Fig. 2.6f shows that the WM-normalized optical density values in the infragranular layers in all areas of the 5-week-old are high (mean 6.5), but undergo a significant decline by 6 weeks of age (mean 3.6). These data corroborate our previous results, and show that the rate and magnitude of decline in the optical density of both the infragranular and supragranular layers are comparable across all five areas.

2.5 Discussion

We have shown that synaptic zinc staining can be used to distinguish visual areas in the adult and developing ferret cerebral cortex. Although zinc staining in the juvenile is darker with less obvious laminar variation than adults, the laminar pattern is discernible; areal boundaries were consistently identifiable and correlated well with

boundaries found in the adult. In both juvenile and adult ferret, laminar staining patterns differ among areas; this differs among species. For example, our results show that layer I is dark in all areas in young animals, and darker in areas 17 and 18 than in 19, 21, and Ssy in the adult. Layer I in adult cat area 17 is dark (and distinguishable from layer II), but is dark and indistinguishable from layer II in areas 18 and 19 (Dyck et al. 1993). Brown and Dyck (2004) showed that layer I stains intensely in multiple cortical areas of the mouse forebrain, but layer Ia is zinc-poor in rat S1 (Land and Shamalla-Hannah 2002) and macaque TEO (Ichinohe et al. 2010). Therefore, it appears that regional and laminar differences are species specific.

To our knowledge, this is the first study to simultaneously investigate the developmental trajectory of zinc circuits in multiple visual cortical areas. We have shown that synaptic zinc staining in all layers of all five areas studied declines dramatically and on a broadly similar timecourse. By 6 weeks of age, we observe a significant decline in visual cortical synaptic zinc; this decline was most pronounced in layer IV of areas 17 and 18, with much less change in higher-order extrastriate areas during the important period in visual cortical development following eye opening. Synaptic zinc is a calcium- and activity- dependent neuromodulator implicated in synaptic function and plasticity (for review see Nakashima and Dyck 2009), and thus likely to play a key role in experience-dependent reorganization of visual circuits.

Previous studies have demonstrated the use of zinc histochemistry in distinguishing cortical areas in adult mouse (Garrett et al. 1991, 1994; Brown and Dyck 2004), developing and adult rat (Pérez-Clausell 1996; Valente et al. 2002), and developing and adult cat (Dyck et al. 1993). We demonstrate here that zinc

histochemistry similarly distinguishes cortical areas in the developing ferret visual cortex. While visual cortical areas in the adult ferret cortex may easily be distinguished based on cyto-, chemo- and myeloarchitecture, it is more difficult to do so in young ferrets as the myelination of visual cortical areas is not complete until the end of the second postnatal month (Barnette et al. 2009). Another criterion used to identify cortical areas is the connectional pattern unique to each area (Kaas 2002). Synaptic zinc histochemistry can be interpreted as another indicator of an area's connectional pattern. This is so because the laminar zinc distribution unique to each area reflects a particular set of afferents.

Zinc histochemistry, like other histochemical markers, at some areal boundaries reveals transition zones and not necessarily sharp boundaries, but one can still distinguish areas reliably. Furthermore, areal boundaries we observe are broadly consistent with previous studies (Homman-Ludiye et al. 2010; Innocenti et al. 2002). Zinc histochemistry may prove useful in other cortical areas or sensory systems, although with some limitations. Many studies have reported that levels of synaptic zinc can be rapidly and dynamically regulated in conditions of sensory deprivation (Brown and Dyck 2002; Dyck and Chaudhuri 2003), so use of zinc as an areal marker necessarily assumes normal visual experience.

What circuits are being revealed?

In the adult ferret, layer IV of areas 17 and 18 receives a substantial LGN input, while areas 19, 21, and Ssy do not. The relative lack of zinc staining in layer IV of adult areas 17 and 18 presumably reflects the lack of zinc in geniculocortical terminals

(Casanovas-Aguilar et al. 1998; Brown and Dyck 2004). The intense zinc staining in layer IV of juvenile ferret areas 17 and 18 suggests a developmental loss of zinc from thalamocortical afferents; this is consistent with Ichinohe et al.'s (2006) report of transient presence of zinc in thalamic afferents to rat barrel cortex. Layer IV of areas 19, 21 and Ssy is instead largely occupied by feedforward corticocortical terminals. Corticocortical terminals have been shown to sequester zinc (Garrett et al. 1992; Casanovas-Aguilar et al. 1995, 1998; Casanovas- Aguilar and Miro-Bernie 2002; Brown and Dyck 2004). Consistent with this finding, the relatively high zinc staining we observe in layer IV of these areas suggests that corticocortical feedforward input terminals are rich in synaptic zinc (though we do note that layer IV in area 18 appeared to stain less intensely for zinc than area 17). Our results suggest that there is either a decrease in the number of thalamocortical terminals in layer IV through postnatal development, or a decrease in the proportion of those terminals containing synaptic zinc, or a decrease in the amount of zinc in each terminal.

Alternatively, the dramatic decline we observe in synaptic zinc in layer IV of areas 17 and 18 could also be a consequence of the loss of early functional inputs from subplate neurons. Subplate neurons are a transient neuronal cell population that is integral in the functional development of thalamocortical connections and ocular dominance column formation (Ghosh and Shatz 1992; Kanold et al. 2003). They provide the first postsynaptic targets for afferent thalamocortical axons (McConnell et al. 1989; Molnar et al. 1998), and project into the cortical plate (Finney et al. 1998; Friauf et al. 1990). This projection is mainly glutamatergic (Finney et al. 1998). We speculate that the synaptic zinc staining we observe in layer IV of areas 17 and 18 reflects transient

input from subplate neurons that sequester high levels of zinc at their terminals; these could later be replaced by thalamic axons that sequester very little zinc at their terminals.

Using intracerebral injections of sodium selenite to retrogradely label zinc-positive neurons, Casanovas-Aguilar et al. (1995) examined the origin of zinc-positive pathways in rat visual cortex and revealed ipsilateral as well as callosal label. This study showed that labeled neurons were present in layers II–III and VI. Similarly, Brown and Dyck (2005b) showed that zinc-positive projections arise exclusively from within the cortex and reciprocally interconnect the mouse barrel cortex with other cortical and limbic regions. Their results demonstrated that the majority of zinc-positive projections to the barrel cortex arose from ipsilateral and callosal neurons, in the superficial and deep layers. Several lines of evidence suggest that a subset of intrinsic connections within an area is also zinc positive. Casanovas-Aguilar et al. (1998) mapped the zinc-positive afferents in rat neocortex by tracing zinc-positive projections to the visual cortex with intracerebral selenite injections. Selenite injections in several visual cortical areas (Oc1, Oc2M, and Oc2L) yielded a substantial number of zinc-positive neurons within each area. Brown and Dyck (2005b) similarly used selenite injections to reveal intrinsic connections in the superficial and deep layers of rat somatosensory cortex. Further evidence that zinc-positive neurons constitute a subset of intrinsic connections comes from Ichinohe et al. (2010). Using focal injections of sodium selenite into multiple visual cortical areas of the macaque ventral stream, they reported zinc-positive labeled intrinsic connections with an area-dependent laminar distribution.

Zinc-rich corticocortical projections appear to be a major component in the general

system of feedforward and feedback circuits. Retrograde tracing of zinc-positive neurons was also utilized by Casanovas-Aguilar and Miro- Bernie (2002). They examined the regional and laminar distribution of zinc-positive neurons in the rat visual cortex. Their findings revealed a laminar distribution of zinc-positive neurons typically observed in feedforward and feedback projections between multiple visual cortical areas. Zinc-positive projections from Oc1 to Oc2L (feed- forward projections) were numerous and arose preferentially from supragranular layers, whereas feedback projection neurons (from Oc2M to Oc2L, or from Oc2L to Oc1) were more abundant in the infragranular layers. Ichinohe et al. (2010) further reported zinc-positive neurons in several feedback pathways after selenite injections in areas V1, V4, and TEO of macaque visual cortex. Surprisingly, unlike the results obtained by Casanovas-Aguilar and Miro-Bernie (2002) showing that zinc-positive neurons were found in both the feedforward and feedback pathways in rat visual cortex, Ichinohe et al. (2010) report that feedforward pathways are zinc negative in macaque. Feedback projections have been shown to originate mainly from the infragranular layers and terminate densely in layer I (Rockland and Pandya 1979). This is consistent with the pattern of zinc staining we observe in the adult ferret visual cortex. Zinc staining in layer I of areas 17 and 18 is consistently more intense than in layer I of areas 19, 21, and Ssy. This presumably reflects corticocortical feedback projections to areas 17 and 18 from higher visual areas. Therefore, it seems that zinc-positive inputs are a subclass of callosal, intra- and interareal connections; the staining we observe reflects the axon terminals of these cells.

Comparison with other developmental events and other species

The ages examined in this study (5–10 weeks postnatal) were chosen to span the period just after eye opening (around P32 in ferret), during which emergent visual responses undergo much of their refinement to the adultlike state. These ages are approximately equivalent to: P12–P24 in a mouse, P15–P30 in a rat, P18–P56 in a cat, and E154– P65 in macaque monkey (extrapolated from Clancy et al. 2001). For example, mice typically open their eyes around P12, rats around P15, cats around P7, and macaque monkeys are born with their eyes open. The ferret brain is perhaps more immature at birth than cats and monkeys; for example, the differentiation and neurogenesis of layer IV of primary visual cortex, as well as the arrival and synapse formation of geniculate axons within layer IV occurs around P21 in the ferret (Johnson and Casagrande 1993; Jackson et al. 1989), but occurs prenatally in the monkey (Rakic 1977).

Several other aspects of cortical function appear to mature during this same postnatal period shortly after eye opening, over which we observe the major decline in zinc staining in layer IV of areas 17 and 18. (1) While ocular dominance columns are established early in the ferret (P16: Crowley and Katz 2000), the critical period for ocular dominance plasticity roughly coincides with the period of major decline in zinc staining in layer IV and continues until the end of the second postnatal month (Issa et al. 1999). (2) The development and refinement of horizontal projections in layers II/III of ferret visual cortex starts around P22 and continues until distinct adult-like clusters are observed at P45 (Durack and Katz 1996; Ruthazer and Stryker 1996); the refinement of this aspect of cortical circuitry appears adult-like just when zinc staining in the

superficial layers of ferret visual cortex first appears adult-like. (3) Chapman and Stryker (1993) showed that orientation selective responses are first detected as early as P23, with 25 % of cells in all layers showing some orientation selectivity. These immature responses continue unchanged until roughly postnatal week five, when the orientation preference of V1 neurons is qualitatively adultlike. (4) Li et al. (2006) used optical imaging and electrophysiological techniques to show that direction selectivity in ferret visual cortex emerges shortly after eye opening, and is qualitatively adultlike by P45. (5) Cortical feedback projections to ferret primary visual cortex also appear to refine to their adultlike state during the second postnatal month (Khalil and Levitt 2008).

The changes in synaptic zinc density we observe during the postnatal development of juvenile ferret visual cortex are consistent with previous studies in other species; cat primary visual cortex (Dyck et al. 1993), rat forebrain (Valente et al. 2002) as well as mouse somatosensory cortex (Czupryn and Skangiel-Kramska 1997; Ichinohe et al. 2006; Land and Shamalla-Hannah 2002). Synaptic zinc has been associated with various forms of experience dependent and developmentally regulated synaptic plasticity. In the rat somatosensory cortex, postnatal reduction in zinc staining is observed in the core of barrels, but high levels can be sustained by depriving the animal of sensory information through whisker trimming (Czupryn and Skangiel-Kramska 2003; Land and Shamalla-Hannah 2002). Furthermore, manipulating sensory experience in adults through whisker trimming causes a rapid and transient elevation of zinc in the core of the barrels (Brown and Dyck 2002, 2005a; Land and Akhtar 1999). Similar effects have been observed in the visual system of the monkey; monocular deprivation provokes a rapid elevation of zinc levels in the deprived eye ocular dominance bands

(Dyck and Chaudhuri 2003). An important unanswered question is the role of neurons that use zinc in the maturation, organization, and function of the cerebral cortex. In addition, it is of great interest to reveal if synaptic zinc is simply an indicator of the maturity of a region, or plays a key role in mediating the maturation process.

Asynchronous versus concurrent refinement of zinc-positive circuits in different cortical areas

While some aspects of cortical circuitry may refine con- currently in a number of areas, other aspects exhibit a hierarchical sequence of maturation with primary areas maturing before secondary and multisensory areas. Rakic et al. (1986) provided evidence in support of the concurrent maturation view. They showed that the rapid proliferation phase of cortical synaptogenesis and subsequent refinement occurs simultaneously in multiple and diverse regions of the cerebral cortex. In contrast, Conde´ et al. (1996) suggested asynchronous postnatal maturation of macaque cortical areas by showing that a subclass of local circuit neurons are adult-like first in primary sensory areas, but later in higher-order association areas. Bourne and Rosa (2006) provided more evidence in support of the concept of hierarchical maturation of cortical areas by noting that a subset of pyramidal neurons in V1, MT, S1, and A1 were histochemically mature at birth in New World monkeys, but not in higher-order association areas.

We have demonstrated reorganization of zinc circuits in ferret visual cortex during the second postnatal month, the period immediately after eye opening. Most strikingly, the reduction in zinc density is greater in layer IV of areas 17 and 18 than in

areas 19, 21, and Ssy. One could argue that our results reveal different rates of zinc circuit refinement in different areas as the rate and magnitude of change differs between areas 17 and 18 versus areas 19, 21, and Ssy. This presumably reflects changes in the relative weight of thalamocortical versus corticocortical inputs to those areas. However, although areas 17 and 18 show a greater decline in zinc staining than areas 19, 21, and Ssy, minimum staining intensity in all areas is reached at the same postnatal age (6 weeks), and therefore developmental trajectories among areas appear fundamentally similar in this respect. In contrast, another indicator of glutamatergic system maturation appears clearly asynchronous; different vesicular glutamate transporters (VGLuT1) and (VGLuT2), which are differentially expressed in particular brain circuits, have been shown to refine on different time scales (Liguz-Lecznar and Skangiel-Kramska 2007; Nakamura et al. 2005). Whether areas 17 and 18 share a different developmental timecourse for zinc staining than areas 19, 21, and Ssy, or all areas manifest a similar rate of change is open to interpretation.

References:

Barnette AR, Neil JJ, Kroenke CD, Griffith JL, Epstein AA, Bayly PV, Knutsen AK, Inder TE (2009) Characterization of brain development in the ferret via MRI. Pediatr Res 66(1):80–84

Beaulieu C, Dyck R, Cynader M (1992) Enrichment of glutamate in zinc-containing terminals of the cat visual cortex. NeuroReport 3(10):861–864

Bourne JA, Rosa MG (2006) Hierarchical development of the primate visual cortex, as revealed by neurofilament immunoreactivity: early maturation of the middle temporal area (MT). Cereb Cortex 3:405–414

Brown CE, Dyck RH (2002) Rapid, experience-dependent changes in levels of synaptic zinc in primary somatosensory cortex of the adult mouse. J Neurosci 22(7):2617–2625

Brown CE, Dyck RH (2004) Distribution of zincergic neurons in the mouse forebrain. J Comp Neurol 479(2):156–167

Brown CE, Dyck RH (2005a) Modulation of synaptic zinc in barrel cortex by whisker stimulation. Neuroscience 134(2):355–359

Brown CE, Dyck RH (2005b) Retrograde tracing of the subset of afferent connections in mouse barrel cortex provided by zincergic neurons. J Comp Neurol 486(1):48–60

Cantone G, Xiao J, McFarlane N, Levitt JB (2005) Feedback connections to ferret striate cortex: direct evidence for visuotopic convergence of feedback inputs. J Comp Neurol 487:312–331

Casanovas-Aguilar C, Miro-Bernie N (2002) Zinc-rich neurones in the rat visual cortex give rise to two laminar segregated systems of connections. Neuroscience 110(3):445–458

Casanovas-Aguilar C, Reblet C, Perez-Clausell J, Bueno-Lopez JL (1998) Zinc-rich afferents to the rat neocortex: projections to the visual cortex traced with intracerebral selenite injections. J Chem Neuroanat 15(2):97–109

Casanovas-Aguilar C, Christensen MK, Reblet C, Martinez-Garcia F, Pe´rez-Clausell J, Bueno-Lopez JL (1995) Callosal neurones give rise to zinc-rich boutons in the rat visual cortex. NeuroReport 6:497–500

Chapman B, Stryker MP (1993) Development of orientation selec- tivity in ferret visual cortex and effects of deprivation. J Neurosci 13(12):5251–5262

Clancy B, Darlington RB, Finlay BL (2001) Translating develop- mental time across mammalian species. J Neurosci 105(1): 7–17

Conde´ F, Lund JS, Lewis DA (1996) The hierarchical development of monkey visual cortical regions as revealed by the maturation of parvalbumin-immunoreactive neurons. Brain Res Dev Brain Res 96(1–2):261–276

Crowley JC, Katz LC (2000) Early development of ocular dominance columns. Science 290(5495):1321–1324

Czupryn A, Skangiel-Kramska J (1997) Distribution of synaptic zinc in the developing mouse somatosensory barrel cortex. JCN 386:652–660

Czupryn A, Skangiel-Kramska J (2003) Switch time-point for rapid experience-dependent changes in zinc-containing circuits in the mouse barrel cortex. Brain Res Bull 61(4):385–391

Danscher G (1982) Exogenous selenium in the brain: a histochemical technique for light and electron microscopic localization of catalytic selenium bonds. Histochemistry 76:4281–4293

Danscher G, Howell G, Pe´rez-Clausell J, Hertel N (1985) The dithizone, Timm's sulphide silver and the selenium methods demonstrate a chelatable pool of zinc in CNS: a proton activation (PIXE) analysis of carbon tetrachloride extracts from rat brains and spinal cords intravitall treated with dithizone. Histochem- istry 83:419–422

Durack JC, Katz LC (1996) Development of horizontal projections in layer 2/3 of ferret visual cortex. Cereb Cortex 6(2):178–183

Dyck RH, Chaudhuri A (2003) Experience-dependent regulation of the zincergic innervation of visual cortex in adult monkeys. Cereb Cortex 13(10):1094–1109

Dyck R, Beaulieu C, Cynader M (1993) Histochemical localization of synaptic zinc in the developing cat visual cortex. J Comp Neurol 329(1):53–67

Finney EM, Stone JR, Shatz CJ (1998) Major glutamatergic projection from subplate into visual cortex during development. J Comp Neurol 398(1):105-118

Frederickson CJ (1989) Neurobiology of zinc and zinc-containing neurons. Int Rev Neurobiol 31:145–238

Frederickson CJ (2003) Imaging zinc: old and new tools. Sci STKE 182:pe18

Frederickson CJ, Danscher G (1988) Hippocampal zinc, the storage granule pool: localization, physiochemistry, and possible func- tions. In: Morley JE, Sterman MB, Walsh JH (eds) Nutritional modulation of neural function. Academic Press, San Diego, pp 289–306

Frederickson CJ, Rampy BA, Reamy-Rampy S, Howell GA (1992) Distribution of histochemically reactive zinc in the forebrain of the rat. J Chem Neuroanat 5:521–530

Friauf E, McConnell SK, Shatz CJ (1990) Functional synaptic circuits in the subplate during fetal and early postnatal development of cat visual cortex. J Neurosci 10:2601–2613

Gallyas F (1979) Silver staining of myelin by means of physical development. Neurol Res 1(2):203–209

Garrett B, Slomianka L (1992) Postnatal development of zinc- containing cells and neuropil in the visual cortex of the mouse. Anat Embryol (Berl) 186(5):487–496

Garrett B, Geneser FA, Slomianka L (1991) Distribution of acetyl- cholinesterase and zinc in the visual cortex of the mouse. Anat Embryol (Berl) 184(5):461–468

Garrett B, Sørensen JC, Slomianka L (1992) Fluoro-gold tracing of zinc-containing afferent connections in the mouse visual corti- ces. Anat Embryol (Berl) 185(5):451–459

Garrett B, Osterballe R, Slomianka L, Geneser FA (1994) Cytoar- chitecture and staining for acetylcholinesterase and zinc in the visual cortex of the Parma wallaby (Macropus parma). Brain Behav Evol 43(3):162–172

Ghosh A, Shatz CJ (1992) Involvement of subplate neurons in the formation of ocular dominance columns. Science 255:1441–1443 Homman-Ludiye J, Manger PR, Bourne JA (2010) Immunohisto- chemical parcellation of the ferret (Mustela putorius) visual cortex reveals substantial homology with the cat (Felis catus). J Comp Neurol 518(21):4439–4462

Ichinohe N, Potapov D, Rockland KS (2006) Transient synaptic zinc-positive thalamocortical terminals in the developing barrel cortex. Eur J Neurosci 24(4):1001–1010

Ichinohe N, Matsushita A, Ohta K, Rockland KS (2010) Pathway-specific utilization of synaptic zinc in the macaque ventral visual cortical areas. Cereb Cortex 20:2818–2831

Innocenti GM, Manger PR, Masiello I, Colin I, Tettoni L (2002) Architecture and callosal connections of visual areas 17, 18, 19 and 21 in the ferret (Mustela putorius). Cereb Cortex 12(4):411–422

Issa NP, Trachtenberg JT, Chapman B, Zahs KR, Stryker MP (1999) The critical period for ocular dominance plasticity in the ferret's visual cortex. J Neurosci 19(16):6965–6978

Jackson CA, Peduzzi JD, Hickey TL (1989) Visual cortex develop- ment in the ferret. I. Genesis and migration of visual cortical neurons. J Neurosci 9:1242–1253

Johnson JK, Casagrande VA (1993) Prenatal development of axon outgrowth and connectivity in the ferret visual system. Vis Neurosci 10:117–130

Kaas JH (2002) Cortical areas and patterns of cortico-cortical connections. In: Cortical areas, unity and diversity. CRC press, Boca Raton, pp 179–191

Khalil R, Levitt JB (2008) Postnatal refinement of cortical feedback connections to ferret primary visual cortex. Society for Neuroscience Abstracts

Kanold PO, Kara P, Reid RC, Shatz CJ (2003) Role of subplate neurons in functional maturation of visual cortical columns. Science 301(5632):521–525

Land PW, Akhtar ND (1999) Experience-dependent alteration of synaptic zinc in rat somatosensory barrel cortex. Somatosens Mot Res 16(2):139–150

Land PW, Shamalla-Hannah L (2002) Experience-dependent plastic- ity of zinc-containing cortical circuits during a critical period of postnatal development. J Comp Neurol 447(1):43–56

Li Y, Fitzpatrick D, White LE (2006) The development of direction selectivity in ferret visual cortex requires early visual experi- ence. Nat Neurosci 9(5):676–681

Liguz-Lecznar M, Skangiel-Kramska J (2007) Vesicular glutamate transporters VGLUT1 and VGLUT2 in the developing mouse barrel cortex. Int J Dev Neurosci 25(2):107–114

Martinez-Guijarro FJ, Soriano E, Del Rio JA, Lopez-Garcia C (1991) Zinc-positive boutons in the cerebral cortex of lizards show glutamate immunoreactivity. J Neurocytol 20(10):834–843

McConnell SK, Ghosh A, Shatz CJ (1989) Subplate neurons pioneer the first axon pathway from the cerebral cortex. Science 245:978–982

Molnar Z, Adams R, Blakemore C (1998) Mechanisms underlying the early establishment of thalamocortical connections in the rat. J Neurosci 18:5723–5745

Nakamura K, Hioki H, Fujiyama F, Kaneko T (2005) Postnatal changes of vesicular glutamate transporter (VGluT)1 and VGluT2 immunoreactivities and their colocalization in the mouse forebrain. J Comp Neurol 492(3):263–288

Nakashima A, Dyck RH (2009) Zinc and cortical plasticity. Brain Res Rev 59:347–373

Pe´rez-Clausell J (1996) Distribution of terminal fields stained for zinc in the neocortex of the rat. J Chem Neuroanat 11(2):99–111

Rakic P (1977) Prenatal development of the visual system in rhesus monkey. Phil Trans R Soc Lond B 278(961):245–260

Rakic P, Bourgeois JP, Eckenhoff MF, Zecevic N, Goldman-Rakic PS (1986) Concurrent overproduction of synapses in diverse regions of the primate cerebral cortex. Science 232(4747):232–235

Rockland KS, Pandya DN (1979) Laminar origins and terminations of cortical connections of the occipital lobe in the rhesus monkey. Brain Res 179(1):3–20

Ruthazer ES, Stryker MP (1996) The role of activity in the development of long-range horizontal connections in area 17 of the ferret. J Neurosci 16(22):7253–7269

Valente T, Auladell C, Pe´rez-Clausell J (2002) Postnatal development of zinc-rich terminal fields in the brain of the rat. Exp Neurol 174(2):215–229

Wong-Riley M (1979) Changes in the visual system of monocularly sutured or enucleated cats demonstrable with cytochrome oxidase histochemistry. Brain Res 171(1):11–28

CHAPTER 3
Developmental remodeling of corticocortical feedback circuits in ferret visual cortex

3.1 Abstract

Visual cortical areas in the mammalian brain are linked through a precise system of interareal feedforward and feedback connections, which presumably underlie different visual functions. We characterized the refinement of feedback projections to primary visual cortex (V1) from multiple sources in juvenile ferrets ranging in age from four to ten weeks postnatal. Our goal was to determine whether the refinement of different aspects of feedback circuitry from multiple visual cortical areas proceeds at a similar rate in all areas. We made injections of the neuronal tracer cholera toxin B (CTb) into V1, and mapped the areal and laminar distribution of retrogradely labeled cells in extrastriate cortex. Around the time of eye opening at four weeks postnatal, the retinotopic arrangement of feedback appears essentially adultlike; however, Suprasylvian cortex supplies the greatest proportion of feedback, whereas area 18 supplies the greatest proportion in the adult. The density of feedback cells and of the supragranular feedback contribution declined in this period at a similar monotonic rate in all cortical areas. The regularity of cell spacing, the proportion of feedback arising from layer IV, and the tangential extent of feedback in each area all remained essentially unchanged during this period, except for the infragranular feedback source in area 18 which expanded. Thus, while much of the basic pattern of cortical feedback to V1 is present before eye opening, there is major synchronous reorganization in its areal, tangential, and laminar organization after eye opening, suggesting a crucial role for visual experience in this remodeling process

3.2 Introduction

The mammalian brain is immature at birth, with major developmental events such as the establishment of basic neural circuitry and its subsequent refinement ensuing during the postnatal period. A major developmental strategy commonly used by many developing corticocortical and intracortical pathways is the initial overproduction of projections, followed by the selective removal of a subset to yield the mature adult pattern (Changeux and Danchin, 1976; Rakic et al., 1986; Innocenti and Price, 2005). Intracortical connections within primary visual cortex (V1) of several species (cat, ferret, human, monkey) undergo substantial postnatal refinement (Huttenlocher, 1979; Price, 1986; Callaway and Katz, 1990; Burkhalter et al., 1993; Coogan and Van Essen, 1996; Durack and Katz, 1996; Ruthazer and Stryker, 1996). Similarly, corticocortical connections between different mammalian visual cortical areas have been shown to refine and reorganize as well (Dehay et al., 1988; Price and Blakemore, 1989; Price and Zumbroich, 1989; Barone et al., 1995; Batardiere et al., 1998, 2002). The anatomical refinement of cortical circuits presumably underlies the maturation of neuronal physiological properties, and is thus one indicator of functional maturity. We are particularly interested in characterizing the postnatal refinement of interareal connections in the ferret visual cortex; specifically we wish to know whether feedback projections to V1 from multiple extrastriate areas refine with a similar postnatal timecourse. Differential development of distinct cortical circuits could underlie the known differences in the rate at which various perceptual abilities mature (Harwerth et al., 1986; Lewis and Maurer, 2005; Braddick and Atkinson, 2011).

There are currently two prevailing theories that describe the developmental sequence of anatomical and functional maturation. The hierarchical theory holds that the maturation of a given functional property or anatomical circuit proceeds in a sequential fashion with more basic functional properties or anatomical circuits maturing before more complex ones. The earliest accounts supporting the concept of hierarchical maturation of cortical areas come from classic studies by Flechsig (1901) on the human brain. He showed that during the first years of postnatal life, pathways to the primary motor, somatosensory, visual, and auditory cortical areas are the first to be myelinated. Consistent with this, Condé et al. (1996) showed that parvalbumin expression in a subset of GABAergic neurons in the monkey brain appears during development in a sequential fashion across the visual cortical hierarchy - first in V1, and later in more rostral areas. More recent in vivo imaging studies in humans have also confirmed Flechsig's findings, showing similar regional differences in the rate of cortical maturation (Girard et al., 1991; Paus et al., 2001). Zhang et al. (2005) provided physiological evidence supporting the hierarchical theory. The authors reported that the receptive field surround of monkey V1 neurons is mature by four weeks of age, whereas in V2 the receptive field surround size and surround suppression were not adultlike until after eight weeks of age. In contrast, the concurrent theory posits that functional or anatomical aspects of multiple brain regions mature in concert. This theory derives from anatomical data in monkey suggesting that synaptogenesis and synapse elimination occur concurrently in multiple diverse regions of cerebral cortex (Rakic et al., 1986; Bourgeois et al., 1994). What remains unclear is which aspects of cortical function and circuitry mature synchronously, and which in a sequential or hierarchical fashion.

Several aspects of corticocortical connectivity refine postnatally, such as the laminar and tangential distribution of cells furnishing interareal projections. In cats and monkeys, there is a developmental refinement of the topography of interareal projections, a decline in the infragranular contribution to feedforward projections (also observed in the rat by Coogan and Burkhalter, 1988), and a decline in the supragranular contribution to feedback projections (Price and Blakemore, 1985; Kato et al., 1991; Price et al., 1994; Barone et al., 1995; Batardiere et al., 1998, 2002). The selective reduction in supragranular feedback cells leads to a unique laminar distribution characteristic of each area in the adult. Feedforward and feedback pathways may not refine similarly. Batardiere et al. (2002) suggested a difference in the development of different types of cortical connections of primate area V4; the laminar distribution of the feedforward pathway from area V2 to V4 is adultlike early in prenatal life, while feedback projections from V4 to V2 undergo extensive remodeling. Burkhalter (1993) demonstrated a similar developmental sequence of events in human infants; the laminar termination pattern of feedforward connections matures before that of feedback connections. Likewise, Berezovski et al. (2011) examined the development of feedforward and feedback connections in mouse visual cortex between V1, anterolateral area (AL), and lateromedial area (LM). Feedforward connections were present at the earliest time point examined (postnatal day 2), while feedback connections were not detectable until postnatal day 11. Thus, changes during postnatal developmental in certain aspects of the interareal connectivity of primary visual cortex have been reported.

What is lacking is simultaneous quantitative descriptions of the organization of the feedback pool to V1 from multiple visual areas at different postnatal ages; this will clarify whether there is synchronous versus sequential development of cortical areas and the links among them. Here we describe the developmental refinement of feedback projections arising from multiple visual areas in ferret visual cortex from four weeks to ten weeks postnatal. We have quantified different anatomical aspects related to the topography of feedback projections. Specifically, we are interested in determining whether different anatomical features of feedback circuitry refine simultaneously in all visual cortical areas. We find that the overall retinotopic pattern of feedback connections from extrastriate cortex is qualitatively adultlike as early as 4 weeks of age (in the period just before eye opening), though there are differences from the adult in areal, tangential, and laminar distribution; these all refine in the weeks after the eyes open. Significantly, the refinement of different anatomical aspects of cortical feedback maturation appears to follow a similar developmental timecourse in all visual cortical areas. Our results suggest that while the overall pattern of feedback projections from extrastriate cortex to primary visual cortex is present before eye opening, the fine scale refinement of the spatial layout of feedback connections in multiple visual areas occurs largely synchronously, and requires early postnatal visual experience.

3.3 Materials and Methods

Anatomical tracer injections:

We studied 16 female sable ferrets (Mustela putorius furo) at six postnatal ages: 4 weeks (n=3), 5 weeks (n=3), 6 weeks (n=2), 7 weeks (n=2), 8 weeks (n=3), and 10 weeks (n=3). Animals were obtained from Marshall Farms (North Rose, NY); kits were housed with the jill under a 12 h light/dark cycle. All procedures conformed to National Institutes of Health guidelines. Prior to surgery, ferrets were sedated with an intramuscular injection of ketamine (25 mg/kg) and xylazine (2 mg/kg). The animal's head was fixed in a stereotaxic apparatus, and secured with ear bars. The animals were respired using a pump, which delivered a mixture of 1%-2% isoflurane, in O_2. A small mask was placed on the nose and snout to administer isoflurane throughout the surgery. The EKG, pulse, tissue oxygenation, and rectal temperature were continuously monitored throughout the rest of the surgery, and maintained at appropriate levels. During a sterile surgery, Lidocaine HCl was injected into the scalp prior to incisions. The scalp was retracted, and a craniotomy and durotomy were performed on either the left or right hemisphere. Cholera toxin B subunit (CTb: List Biological Laboratories, Campbell CA) was reconstituted in 0.1M potassium phosphate buffer (1%, pH.6), and either pressure injected or delivered with current into primary visual cortex. Iontophoretic injections using glass micropipettes (aperture 10-15 µm) were made by passing current at 2 µA for 10 minutes with a 7-second on-off cycle at two cortical depths to ensure that the extent of the injection site spanned both the upper and lower layers of the cortex. This method of injection typically yields an injection core with a

diameter of 800-1000 µm. Pressure injections were delivered with a Picospritzer (Parker Hannifin, Fairfield, NJ), using glass micropipettes (aperture 30-40 µm) at two cortical depths with 2 X 10 msec pulses at each location. Both injection methods yielded comparable injection core volumes.

Following the injections, craniotomies were filled with sterile Gelfoam. Lidocaine was injected into the wound margins before the scalp was sutured, and an intramuscular injection of a broad spectrum antibiotic (ampicillin: 25 mg/kg) and analgesic (buprenorphine: 0.05 mg/kg) was administered for 2 days postoperatively. After a survival period of five to seven days, the animals were sedated with ketamine (25 mg/kg) + xylazine (2 mg/kg), given an intraperitoneal injection of sodium selenite (15 mg/kg) for subsequent labeling of synaptic zinc, then euthanized with an intraperitoneal overdose of pentobarbital (100 mg/kg).

Tissue fixation and histological processing:

Animals were transcardially perfused with a 0.9% NaCl solution followed by a 4% paraformaldehyde in 0.1M phosphate buffer (PB) solution, then a 4% paraformaldehyde plus 10% sucrose solution. The brains were removed from the skull, then the posterior cortex was blocked and placed in a postfix solution of 4% buffered paraformaldehyde plus 30% sucrose for 2-3 hours. The brains were then placed into a 0.1 M PB solution with 30% sucrose for 2 days until they were sunk.

Frozen tangential or sagittal sections were cut at 40 microns using a sliding microtome. The sections were separated into four numbered series. The first and the third series were processed to reveal the CTb label using a modified version of the

standard CTb protocol (Angelucci et al., 1996; Cantone et al., 2005). All procedures were done on free-floating sections, and all solutions were made with 0.1M phosphate buffered saline (PBS) (pH 7.4). Sections were rinsed in PBS, incubated in a 1% H_2O_2 solution to eliminate endogenous peroxidase, and rinsed again in PBS. This was followed by a short incubation in 0.1M glycine solution, rinsed in PBS, then incubated overnight at 4° C in a blocking solution containing 4% normal rabbit serum (NRS), 2.5% bovine serum albumin (BSA), and 1% Triton-X solution or 4% fish gelatin to reduce non-specific staining. The sections were rinsed in PBS, then incubated for 48 hours in a solution containing a 1:5,000 dilution of goat anti-choleraganoid (primary antibody, List Biological Laboratories, Campbell CA), 2% NRS, 2.5% BSA, and 1% Triton-X. The sections were then rinsed in PBS, and incubated in a 1:200 dilution of biotinylated rabbit anti-goat IgG (secondary antibody, Vector Laboratories, Burlingame CA), 2% NRS, 2.5% BSA, and 2% Triton. After several rinses in PBS and a brief incubation in blocking solution, the tissue sections were incubated in a solution containing Standard Elite ABC Kit (Vector Laboratories, Burlingame CA). Finally the tracer was developed with diaminobenzidine, and sections were mounted on subbed slides, dehydrated and cleared in xylene, and coverslipped in Permount.

Sections from the remaining series were processed for cytochrome oxidase (CO) (Wong-Riley, 1979), Nissl substance, or synaptic zinc following the protocol described in Khalil and Levitt (2012). These were compared with adjacent CTb stained sections to assign cells to particular areas and layers.

Reconstruction of label:

We relied on the following criteria to ensure that our injections were restricted to area 17 and did not intrude onto area 18 or white matter. The laminar location of the injection core was visually inspected using adjacent sections stained for Nissl, CO, or synaptic zinc to ensure that none of our cases intruded on white matter. Injection core was defined as the uniform, densely labeled region of CTb. We observed a typical pattern of label in all the layers (A, A1, and C) of the lateral geniculate nucleus (LGN) following our area 17 injections. Consistent with previous reports (Baker et al., 1998), the density of labeled cells was greatest in the two A layers, but a small number of cells were also present in the C layers. In contrast, if the injection intruded on area 18, there would be many more cells in the C-layers of the LGN. Furthermore, the lack of extensive label in ventral cortex (which results from area 18 injections) was interpreted as further evidence that the location of our injections was indeed restricted to area 17. All the cases analyzed in this study had injection cores that were restricted to area 17 without intruding onto area 18 or white matter.

Section outlines from every fourth semi-tangential section containing CTb label were traced, and retrogradely labeled cells found within each visual area were plotted in the Neurolucida tracing and reconstruction program (MicroBrightField, Williston VT). Fiducial landmarks such as blood vessels were marked, and comparison of CTb tracings with adjacent CO, synaptic zinc, or Nissl stained sections was used for precise local alignment. CTb-labeled cells were then assigned to a cortical area and layer. Accurate laminar assignment of cells was further verified by measuring the distance from the pial surface to the bottom of particular layers and subsequently compared with

similar measurements in adjacent CO, synaptic zinc, or Nissl stained sections. Three-dimensional reconstructions of section outlines containing CTb label were generated by carefully stacking and aligning tracings of serial sections containing retrogradely labeled cells. Vascular landmarks and other anatomical features were used to accomplish precise alignment by pairing two consecutive tracings. Correct determination of laminar and areal boundaries was critical to our analysis. We have previously shown that visual cortical areas in juvenile ferrets may reliably be distinguished in sections stained for synaptic zinc (Khalil and Levitt, 2012); observed areal boundaries in zinc-stained sections were well correlated with adjacent CO sections and prior descriptions (Innocenti et al., 2002). Histochemical methods did not always reveal sharp areal boundaries, but rather showed transition zones. Therefore, cells found in transition zones were assigned to border zones 18/19 and 19/21. The proportion of cells that were assigned to border zones was less than 2% of the total pool of feedback cells and were therefore not included in subsequent figures.

We note that oftentimes, clusters of feedback cells were offset from one another, which further facilitated the assignment of cells to areas. Sections containing CTb-labeled cells or stained for CO, zinc, or Nissl were examined and photographed with bright field illumination using a Nikon Eclipse Ti inverted scope with a low power (4x) lens. Contrast and brightness of photomicrographs were enhanced in image processing software (Adobe Photoshop CS5, v.12) for display purposes, but were otherwise unaltered. All figures were assembled in Adobe Photoshop (CS5, v.12), and all line graphs and histograms were generated in MATLAB (The Mathworks, Natick, MA).

Cell counts and cell densities:

Because of variation in the absolute number of labeled cells in extrastriate cortex due to differences in injection core size and extent of laminar intrusion, we determined the proportion of labeled feedback cells in each area as a fraction of the total pool of labeled cells to more accurately reflect developmental changes in the distribution across areas. The relative proportion of labeled cells located in each visual area was determined by dividing the number of cells in a given visual area by the total number of labeled cells in extrastriate cortex. Similarly, the proportion of labeled cells located in the different layers of each area was determined by dividing the number of labeled cells in the supragranular or infragranular layers of a given area by the total number of labeled cells found within that area. We then computed supragranular to infragranular ratios (supra/infra) to determine the relative contribution of the upper vs. lower layers, and used this ratio as a measure to assess developmental changes in the contribution of each set of layers. We also determined the proportion of feedback to area 17 arising from layer IV of each extrastriate area. We determined the peak density of feedback cells in each area, defined in the region in each area with the highest density within a cluster of cells in any section of the reconstructed stack (this was often found in at least 5-6 sections in the stack). A circumscribed area that contained the highest peak density was subsequently delineated with a 200 μm diameter circle. We chose a small area to include the highest peak density in the middle of the cluster, and to exclude cells in the periphery of the cluster. The volume of each sample was then calculated by multiplying the area of the circle by the section thickness (40 μm). Peak density values were then calculated using the sample volumes obtained.

To further assess the spatial distribution of feedback cells, we assessed the distribution of nearest neighbor distances (NND) of labeled cells in a given visual area. The nearest neighbor distance represents the distance of a single cell to that of the closest adjacent cell in a 2D plane within that visual area. We determined nearest neighbor distances within a 300 μm diameter circle centered over a cluster of feedback cells. This region includes cells in the densest region of the cluster as well as those in the periphery. We separately computed nearest neighbor distances in the supra- and infragranular layers in each area, and constructed frequency histograms of these values. To assess developmental changes in the spatial distribution of nearest neighbor distances, we computed the median and third quartile values (Q3) in each area at each developmental age. The Q3 is the value below which 75% of the NND values lie.

Neuronal density was determined using Nissl-stained sections from areas 17, 18, 19, 21, and SSy at 4 and 6 weeks of age, as well as in adults. Using Neurolucida, columns encompassing a region of interest were drawn perpendicular to the pial surface, extending to the white matter. Each column contained a sample box superimposed on each of the five layers, except for layer 1, which is cell sparse. Sample boxes were 45 μm x 45 μm. Three sections were used from each animal and two to three samples were obtained from each section. Neurons were counted using a light microscope at 100x oil immersion. Neurons with a reliably distinct nucleolus were counted through the depth of each box, with an exclusion zone of 4 μm at the top and bottom of the section. To minimize over counting, nucleoli were counted if they fell entirely within the box, or touched the top and right sides; nucleoli touching the bottom and left sides of the counting box were excluded. Glial cells containing multiple granules

(lacking clear single nucleoli) were not counted. Section shrinkage in the z-plane varied from 50 to 75% and the resulting sample volumes were adjusted accordingly.

To more explicitly reveal an underlying regularity in the spatial distribution of nearest neighbor distances we also computed a "conformity ratio" (Cook, 1996), which reflects "the degree of conformity of the measured set of NNDs to their own mean value". This CR value is simply the mean of the NND divided by the standard deviation; the more regular the arrangement of neurons, the higher the CR. This ratio is immune to boundary effects as well as undersampling effects in the region of interest. To test if any of our NND distributions were significantly different from a random arrangement of neurons (at the $p<0.01$ significance level), we compared our values to Cook's calculations of critical values of conformity ratios (Figure 2, Cook 1996).

All statistical analyses were performed in MATLAB (The Mathworks, Natick, MA). Initially, Barlett's test was used to confirm that each data set had a normal distribution; we then assessed statistical differences between slopes (the slope of each line corresponding to the change with time of a particular measure in an area) by applying the ANCOVA (analysis of covariance) with a significance level of $p<0.05$. When a value of $p<0.05$ was obtained, post hoc pair-wise comparisons between slopes were then computed using a Bonferroni correction. Where appropriate, a non-parametric permutation test was used to address whether there was a significant correlation between other measured variables in each area and developmental age. The permutation test estimates the probability of obtaining our data by chance. Statistical testing consisted of randomly permuting the raw data points within a single visual area between different age groups 10,000 times (without replacement). On each iteration, a

random reassignment is accomplished and a correlation is computed. After many iterations, we compared the distribution of reshuffled correlations with our observed correlation. Our observed correlation was deemed significant if it resulted in a $p<0.05$. We used a more stringent criterion value of $p<0.01$ to test for a significant change in the conformity ratios. A permutation test was separately conducted for each visual area. To asses statistical significance among age groups, areas, and layers in our neuron density counts we used the Kruskal-Wallis test with a significance level of $p < 0.05$. Subsequent post hoc comparisons were computed using a Bonferroni correction when significance was observed.

3.4 Results

All injection cases are summarized in Table 1. The injection core was defined as the uniformly dense region of CTb label, with a mean diameter of 1020 μm at all ages studied. We confirmed that all injection sites were confined to area 17, and spanned all six layers without intruding on the white matter. This was verified by comparing tracings of the injection core with adjacent sections stained for CO, synaptic zinc, and Nissl substance; this allowed us to identify the areal borders between areas 17 and 18 in juvenile visual cortex (Innocenti et al., 2002; Khalil and Levitt, 2012). Correct identification of visual cortical areas in the juvenile was crucial to our analysis as one of our primary goals was to track simultaneously the postnatal refinement of feedback projections from multiple visual areas to primary visual cortex.

Table 1.1. Characteristics of injection cases

Age	Case	Core diameter (µm)	Core volume (mm^3)	Mean Core volume (mm^3)	Max DV extent (µm)	Max ML extent (µm)	Laminar intrusion	Total # labeled cells	Normalized # labeled cells	Mean # labeled cells
4 wks	219	800	0.32		900	480	Mostly SG/ very little IG	1180		
	220	900	0.42	1.156	1000	800	More SG/little less IG	2412	2271	2644
	247	1450	2.73		2300	1280	Equal uptake SG & IG	4340		
5 wks	231	1100	1.54		1500	1280	Equal uptake SG & IG	4912		
	241	900	1.03	1.193	1000	960	Mostly SG/ very little IG	3642	3225	3848
	249	1000	1.01		1500	960	Mostly SG/ some IG	2990		
6 wks	255	1100	1.26	1.92	1500	800	Equal uptake SG & IG	3683	6193	11890
	256	1500	2.58		2400	1280	Equal uptake SG & IG	8207		
7 wks	215	950	0.97	1.04	1600	800	Equal uptake SG & IG	4850	3668	3815
	248	900	1.11		1300	800	Mostly SG/ some IG	2779		
8 wks	200	850	0.46		800	640	Mostly SG/ some IG	1221		
	229	800	0.46	0.446	900	800	Mostly SG/ very little IG	2200	4626	2066
	235	700	0.42		1000	640	Mostly SG/ some IG	2778		
10 wks	250	1600	2.51		2300	1440	Equal uptake SG & IG	15351		
	251	600	0.21	1.34	700	480	Mostly SG/ very little IG	1677	4808	6443
	258	1000	1.30		1300	640	Mostly SG/some IG	2300		

Age	Case	Area 18 # cells %Supra/Infra	Area 19 # cells %Supra/Infra	Area 21 # cells %Supra/Infra	Area Ssy # cells %Supra/Infra	Area 18/19 border	Area 19/21 border
4 wks	219	228 / 0.62 / 0.33	136 / 0.46 / 0.54	273 / 0.24 / 0.75	535 / 0.42 / 0.33		
	220	850 / 0.65 / 0.16	553 / 0.56 / 0.44	219 / 0.73 / 0.27	790 / 0.56 / 0.26		
	247	1285 / 0.64 / 0.23	888 / 0.41 / 0.22	866 / 0.64 / 0.21	1208 / 0.53 /0.29	31	25
5 wks	231	810 / 0.31 / 0.43	1178 / 0.36 / 0.42	943 / 0.35 / 0.60	1690 / 0.54 / 0.35		
	241	1736 / 0.30 / 0.44	900 / 0.39 / 0.41	180 / 0.34 / 0.66	808 / 0.50 / 0.25		
	249	944 / 0.31 / 0.49	138 / 0.38 / 0.60	594 / 0.60 / 0.40	1186 / 0.42 / 0.33	19	
6 wks	255	2109 / 0.24 / 0.53	727 / 0.29 / 0.55	365 / 0.36 / 0.53	455 / 0.40 / 0.37		18
	256	2544 / 0.36 / 0.47	1688 / 0.28 / 0.64	892 / 0.14 / 0.86	2359 / 0.35 / 0.50		53
7 wks	215	1631 / 0.21/ 0.61	1137 / 0.28 / 0.63	969 / 0.41 / 0.59	947/ 0.36 / 0.44		
	248	1590 / 0.21 / 0.53	313 / 0.47 / 0.35	150 / 0.08 / 0.98	699 / 0.29 / 0.34		
8 wks	200	743 / 0.17 / 0.53	235 / 0.26 / 0.65	92 / 0.29 / 0.65	151 / 0.26 / 0.44		
	229	1166 / 0.39 / 0.46	489 / 0.27 / 0.49	154 / 0.32 / 0.58	391 / 0.39 / 0.47		
	235	1092 / 0.25 / 0.52	710 / 0.37 / 0.47	314 / 0.31 / 0.61	639 / 0.26 / 0.48		
10 wks	250	6296 / 0.22 / 0.52	2935 / 0.27 / 0.34	1818 / 0.16 / 0.77	2805 / 0.29 / 0.45	130	234
	251	1078 / 0.24 / 0.43	267 / 0.24 / 0.55	130 / 0.26 / 0.82	202 / 0.32 / 0.49		
	258	1315 / 0.26/ 0.49	419 / 0.15 / 0.80	285 / 0.33 / 0.66	281 / 0.38 / 0.48		

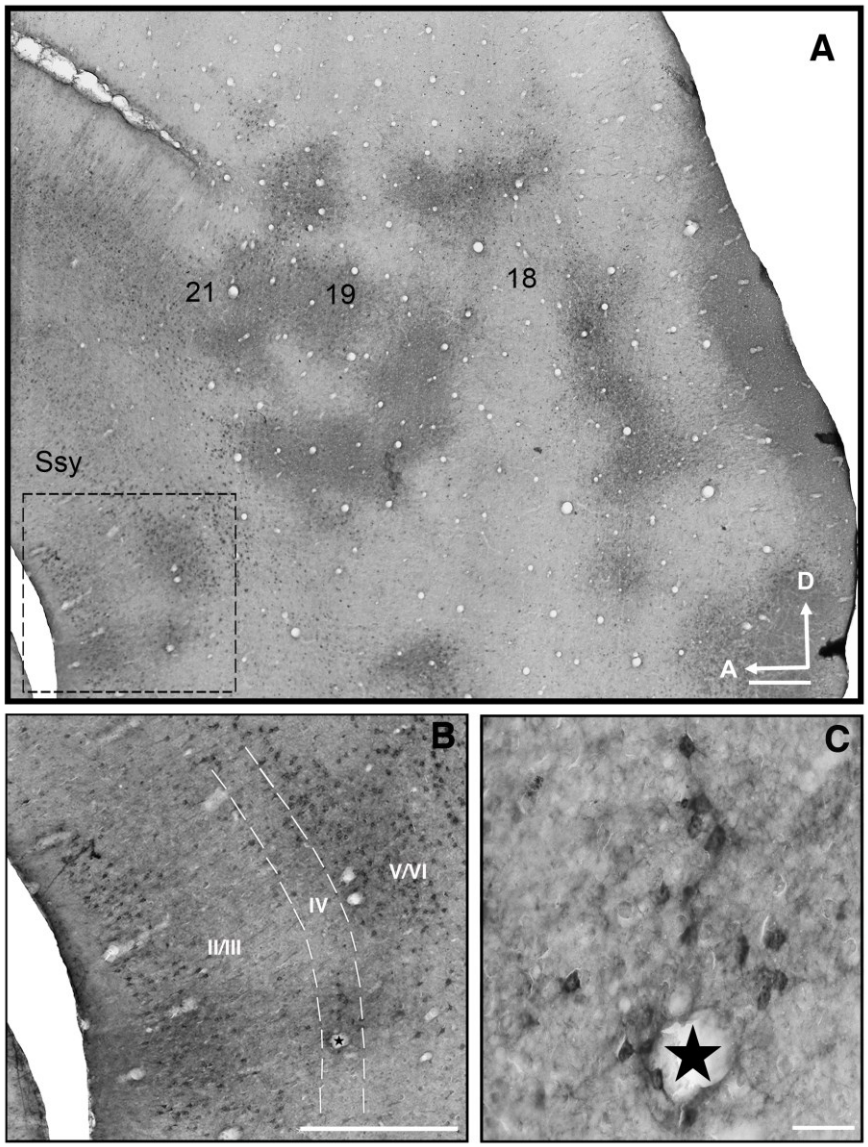

Figure 3.1. Representative area 17 injection in a 5 week old ferret with feedback label in extrastriate cortex. Photomicrographs of a semi-tangential brain section showing the typical pattern of feedback labeling in extrastriate cortex after a CTb injection in area 17. A: Area 17 injection site with overlapping clusters of orthogradely labeled terminals and retrogradely labeled cells in areas 18, 19, 21, and Ssy. Dashed square indicates region shown at higher magnification in B. B: Laminar distribution of feedback cells in Suprasylvian cortex (Ssy). Dashed lines indicate boundaries of layer IV. Most labeled cells are found in the infragranular layers, but supragranular and layer IV cells are labeled as well. C: High power photomicrograph of feedback cells in area 18. Arrows point to feedback cells. Stars in panels B and C indicate corresponding blood vessel. Ssy: Suprasylvian cortex, A: anterior, D: dorsal. Scale in A= 500 µm, scale in B= 200 µm, scale in C= 50 µm.

The pattern of feedback labeling in extrastriate cortex of a juvenile ferret (5 weeks old) is depicted in a representative photomicrograph of a semi-tangential section in Fig. 3.1A. The numbers indicate visual areas that provide substantial feedback to area 17. We find that in all areas examined, feedback cells and feedforward terminal clusters are typically found at corresponding locations, reflecting the reciprocity of connections between primary visual cortex and these extrastriate visual areas. Genuine cell label was distinguished from nonspecific labeling by its greater intensity and discontinuous cellular distribution. The ringlike pattern of feedback label found in Fig. 3.1A is qualitatively similar to the pattern of label we observe in the visual cortex of the adult. Fig. 3.1B is a higher magnification image of the dashed rectangle in panel A within the Suprasylvian region (Ssy); feedback cells can be found throughout all laminae. Although the majority of feedback cells were found in layers II/III and V/VI, labeled cells are also found in layer IV (see Fig 3.3C below). Fig. 3.1C is a higher magnification image of layer IV of Ssy with labeled feedback cells.

To examine the overall pattern of feedback label in extrastriate cortex, and to assess developmental changes in the pattern, we generated serial reconstructions of semi-tangential sections in a young and an older juvenile (Fig. 3.2). We accomplished this by outlining the contour of every fourth section, and plotting every labeled feedback cell in extrastriate cortex. Each dot represents a single feedback cell. In both reconstructions (Fig. 3.2A,B), superficial sections are to the left with successive sections being more medial. Fiducial landmarks and blood vessels were used for precise local alignment of all the serial sections in Fig. 3.2A and 3.2B to yield a collapsed image of the overall pattern in Fig. 3.2C and 3.2D.

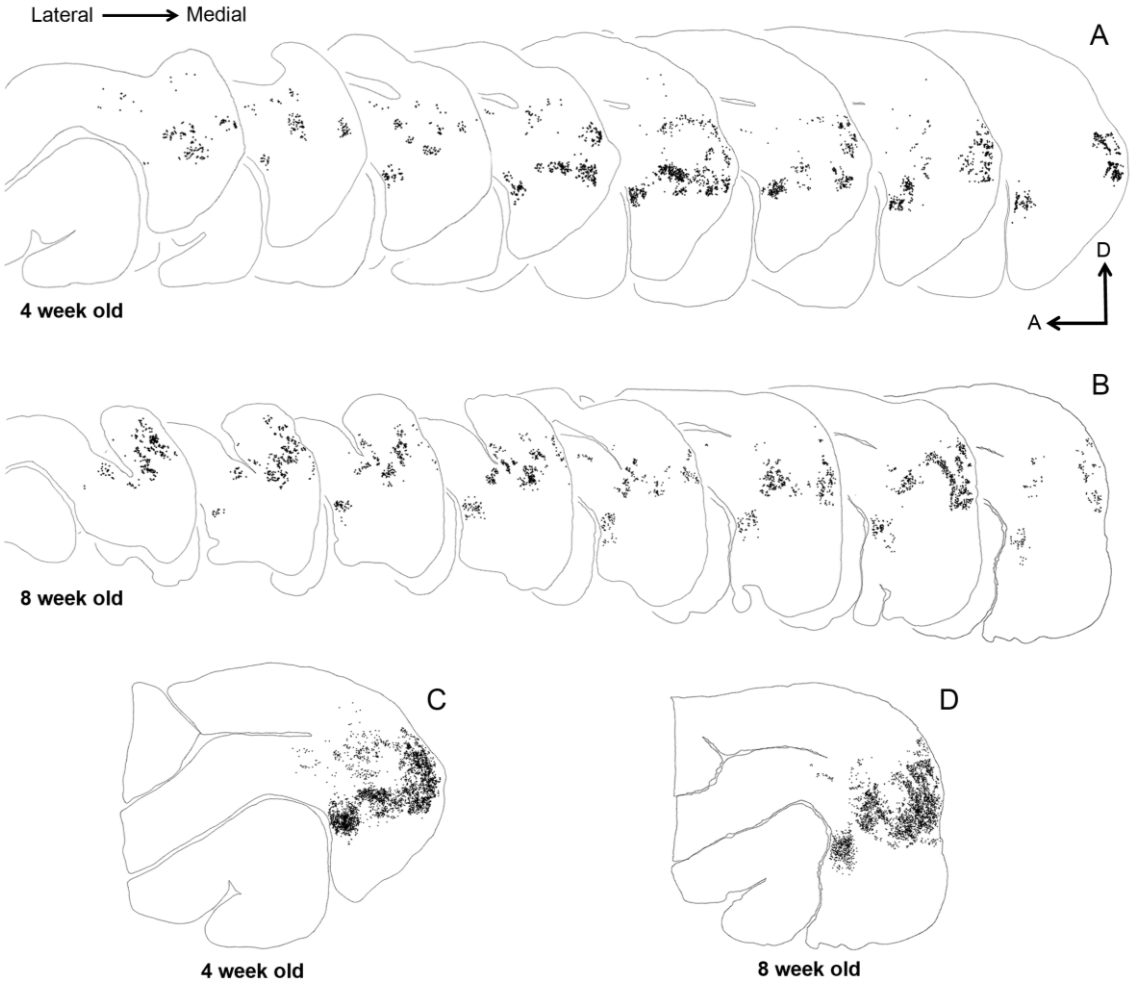

Figure 3.2. Serial reconstructions of retrogradely labeled cells in the visual cortex of juvenile ferrets. The semi-tangential sections are arranged serially (lateral=left). Black dots represent retrogradely labeled cells. A,B: Feedback label in every fourth section in a 4 week old (A) and an 8 week old (B) ferret. C, D: Superimposed and aligned images of the serial sections from the reconstructions shown in A and B to reveal the complete pattern of label. At 4 weeks postnatal, the overall label pattern resembles that seen in the adult. The sparse labeling anterior to area 21 and dorsal to the suprasylvian area (Ssy) is located in areas PPr and PPc. A: anterior, D: dorsal.

One clear and striking similarity between the 4 week old (Fig. 3.2C) and 8 week old (Fig. 3.2D) reconstructions is the stereotypical ring-like pattern of feedback label that is qualitatively similar to the pattern observed in adult ferret visual cortex. (Cantone et al., 2005). Therefore, it appears that by 4 weeks of age (shortly before eye opening) the

pattern of feedback label is broadly comparable to the feedback pattern of adult labeling for an injection at a similar retinotopic location. We observed this ring-like pattern at all postnatal ages studied.

We first asked whether the absolute number of extrastriate cells providing feedback to area 17 decreases with age. Table 1 shows that mean injection volumes were essentially the same at all ages studied (with the exception of 8 week olds, in which injection volumes were somewhat smaller than at other ages). We determined the total number of feedback cells labeled in extrastriate cortex as a function of injection core total volume (reasoning that injection core total volume was a better metric than maximal tangential extent, as the spread of CTb tracer is usually anisotropic). We found a highly significant linear correlation between the total number of labeled cells in extrastriate cortex and injection core total volume (r^2= 0.82, p =0.0006), with no differences among areas in this relationship. Since absolute number of labeled cells in extrastriate cortex scaled linearly with injection core volume, we determined a normalized number of labeled cells at each age by using the regression line to determine the number of cells in each case if the injection volume had been1 mm^3. Normalized cell counts for each age group are recorded in Table 1. With the exception of a few cases (250, 256) that had larger injection cores and thus a greater number of labeled cells, there was no obvious change with age in the number of cells in extrastriate cortex providing feedback to area 17. Therefore, it appears that at all of the postnatal ages studied here, similarly sized injection cores in area 17 yielded comparable number of labeled feedback cells in extrastriate cortex. We see no

compelling evidence for a decrease with age in absolute numbers of feedback cells, yet we show that peak density of feedback projections declines with age.

Given that the total number of feedback cells resulting from an area 17 injection appears not to change significantly with age, we wondered what spatial features of the feedback pool change throughout development. In the adult ferret, Cantone et al. (2005) have shown that area 18 provides the greatest proportion of the total number of cells providing feedback to area 17 (mean 45.5%). Areas 19, 21, and Ssy each provide similar smaller feedback contributions. We were therefore interested in revealing whether the proportion of feedback arising from each visual area changes throughout postnatal development. Secondarily, we wanted to know whether the refinement of feedback connections in each visual area proceeds at a similar rate or if each visual area has a unique developmental trajectory. Since absolute number of labeled feedback cells could vary with injection core size and laminar intrusion, the proportion of feedback from each area is a normalized measure that more appropriately reflects changes in the total pool of feedback to area 17.

The change in the relative proportion of feedback connections arising from each visual area as a function of age is plotted in Fig. 3.3A. Adult values are plotted on the right for comparison. Unlike the adult, in which area 18 (black squares) provides the greatest proportion of feedback, at 4 weeks of age we find that area Ssy provides the greatest feedback input (about 36% of the total), somewhat greater than that from area 18. Within 2 weeks, bye the age of 6 weeks (soon after eye opening), the adultlike distribution of feedback is attained: area 18 provides the greatest amount of feedback

(mean 44%), while areas 19, 21, and Ssy provide roughly the same amount of feedback (areal means range from 10%-20%).

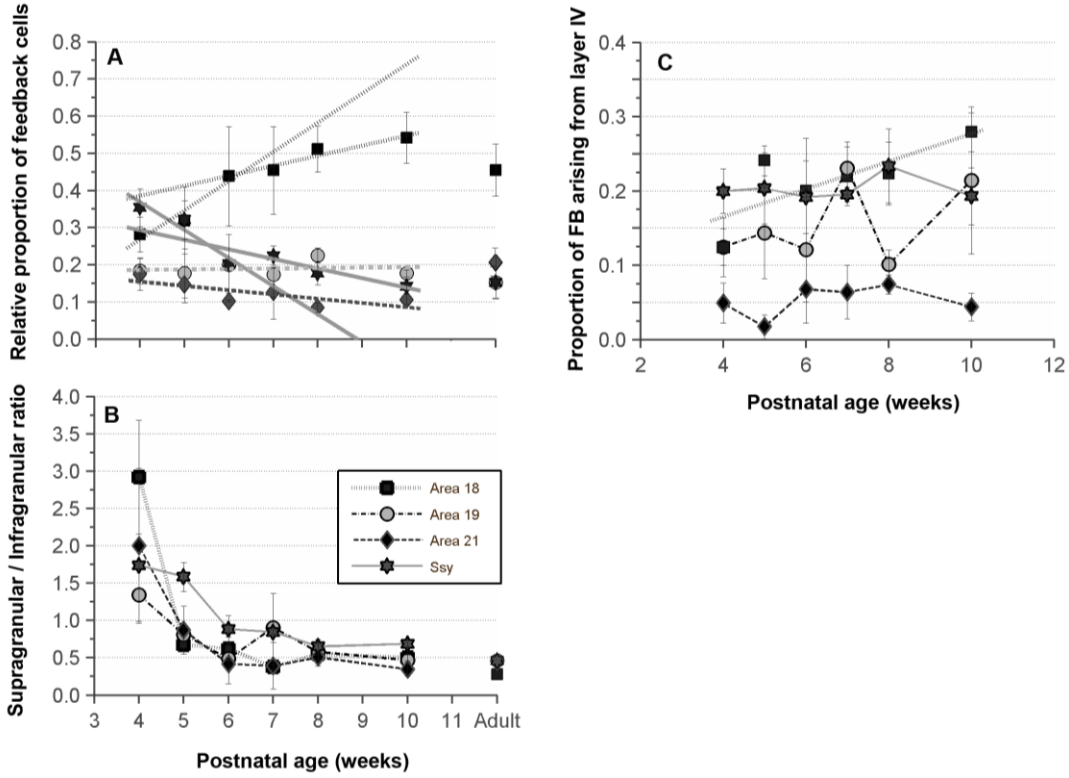

Figure 3.3. Developmental changes in the areal and laminar distribution of feedback cells in the visual cortex of juvenile ferrets. A: Proportion of feedback projections to area 17 arising from areas 18, 19, 21, and Ssy as a function of age. Before eye opening, Ssy makes the largest feedback contribution to area 17; by 6 weeks postnatal, area 18 feedback input is largest. B: Ratio of the proportion of feedback to area 17 arising from supragranular to that of infragranular layers in each area. The supragranular contribution to feedback declines synchronously in all extrastriate areas from 4 to 6 weeks. C: The proportion of feedback arising from layer IV in each area changes little in this period, except for feedback from area 18 whose layer IV contribution increases. Regression line is plotted for area 18. Adult mean values are plotted on the right for comparison in panels A and B. Error bars represent ±SEM

The proportion of feedback arising from area 18 shows a positive linear correlation with age from 4 to 8 weeks (r^2= 0.90), while the change in the proportion of feedback arising from Ssy shows a negative linear relationship over this same period (r^2= 0.85). There was no significant change in the feedback contribution made by areas 19 and 21 (r^2= 0.021 and r^2= 0.51, respectively). After 6 weeks, there is little change in the proportion of feedback arising from different cortical areas. A permutation test was separately conducted for each area to determine whether there was a significant correlation between the proportion of feedback in each area and developmental age.

The permutation test estimates the probability of obtaining our data by chance. Statistical testing consisted of randomly permuting the raw data points within a single visual area between different age groups 10,000 times (without replacement). This repeated random reassignment between age groups was used to test the null hypothesis that there is no relationship between proportion of feedback and developmental age. The permutation test yielded a $p<0.0032$ for area 18, $p<0.5077$ for area 19, $p<0.05832$ for area 21, and $p<0.0002$ for Ssy. Thus, there is a significant change with age in the proportion of feedback to area 17 arising from areas 18 and Ssy, but there is not a significant change in the proportion of feedback arising from areas 19 and 21. Feedback cells were also labeled in the lateral temporal (LT), posterior parietal (PP), and auditory areas in the younger animals. The proportion of feedback deriving from PP was about 3%, 6% in LT, and less than 1% in auditory cortex. These small contributions did not appear to change with age. We also assessed the developmental change in the laminar distribution of feedback cells in each visual area. Fig. 3.3B shows the ratio of the proportion of feedback

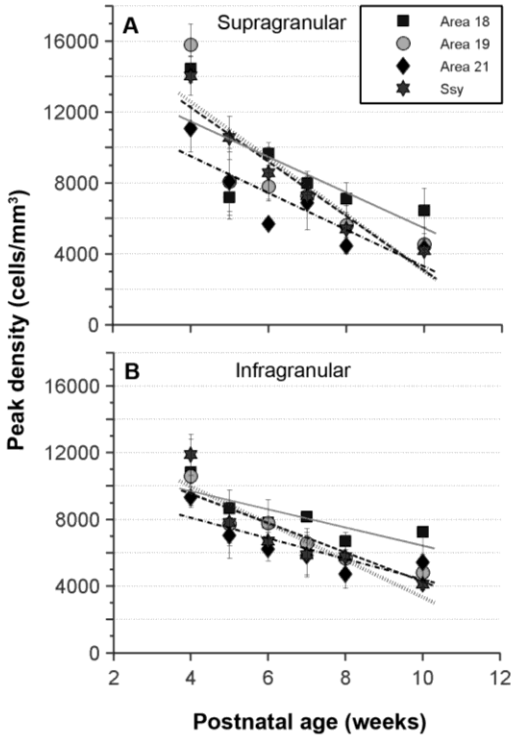

Figure 3.4. Developmental decreases in the peak densities of labeled cells within the cortical areas providing feedback to area 17. Peak density of feedback cells in the supragranular (A) and infragranular (B) layers of areas 18, 19, 21, and Ssy declines monotonically with age. Regression lines are plotted for each visual area. Error bars represent ±SEM.

arising in each area from the supragranular layers to that from the infragranular layers. Higher supra/infra ratios reflect a greater proportion of feedback arising from the supragranular layers. At 4 weeks of age, the majority of labeled cells in all areas were found in the supragranular layers; area 18 seems to have the greatest proportion of feedback arising from the supragranular layers, while area 19 appears to have a more balanced contribution from the supragranular and infragranular layers (ratio 1.3).

A permutation test was separately conducted for each area to determine whether there was a significant correlation between the ratio of supra- to infragranular neurons in each area and developmental age. The permutation test yielded a $p<0.0032$ for area 18, $p<0.0077$ for area 19, $p<0.01832$ for area 21, and $p<0.0002$ for Ssy. Thus, with age, there is a significant change in the supragranular contribution resulting in lower

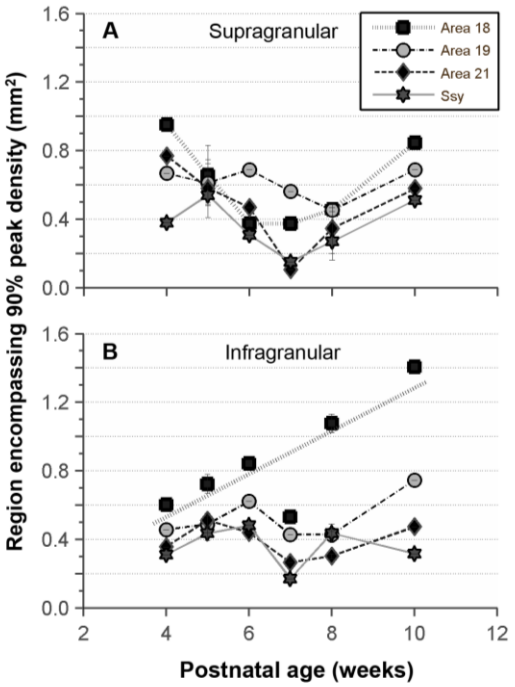

Figure 3.5. Developmental changes in the tangential extent of feedback label. Area of region that encompasses 90% of the peak density of feedback cells in the supragranular (A) and infragranular (B) layers of areas 18, 19, 21, and Ssy as a function of age. With the exception of infragranular area 18, the region in each cortical area furnishing area17 feedback remains essentially unchanged in extent. Regression line is plotted for area 18. Error bars represent ±SEM.

supra/infra ratios. By 6 weeks of age, similar to the areal rearrangements described above, the laminar pattern of feedback appears similar to that in the adult.

We consistently found labeled feedback cells in layer IV of all the visual areas that provide input to area 17. We therefore quantified the relative proportion of feedback cells in layer IV of areas 18, 19, 21, and Ssy to determine if the contribution from layer IV changes with age (Fig. 3.3C). Areas 18, 19, and Ssy had a substantial proportion of their feedback arise from layer IV (means 10-20%). At all ages, Layer IV of area 21 seems to provide a minor feedback contribution (roughly 5%). We performed a permutation test to reveal if there was a significant change with age in the proportion of feedback arising from layer IV of each visual area. We found that the proportion of feedback arising from layer IV of areas 19, 21, and Ssy does not change significantly with age (area 19: $p=0.297$; area 21: $p=0.298$; Ssy: $p=0.369$). However, we found that

the increase in the proportion of feedback arising from layer IV of area 18 is statistically significant (p=0.01).

We next compared the peak densities of labeled cells in these areas at different developmental stages. We defined the peak density within a cortical area as the region of highest density in any one of the reconstructed sections, delineated with a 200 μm diameter circle. The peak density of feedback cells in the supragranular layers of all areas at 4 weeks of age is initially very high (mean=13,840 cells/mm^3) (Fig. 3.4A). The peak density of feedback cells in the supragranular layers of all areas examined decreased monotonically with age. By 10 weeks of age, the peak densities declined dramatically (mean=4,860 cells/mm^3). Comparison of the regression lines for each area's data revealed that the slopes were not significantly different from each other (ANCOVA, p=0.6004); this indicates that feedback cell density declined at a similar rate in all areas. We similarly plotted the peak density of feedback cells in the infragranular layers of all areas as a function of age (Fig. 3.4B). The peak density at 4 weeks of age averages 10,600 cells/mm^3 across all areas. Like the supragranular layers, the peak density of cells in infragranular layer also declines linearly, albeit at a slower rate. We likewise found that the slopes were not significantly different from each other (ANCOVA, p=0.2730), indicating indistinguishable rates of feedback loss.

Declining density of feedback cells could result either because a fixed proportion of cells in the neuropil provide feedback but overall neuronal density declines with age, or because neuron density remains unchanged but fewer of those cells furnish feedback axons to area 17. To distinguish these possibilities, we measured neuronal density in Nissl-stained material from each extrastriate area. We find that in area 18, neuronal

density declined by 10 weeks postnatal to about 75% of the value in 4 week olds (layer II: 53,000 to 38,000 cells/mm^3; layer III: 42,000 to 31,000 cells/mm^3; layer V: 25,000 to 19,000 cells/mm^3; layer VI: 43,000 to 32,000 cells/mm^3. Similarly, in area Ssy, neuronal density declined by 10 weeks postnatal to 56-75% of the value in 4 week olds (layer II: 55,000 to 31,000 cells/mm^3; layer III: 40,000 to 30,000 cells/mm^3; layer V: 30,000 to 19,000 cells/mm^3; layer VI: 36,000 to 26,000 cells/mm^3. We found no clear evidence for declines in cell density in areas 19 and 21. For comparison, peak density of feedback cells in areas 18 and Ssy declined to about 43% and 29% (respectively) of the 4 week old value in the supragranular layers, and to about 64% and 33% in the infragranular layers; in areas 19 and 21, the declines in feedback cell density were to 25-50% of the 4 week value (Fig. 3.4). Thus, the developmental decline in density of feedback cells may in part reflect decreasing neuronal density. However, this cannot be entirely attributed to declines in overall neuronal density (presumably reflecting not neuronal loss but rather brain growth due to increased volume occupied by axons, dendrites, and glial cells).

The decline in peak density could reflect an increase with age in the areal extent of the region providing feedback. We determined whether the size of the region in each area encompassing 90% of the peak density of feedback cells changes with age. Fig. 3.5A shows that there is no significant change with age in the areal extent of this region in the supragranular layers of all areas examined (permutation test, $0.661 < p < 0.829$). Fig. 3.5B similarly shows that the areal extent of the region that encompasses 90% of the peak density of feedback cells in the infragranular layers remains unchanged throughout development in areas 19, 21, and Ssy ($0.156 < p < 0.793$). However, in area 18 the areal extent of the region that encompasses 90% of the peak density in the

infragranular layers does appears to increase with age (permutation test, p=0.004; r^2=.62).

We next assessed developmental changes in the spatial distribution of the feedback population by quantifying nearest neighbor distances (NND) between cells in each visual area providing feedback to area 17. For every cell within a region of interest, the distance to its nearest neighbor was computed and a frequency histogram for all the nearest neighbor distances was subsequently constructed. This measure also indicates the density of feedback projections from each visual area (high NND values reflecting lower cell density). but also reveals more about the spatial layout of the feedback pool. Specifically, it can reveal if the distribution reflects spatial randomness, clustering, uniform tiling, or a more dispersed distribution.

Figures 3.6A and 3.6B illustrate the distribution of nearest neighbor distances between feedback cells in the supra- and infragranular layers of each area at all postnatal ages studied. The black and gray arrowheads indicate the median and third quartile values, respectively. The shape of the distribution is positively skewed for all areas at all postnatal ages. However, at younger ages (4 and 5 weeks), the distribution of NNDs is more peaked, with lower median NND values in all areas. With age, the median NND values as well as the Q3 values shift towards longer distances. The shape of the distribution also changes with age; the tail of the distribution becomes more prominent, indicating that with age the proportion of longer NND distances increases (indicated by bins with dark shading, representing values exceeding 60 µm).

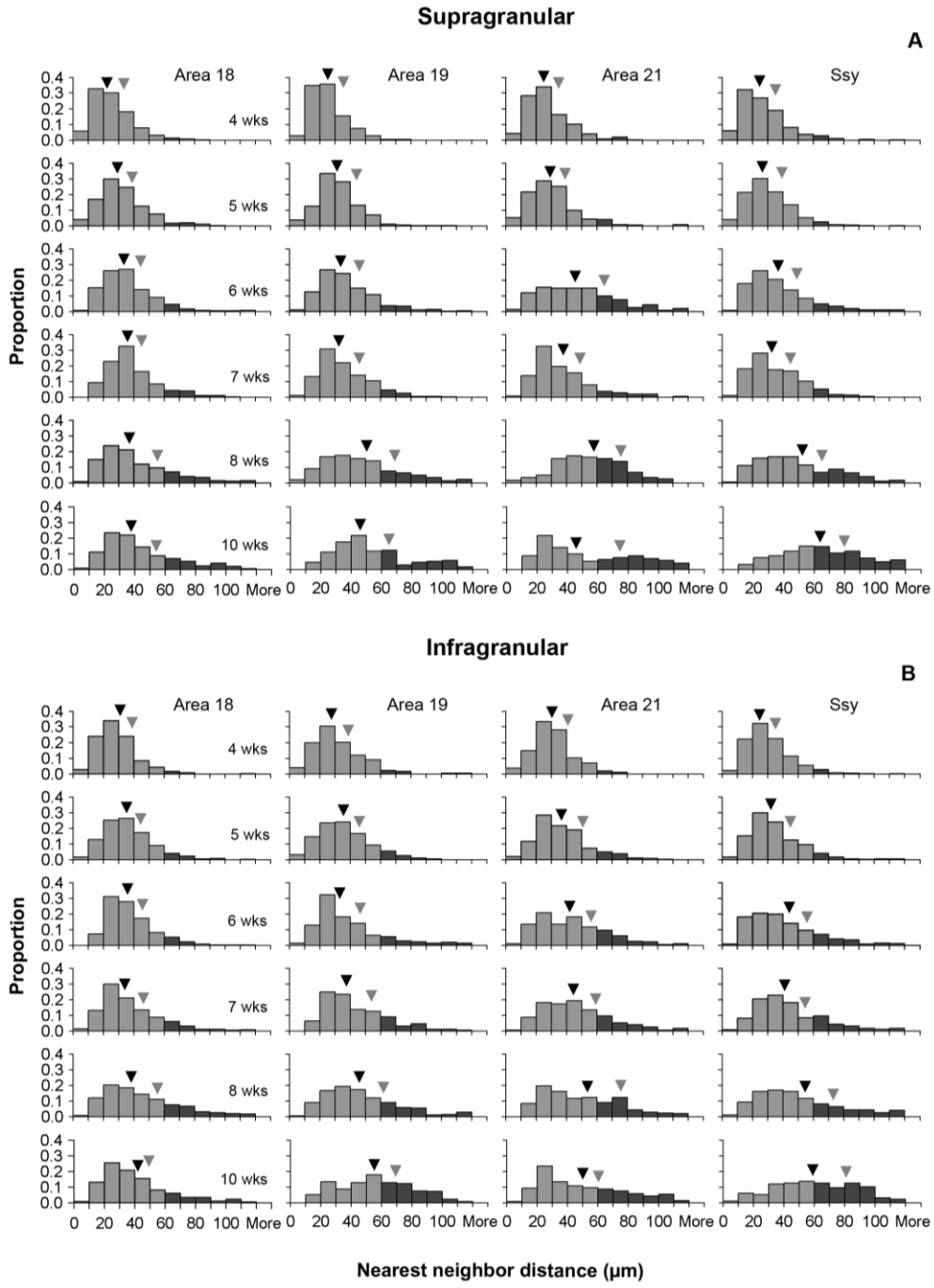

Figure 3.6. Developmental changes in the distribution of nearest neighbor distances (NNDs) between feedback cells in juvenile visual cortex. Frequency distribution histograms of NNDs in the supragranular (A) and infragranular (B) layers of areas 18, 19, 21, and Ssy. Dark shaded bins represent NND values exceeding 60 μm. Black arrowheads indicate median NND values, and gray arrowheads indicate the 3rd quartile NND values. In all areas, with age there is an increase in median NND, and an increase in the proportion of NNDs exceeding 60 μm.

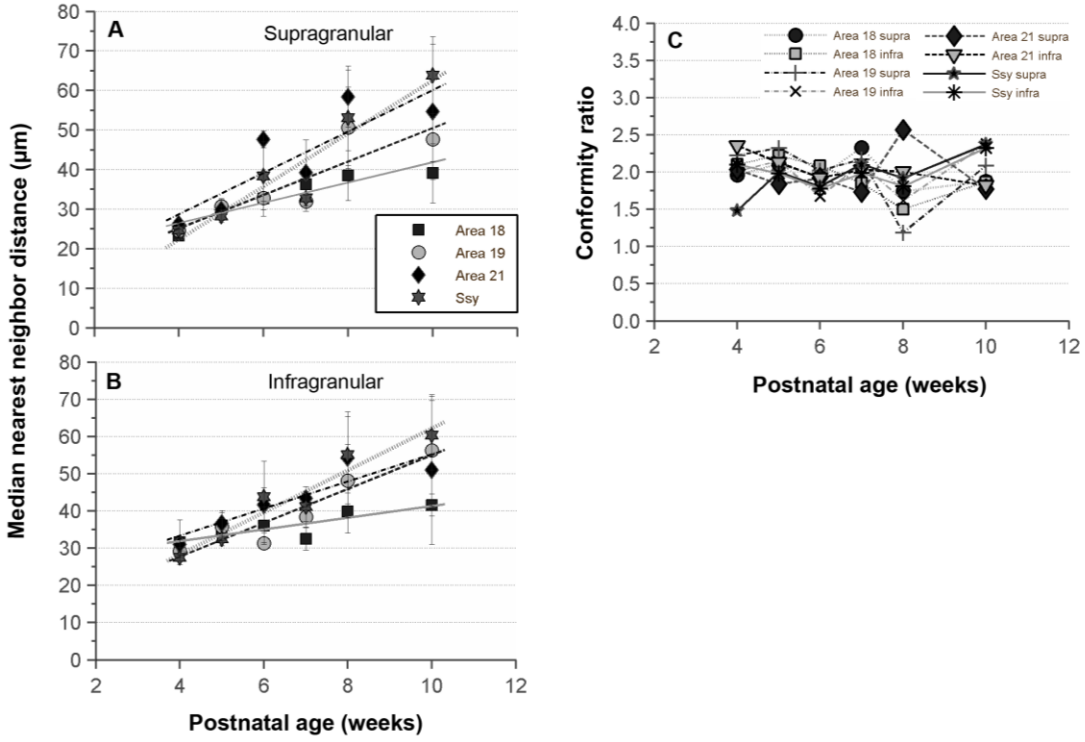

Figure 3.7. Age dependent increase in the median nearest neighbor distance (NND) between feedback cells in the juvenile ferret visual cortex. A,B: Median nearest neighbor distance between feedback cells in the supragranular (A) and infragranular (B) layers of areas 18, 19, 21, and Ssy as a function of age. Median NND increases monotonically at the same rate in all areas. Regression lines are plotted for each visual area. Error bars represent ±SEM C: Conformity ratio (mean NND/Standard deviation of NND) in supra- and infragranular layers of each area as a function of age. This measure of regularity of spacing between feedback cells remains unchanged with age, and provides no strong evidence for a nonrandom distribution of cells.

We plotted the median nearest neighbor distance value in the supragranular layers of each visual area as a function of age (Fig. 3.7A). At 4 weeks of age, the median NND value in all areas is quite low and similar in all areas (mean= 25 µm). To 10 weeks postnatal, the median NND value appears to increase in all areas to a value between 40-60 µm, and the median NND values seem to diverge among areas. We

compared regression lines among areas, and find that there are no significant differences among the slopes (ANCOVA, p=0.1205). We also plotted the change with age in median nearest neighbor distance in the infragranular layers of each visual area (Fig. 3.7B). At 4 weeks of age, the median NND value in all areas is quite low and similar in all areas (mean= 30 μm). We find that there is a significant difference between area 18 and Ssy's slope (ANCOVA, posthoc test; p=0.009); the increase in the median NND value in the infragranular layers of area 18 seems to occur at a slower rate than in Ssy. Therefore, it appears that the median NND value in the supragranular and infragranular layers of all areas share a broadly similar developmental trajectory. However, the increase in the median NND values in the infragranular layers of all areas seems to proceed at a slower rate.

The nearest neighbor analysis is informative in revealing details of how the spacing of neurons changes with age. To more explicitly reveal an underlying regularity in the spatial distribution of nearest neighbor distances we also computed conformity ratios (Cook, 1996) for our NND samples. This measure is the mean of the NND divided by the standard deviation; the more regular the arrangement of neurons, the higher the conformity ratio. In (Fig.3.7C) the conformity ratios in the supra- and infragranular layers of areas 18, 19, 21, and Ssy are plotted as a function of age. The conformity ratios appear to fluctuate around the value of 2 during this postnatal period, but appear not to change with age. A permutation test was separately conducted for each area to assess whether there was a significant correlation between the conformity ratio in each area and developmental age. We found no significant change in conformity ratio with age ($p<0.01$). We also tested whether conformity ratios for any of the NND distributions were

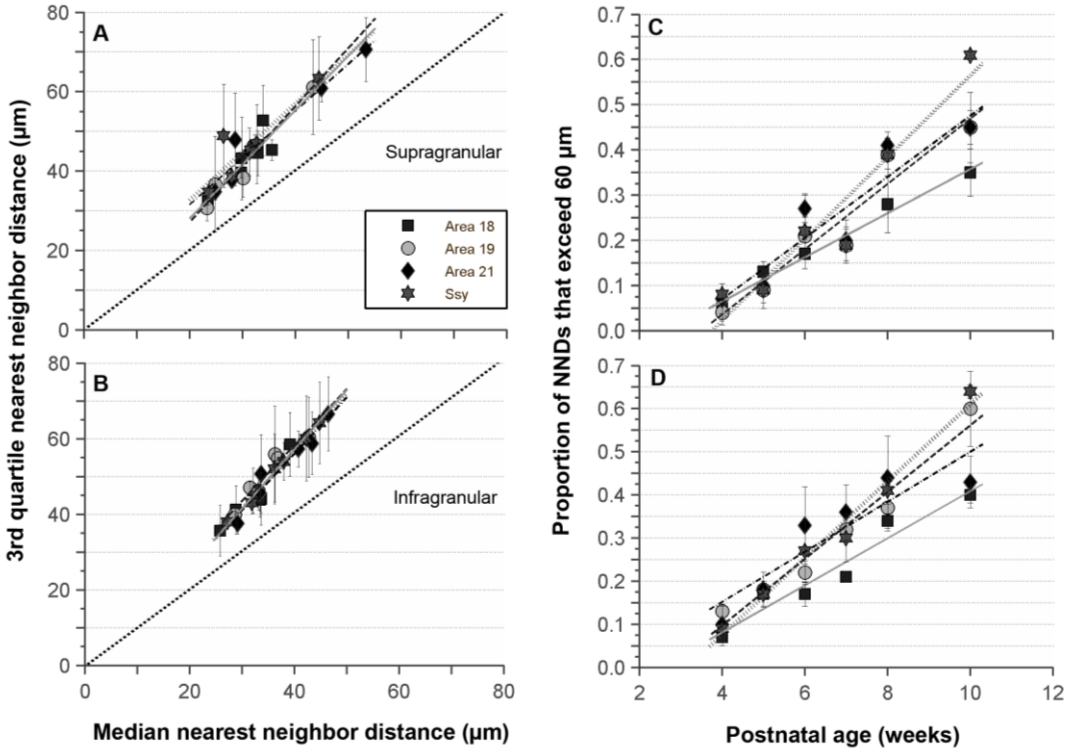

Figure 3.8. Developmental changes in the distribution of nearest neighbor distances (NND) between feedback cells in juvenile ferret visual cortex. A,B: Correlation between the 3rd quartile NND values (Q3) and median NND values in the supragranular (A) and infragranular (B) layers of areas 18, 19, 21, and Ssy. In all areas, the Q3 NND similarly increases with age faster than the median NND, indicating that the distribution of NNDs is not simply uniformly shifting with age to larger values, but is also specifically developing a subset of larger NND values. C,D: The proportion of NNDs in the supragranular (C) and infragranular (D) layers of areas 18, 19, 21, and Ssy that exceed 60 µm as a function of age. These increase with age at the same rate in all areas. Regression lines are plotted for each visual area. Error bars represent ±SEM

significantly different from a random arrangement. Almost all conformity ratio values were not significantly different from complete randomness ($p<0.001$: although conformity ratios for at least one area at each postnatal age suggested statistically significant deviation from randomness). Thus, during this postnatal period while peak density declines and nearest neighbor distances increase, the underlying regularity of

the feedback pool in each area seems indistinguishable from a random arrangement, and does not change with age.

To further examine the refinement of feedback connections, we used the 3rd quartile (Q3) value in conjunction with the median NND value to better characterize the change in the shape of the NND distribution. An increase in the median NND with age reflects a decrease in the density of feedback cells. However, this measure alone does inform about the underlying distribution. The median NND value could conceivably increase without reflecting a change in the distribution. For example, with age the entire distribution of NND values could simply shift to the right and subsequently yield a higher median NND value; in this case the Q3 value would increase by the same amount as the median value. However, if the change in the Q3 value differs from that of the median NND value, this suggests a change in the shape of the NND distribution (and hence the underlying arrangement of feedback cells). We plotted the Q3 value in the supragranular layers of each area as a function of median NND value (Fig. 3.8A); individual data points represent values at different ages. The dashed line through the origin with a slope of one indicates equal change in Q3 and median values. We find a strong correlation between median NND and the Q3 value in each area ($0.75 < r^2 < 0.95$). The slopes do not differ significantly among areas (ANCOVA, $p=0.779$). However, the slopes do differ significantly from 1 (slope test, $p=0.01$). Thus, in all areas examined, the rate at which the Q3 value increases is greater than that for median NND. The same holds in the infragranular layers (Fig. 3.8B). We find a strong correlation between median NND and Q3 value ($0.89 < r^2 < 0.99$). Taken together, the results suggest that both the median NND value and Q3 value in the supragranular and infragranular layers

of all areas examined are monotonically increasing with age, but the Q3 value is increasing at a greater rate. The greater rate of increase in the Q3 value confirms a change in shape of the NND distribution (emergence of larger values), rather than a simple shift of the entire distribution to larger values.

We quantified the emergence of these longer nearest neighbor distances among feedback cells in each area. We chose a criterion distance of 60 μm, since at 4 weeks of age almost no NNDs exceeded this value. We determined whether the proportion of NNDs in each area that exceeded 60 μm changed with age. In both the supra- and infragranular layers of all areas examined, the proportion increased linearly (Fig. 3.8C, 3.8D). At 4 weeks of age, the proportion of NNDs that exceed 60 μm is on average 6-10%. However, by 10 weeks of age, that proportion rises considerably (areal mean range between 35% to 64%). The rate of increase of this population did not significantly differ among areas in the supragranular layers (ANCOVA, $p=0.103$). The rate of increase did not differ among areas in the infragranular layers as well (ANCOVA, $p=0.0472$).

3.5 Discussion

We have shown substantial refinement in the spatial organization of feedback projections from multiple visual areas to ferret primary visual cortex during the period after eye opening. There is major reorganization in the areal and laminar proportion of feedback arising from each visual area from 4 to 6 weeks postnatal (in the period after eye-opening). However, peak density, median NND, and Q3 values decline monotonically from 4 to 10 weeks postnatal. Our results also indicate that much of the

overall pattern of feedback label in extrastriate cortex is present as early as four weeks postnatal, before the eyes open. Our results are in agreement with previous studies showing that feedback projections undergo a period of prolonged remodeling (Barone et al., 1995; Batardiere et al., 1998, 2002; Burkhalter, 1993). Our results provide evidence for a developmental process operating with the same time constant in all visual areas to refine peak density, median NND and Q3 values, with another process governing the refinement of areal and laminar distribution of feedback projections to area 17.

1) Relationship to feedback circuitry in the adult ferret

In the adult ferret, (Cantone et al., 2005) have shown that area 18 provides the greatest proportion of the total number of cells providing feedback to primary visual cortex. Areas 19, 21, and Ssy each provide similar smaller feedback contributions. However, at four weeks of age, we find that area Ssy provides the greatest proportion of feedback to primary visual cortex. Moreover, in the adult ferret, the majority of feedback cells are found in the infragranular layers with fewer cells in the supragranular layers. The inverse relationship exists in the juvenile ferret; at the youngest age examined (4 weeks postnatal) the contribution from the supragranular layers is greater than that from the infragranular layers. Our results are in agreement with previous studies showing that feedback cells are more numerous in the supragranular layers of visual cortical areas early in development (Barone et al., 1995; Batardiere et al., 1998). Peak density of feedback cells in both the supragranular and infragranular layers was roughly six to eight times greater in each area at four weeks of age than in the adult. Peak density of feedback cells declines monotonically with age, yet adult values are not reached by ten

weeks of age. Thus, it appears that there is a prolonged period that extends later than ten weeks in which the peak density continues to decrease.

The decline in peak density of feedback projections we observe is partly due to the decline in overall neuronal density (presumably because of brain growth and not cell death). However, the developmental decline in peak density cannot be entirely attributed to declines in overall neuronal density. We also show that the area encompassing 90% of the peak density does not change significantly with age (except for area 18, which increases with age). Further, the NND value declines with age. These data may seem incompatible. However, it is certainly possible that the areas encompassing 90% of the peak density does not change with age, yet the remaining 10% of the peak density does change with age. To clarify, the region used to calculate the peak density in each area was a 200 μm diameter circle and the region used to calculate the NND values encompassed more of the feedback cluster (300 μm diameter circle)

Our nearest neighbor analysis data corroborate our very high peak density counts as the median nearest neighbor distance is substantially lower at four weeks of age and increases monotonically with age. The fact that the median nearest neighbor distance is much lower in the younger animals suggests that feedback cells are more closely spaced per unit area. To our knowledge, this is the first study to quantify the nearest neighbor distance of feedback cells in multiple visual areas throughout developmental. Cantone et al. (2005) did not quantify the spatial distribution of feedback cells in the adult ferret, therefore we can not unequivocally claim that the nearest

neighbor values at ten weeks of age are comparable to adult values. Interestingly, the authors do claim that feedback label in Ssy of the adult was observed as sparse. This is in agreement with our NND analysis as the median NND value in Ssy in both the supra- and infragranular layers remains the highest by ten weeks of age. Our data reveal that the Q3 value shifts towards longer distances throughout development, as does the median NND value. This is not surprising given that the peak density value of feedback cells also decrease in all visual areas. This could reflect a selective developmental loss of inappropriate feedback connections from extrastriate visual areas to primary visual cortex to attain the adult like spatial configuration. Moreover, we plotted the change in the Q3 value as a function of median NND value and our results suggest that the rate at which the Q3 value is increasing is greater. This implies that the nearest neighbor distribution is not simply shifting towards longer distances, but rather the distribution is developing a tail.

2) Comparison with other aspects of anatomical developmental in the ferret

A number of other anatomical features appear to refine during this same postnatal period shortly after eye opening. We have shown (Khalil and Levitt, 2012) that the major period of zinc circuit refinement (reflecting a subset of feedforward and feedback pathways) occurs shortly after eye opening. This phase of major decline in the synaptic zinc levels in areas 17 and 18 (particularly in layer IV) coincides with the period of reorganization of feedback projections from multiple visual areas to area 17. This is not surprising given that zinc-positive inputs to area 17 are a subset of feedback projections from multiple visual cortical areas. Similarly, the refinement of horizontal

projections in layers II/III of ferret visual cortex begins around P22 and continues until distinct adult-like terminal clusters are observed at P45 (Durack and Katz, 1996; Ruthazer and Stryker, 1996). Around the time of eye opening, these long-range horizontal connections are limited in spatial extent, and are less clustered than in the adult. While ocular dominance columns are established early in the ferret (P16: Crowley and Katz, 2000), the critical period for ocular dominance plasticity roughly coincides with the period of major reorganization of feedback circuitry, and continues until the end of the second postnatal month (Issa et al., 1999).

Therefore, it appears that the period of major refinement of feedback circuitry in ferret visual cortex occurs on a similar timescale as the refinement of certain other features of anatomical circuitry. The onset of visual experience seems to be a critical factor for this refinement process of feedback projections as well as other anatomical features of the visual cortex. For example, the density of thalamocortical synapses in layer 4 of ferret area 17 increases rapidly in the month that follows the onset of patterned visual experience (Erisir and Harris, 2003). Furthermore, manipulation of sensory experience has been shown to affect the anatomical refinement of circuits. For instance Callaway and Katz (1991) demonstrated that depriving young cats of patterned visual experience by binocular lid suture prior to eye opening reduced the specificity of terminal clusters of horizontal connections in V1. The refinement of different aspects of feedback projections we document here appears to be differentially affected by visual experience. The slow monotonic rate of refinement in peak density, median NND, and Q3 values (which start before eye opening), contrasts with the sharp decline in areal and laminar proportion of feedback we observe right after eye-opening. We suggest that

the critical period for the refinement of the areal and laminar proportion of feedback is from four to six week postnatal. However, since peak density, median NND, and Q3 values seem to decline prior to eye opening, the critical period for their normal refinement may start before eye opening and extend for a longer period of time.

3) Comparison with anatomical development in other species

Other studies in monkey (Barone et al., 1995; Batardiere et al., 2002) have shown that feedback connections undergo extensive remodeling involving selective pruning of a subset to yield the adultlike pattern of connections. Barone et al.(1995) investigated the refinement of the laminar distribution of feedback connections reporting a decrease in the proportion of supragranular neurons that differs among areas. This laminar refinement of feedback connections is largely complete by one to two months after birth. Similarly, the laminar distribution of feedback neurons to area 17 in kittens is uniform across individual extrastriate areas and the selective reduction in the supragranular neurons yields the laminar distribution characteristic of each area in the adult (Batardiere et al., 1998). Price and Blakemore (1985) have reported that feedforward neurons in area 17 projecting to area 18 in the kitten are distributed in bands of uniform density. These bands refine in the following two weeks to yield discrete dense clusters of feedforward projections, characteristic of the adult pattern.

Developmental studies investigating the sequence of refinement of interareal feedforward and feedback connections in the visual cortex of human infants have concluded that while the laminar distribution of labeled fibers and cell bodies in V1 and V2 indicate that feedforward and feedback connections emerge shortly before birth, the

laminar termination pattern of feedforward connections appears relatively mature before feedback connections reach their mature form (Burkhalter, 1993). A similar study in mouse visual cortex was conducted more recently by Berezovski et al (2011). The authors examined the development of feedforward and feedback connections between mouse V1, anterolateral area (AL), and lateromedial area (LM). The findings showed that FF connections were present at the earliest time point examined (postnatal day 2), while FB connections were not detectable until P11 and suggests that feedforward connections refine earlier than feedback connections.

4) Relationship to V1 neuronal properties

Feedback projections from extrastriate visual areas have been shown to influence the response properties of V1 neurons. It is now accepted that different visual response properties of V1 neurons mature and attain adultlike characteristics at different times and rates in postnatal development. Orientation and direction selectivity of V1 neurons appear to refine and become adult like during the same refinement period of feedback projection. There appears to be some degree of orientation selectivity as early as visual responses can be elicited, two weeks before the time of natural eye opening, but that adult-like selectivity is not reached until about a week after eye opening (Chapman and Stryker 1993, Krug et al., 2001). Moreover, orientation maps in V1 are present prior to eye opening and the overall map layout does not change much throughout development (Chapman et al., 1996). The basic structure of orientation maps is therefore innate, but experience is necessary for specific features of these maps, and for maintaining selectivity of cortical neurons. Optical imaging and

electrophysiological techniques have revealed the absence of direction selectivity in ferret visual cortex at eye-opening, which develops during the subsequent two weeks from P30 to P45 (Li et al., 2006). Patterned visual input appears to be critical in the development of cortical direction selectivity, as dark rearing ferrets after eye opening precludes the formation of direction maps and V1 neurons lack direction tuning.

Our results are in agreement with the developmental timeline for direction selectivity (Li et al., 2006) as the proportion of feedback from Ssy decreases from four to six postnatal and remains fairly stable throughout development. This suggests the adultlike proportion of feedback from Ssy is achieved by six weeks of age. Ssy has been shown to be the primate homologue of area MT, an area implicated in motion perception. Feedback connections from Ssy presumably shape direction selective-responses of V1 cells. Therefore, if feedback circuits from Ssy to V1 are adultlike by 6 weeks of age, it is likely that these circuits contribute to the direction selective responses of V1 cells. In addition, it seems that the maturation of direction selectivity in area 17 in the ferret is in accord with the maturation of feedback circuits from Ssy, the input of which presumably shapes direction-selective responses.

Understanding how the spatial organization of feedback projections refines in ferret visual cortex during development to generate the adult like pattern is a prerequisite for assessing their physiological development. In the monkey, Zhang et al. (2005) have shown that the size of receptive field center of V1 neurons in infants are considerably larger than that of the adult receptive field center. The RF centers of V2 neurons at 2 weeks of age can be up to three times larger than the size of adult RF center. Their results suggest that at the time that certain receptive field properties are

mature in V1 and V2 the modulatory surround effects are not. Feedback projections in visual cortex have been implicated in these modulatory surround effects. Therefore, it is likely that feedback projections to V1 and V2 from other extrastriate visual areas have not yet assumed their adultlike organization. Taken together, their results suggest that the spatial extent of both the RF center and surround refine throughout the course of development.

5) Comparison with behavioral studies

The anatomical refinement of feedback circuits presumably parallels or precedes the maturation of neuronal physiological properties and more broadly visual perceptual abilities, and is therefore one indicator of functional maturity. Visual cortical areas subserve different perceptual functions as a result of their interareal anatomical circuits, and feedback circuits are one class of interareal projections. Feedback circuits must first be assembled during development and visual experience subsequently fine-tunes these circuits yielding mature anatomical connections. It is known that different visual functions mature and become adultlike at different times and rates in development. The timecourse and duration of refinement varies significantly as more basic visual functions mature earlier and require less time than more complex ones, which require considerable postnatal time to refine. The variability in the rates and duration of the postnatal refinement period appears to reflect the maturational status of distinct cortical circuits that mediate these specific perceptual abilities.

Behavioral studies on human infants have revealed that many basic visual functions are absent at birth, but develop soon thereafter. For instance, by isolating

infants' VEPs (visual evoked potentials) Braddick et al. (1986) found that orientation-selective responses first appeared around 6 weeks of age. Wattam-Bell (1991) reported that responses to direction of motion by isolating VEPs was not possible until 10–12 weeks of age. Interestingly, comparison of orientation selective and direction-selective VEP responses in the same infants shows that these two perceptual abilities do not emerge together, but that direction consistently lags orientation in development (Braddick, 1993; Braddick et al., 2005). These studies are also consistent with studies in ferret V1 showing that orientation selectivity develops and matures somewhat earlier than direction selectivity (Chapman and Stryker, 1993; Li et al., 2006). Furthermore, human infants do not show stereopsis until about 4 – 6 months of age (Birch, 1993; Birch et al., 1983; Brown et al., 2007; Held et al., 1980). Similarly, newborn monkeys are also unable to detect objects embedded in random dot stereograms and stereopsis emerges suddenly around 4 weeks of age (O'Dell et al., 1991).

Complex visual functions that presumably depend on the maturation of extrastriate visual areas have an extended developmental timecourse. For instance, contour integration abilities develop comparatively late. Kovacs et al. (1999) reported that children younger than 3 years of age were unable to identify a coherent contour defined by a circular ring of Gabor patches imbedded in noise, and their ability to perform the task improved into their teenage years. In monkeys, this integrative task is late to develop as well, with an inability to perform contour integration prior to about 16 weeks and full maturation requiring at least one year (Kiorpes and Bassin, 2003). Kiorpes and Movshon (2004) showed that unlike contour integration tasks, monkeys could perform a motion direction discrimination task at the earliest ages studied (3–5

weeks), but the maturation of this visual function continued up to 3 years. Although, human infants can detect directional motion cues at about 2 months of age (Braddick et al., 2003), coherent motion sensitivity was found to be adultlike at around 3 years of age (Parrish et al., 2005). However, some aspects of motion perception appear immature up to 7 years or more (Ellemberg et al., 2003; Giaschi and Regan, 1997; Parrish et al., 2005), and even perhaps even into adolescence (Bucher et al., 2006). Therefore, the different developmental trajectories of different aspects of feedback connections (drastic change in areal and laminar proportion from 4-6 weeks versus the slow monotonic rate of refinement in peak density, median NND and Q3 values) mirrors the multiple developmental trajectories of different visual functions.

We have shown that feedback connections to ferret primary visual cortex from the supra- and infragranular layers of multiple visual areas undergo extensive remodeling in their spatial layout during the period after eye-opening. Remarkably, the presence of aspects of 'adult-like' connections at four weeks of age suggests that the basic pattern of feedback connections to primary visual cortex is present before eye opening. Baldwin et al. (2012) recently demonstrated that the adultlike pattern of cortical connections between V1 and V2 is also present in early postnatal monkeys. However, they also show refinement of connections between 2 to 8 weeks postnatal. Lastly, we show that while the change in the areal and laminar proportion of feedback from each visual area takes on a different developmental trajectory, many features of feedback circuitry from multiple sources do in fact refine at similar rates. Our results confirm and extend the notion that at least some aspects of cortical maturation occur in concert in multiple visual areas.

References:

Angelucci A, Clasca F, Sur M. 1996. Anterograde axonal tracing with the subunit B of cholera toxin: a highly sensitive immunohistochemical protocol for revealing fine axonal morphology in adult and neonatal brains. J Neurosci Methods 65:101–112.

Baker GE, Thompson ID, Krug K, Smyth D, Tolhurst DJ. 1998. Spatial-frequency tuning and geniculocortical projections in the visual cortex (areas 17 and 18) of the pigmented ferret. European Journal of Neuroscience. 10:2657-2668.

Baldwin MK, Kaskan PM, Zhang B, Chino YM, Kaas JH. 2012. Cortical and subcortical connections of V1 and V2 in early postnatal macaque monkeys. J Comp Neurol. 520(3):544-69.

Banks MS, Stephens BR, Hartmann EE. 1985. The development of basic mechanisms of pattern vision – Spatial-frequency channels. Journal of Experimental Child Psychology, 40, 501–527.

Barone P, Dehay C, Berland M, Bullier J, Kennedy H. 1995. Developmental remodeling of primate visual cortical pathways. Cereb Cortex.5(1):22-38.

Batardiere A, Barone P, Dehay C, Kennedy H. 1998. Area-specific laminar distribution of cortical feedback neurons projecting to cat area 17: quantitative analysis in the adult and during ontogeny. J Comp Neurol. 396(4): 493-510.

Batardière A, Barone P, Knoblauch K, Giroud P, Berland M, Dumas AM, Kennedy H. 2002. Early specification of the hierarchical organization of visual cortical areas in the macaque monkey. Cereb Cortex.12(5):453-65.

Berezovskii VK, Nassi JJ, Born RT. 2011. Segregation of feedforward and feedback projections in mouse visual cortex. J Comp Neurol. 519(18):3672-83.

Birch EE, Gwiazda J, Held R. 1983. The development of vergence does not account for the development of stereopsis. Perception, 12:331–336.

Bourgeois JP, Patricia S, Goldman-Rakic, Rakic P. 1994. Synaptogenesis in the Prefrontal Cortex of Rhesus Monkeys. Cerebral Cortex. 4:78-96.

Braddick OJ, Wattam-Bell J, Atkinson J. 1986. Orientation specific cortical responses develop in early infancy. Nature. 320:617-619.

Braddick OJ. 1993. Orientation- and motion-selective mechanisms in infants. In K. Simons (Ed.), Early visual development: Normal and abnormal (pp. 163–177).
New York: Oxford University Press.

Braddick OJ, Atkinson J, Wattam-Bell J. 2003. Normal and anomalous development of visual motion processing: Motion coherence and ‘dorsal stream vulnerability’. Neuropsychologia. 41:1769–1784.

Braddick OJ, Birtles D, Wattam-Bell J, Atkinson J. 2005. Motion- and orientation-specific cortical responses in infancy. Vision Research, 45, 3169–3179.

Braddick OJ, Atkinson J. 2011. Development of human visual function. Vision Res. 51(13):1588-609.

Brown AM, Lindsey DT, Satgunam P, Miracle JA. 2007. Critical immaturities limiting infant binocular stereopsis. Invest Opthalmol Vis Sci. 48(3):1424-34.

Bucher K, Dietrich T, Marcar VL, Brem S, Halder P, Boujraf S. 2006. Maturation of luminance- and motion-defined form perception beyond adolescence: A combined ERP and fMRI study. Neuroimage, 31(4):1625–1636.

Burkhalter A, Bernardo KL, Charles V. 1993. Development of local circuits in human visual cortex. J Neurosci. 13(5):1916-31.

Burkhalter A. 1993. Development of forward and feedback connections between areas V1 and V2 of human visual cortex. Cereb Cortex. 3(5):476-87.

Callawy EM, Katz LC. 1990. Emergence and refinement of clustered horizontal connections in cat striate cortex. J. Neurosci. 10(4):1134-53.

Callawy EM, Katz LC. 1991. Effects of binocular deprivation on the development of clustered horizontal connections in cat striate cortex. Proc Natl Acad Sci. 88(3):745-9.

Cantone, G, Xiao J, McFarlane N, Levitt, JB. 2005. Feedback connections to ferret straite cortex: Direct evidence for visuotopic convergence of feedback inputs. JCN. 487:312-331.

Changeux JP, Danchin A. 1976. Selective stabilisation of developing synapses as a mechanism for the specification of neuronal networks. Nature. 264(5588):705-12

Chapman B, Stryker MP. 1993. Development of orientation selectivity in ferret visual cortex and effects of deprivation. J Neurosci. 13(12):5251-62.

Chapman B, Stryker MP, Bonhoeffer T. 1996. Development of orientation preference maps in ferret primary visual cortex. J Neurosci. 16(20):6443-53.

Condé F, Lund JS, Lewis DA. 1996. The hierarchical development of monkey visual cortical regions as revealed by the maturation of parvalbumin-immunoreactive neurons. Brain Res Dev Brain Res. 96(1-2):261-76.

Coogan TA, Burkhalter A. 1988. Sequential development of connections between striate and extrastriate visual cortical areas in the rat. J Comp Neurol. 278(2):242-52.

Coogan TA, Van Essen DC. 1996. Development of connections within and between areas V1 and V2 of macaque monkeys. J Comp Neurol. (3):327-42.

Crowley JC, Katz LC. 2000. Early development of ocular dominance columns. Science. 290(5495):1321-4.

Dehay C, Kennedy H, Bullier J. 1988. Characterization of transient cortical projections from auditory, somatosensory, and motor cortices to visual areas 17, 18, and 19 in the kitten. J Comp Neurol. 272(1):68-89.

Durack JC, Katz LC. 1996. Development of horizontal projections in layer 2/3 of ferret visual cortex. Cereb. Cortex. 6: 178-183.

Ellemberg D, Lewis TL, Meghji KR, Maurer D, Guillemot JP, Lepore F. 2003. Comparison of sensitivity to first- and second-order local motion in 5-year olds and adults. Spatial Vision. 16(5):419-428.

Erisir A, Harris JL. 2003. Decline of the critical period of visual plasticity is concurrent with the reduction of NR2B subunit of the synaptic NMDA receptor in layer 4. J Neurosci. 23(12):5208-18.

Flechsig, P. 1901. Developmental (myelogenetic) localisation of the cerebral cortex in the human subject. Lancet, 2:1027-1029.

Giaschi D, Regan D.1997. Development of motion-defined figure-ground segregation in preschool and older children, using a letter-identification task. Optometry and Vision Science. 74:761–767.

Harwerth RS, Smith EL 3rd, Duncan GC, Crawford ML, von Noorden GK. 1986. Multiple sensitive periods in the development of the primate visual system. Science. 232(4747):235-8.

Held R, Birch EE, Gwiazda J. 1980. Stereoacuity of human infants. Proceedings of the National Academy of Sciences of the United States of America, 77,5572–5574.
Huttenlocher PR. 1979. Synaptic density in human frontal cortex - developmental changes and effects of aging. Brain Res. 163(2):195-205
Innocenti GM, Price DJ. 2005. Exuberance in the development of cortical networks. Nat Rev Neurosci. 6(12):955-65.
Issa NP, Trachtenberg JT, Chapman B, Zahs KR, Stryker MP. 1999. The critical period for ocular dominance plasticity in the ferret's visual cortex. J Neurosci. 19(16):6965-78.
Kato N, Ferrer JM, Price DJ. 1991. Regressive changes among corticocortical neurons projecting from the lateral suprasylvian cortex to area 18 of the kitten's visual cortex. Neuroscience 43(2-3):291-306.
Khalil R, Levitt JB. 2012. Zinc histochemistry reveals circuit refinement and distinguishes visual areas in the developing ferret cerebral cortex. Brain Struct Funct. 218(5):1293-1306.
Kiorpes L, Bassin SA. 2003. Development of contour integration in macaque monkeys. Vis Neurosci. 20(5):567-75.
Kiorpes L, Movshon JA. 2004. Development of sensitivity to visual motion in macaque monkeys. Visual Neuroscience, 21, 851–859.
Kovács I, Kozma P, Fehér A, Benedek G. 1999. Late maturation of visual spatial integration in humans. Proceedings of the National Academy of Sciences, USA, 96, 12204–12209.
Lewis TL, Maurer D. 2005. Multiple sensitive periods in human visual development: evidence from visually deprived children. Dev Psychobiol.46(3):163-83.
Li Y, Fitzpatrick D, White LE. 2006. The development of direction selectivity in ferret visual cortex requires early visual experience. Nat Neurosci. 9(5):676-81.
Manger PR, Kiper D, Masiello I, Murrilo L, Tettoni L, Hunyadi Z, Innocenti GM. 2002. The representation of the visual field in three extrastriate areas of the ferret (Mustela putorius) and the relationship of retinotopy and field boundaries to callosal connectivity. Cerebral Cortex. 12:423-437.
O'Dell C, Boothe RG. 1997. The development of stereoacuity in infant rhesus monkeys. Vision Res. 37(19):2675-2684.
Parrish EE, Giaschi DE, Boden C, Dougherty R. 2005. The maturation of form and motion perception in school age children. Vision Research. 45:827-837.
Price DJ. 1986. The postnatal development of clustered intrinsic connections in area 18 of the visual cortex in kittens. Brain Res. 389(1-2):31-8.
Price DJ, Blakemore C. 1985. Regressive events in the postnatal development of association projections in the visual cortex. Nature. 316(22)721-724.
Price DJ, Ferrer JM, Blakemore C, Kato N. 1994. Postnatal development and plasticity of corticocortical projections from area 17 to area 18 in the cat's visual cortex. J Neurosci. 14:2747-62.
Price DJ, Zumbroich TJ. 1989.Postnatal development of corticocortical efferents from area 17 in the cat's visual cortex. J Neurosci. 9(2):600-13.
Rakic P, Bourgeois JP, Eckenhoff MF, Zecevic N, Goldman-Rakic PS. 1986. Concurrent overproduction of synapses in diverse regions of the primate cerebral cortex. Science. 232(4747):232-5.

Ruthazer ES, Stryker MP.1996. The role of activity in the development of long-range horizontal connections in area 17 of the ferret. J. Neurosci. 15(22): 7253-69.

Wattam-Bell J. 1991. The development of motion-specific cortical responses in infants. Vision Research. 31:287-297.

Wong-Riley M.1979. Changes in the visual system of monocularly sutured or enucleated cats demonstrable with cytochrome oxidase histochemistry. Brain Res 171(1):11–28

Zhang B, Zheng J, Watanabe I, Maruko I, Bi H, Smith EL 3rd, Chino Y. 2005. Delayed maturation of receptive field center/surround mechanisms in V2. Proc Natl Acad Sci 102(16):5862-7.

CHAPTER 4
Postnatal maturation of feedforward projections from ferret primary visual cortex

4.1 Abstract

The mammalian visual cortex is comprised of multiple areas interconnected by a complex network of interareal feedforward and feedback circuits. We studied the postnatal development of feedforward projections from ferret primary visual cortex (V1) to multiple cortical targets from four to eight weeks postnatal. Our objective was to determine whether the postnatal refinement of feedforward projections parallels that of feedback cortical circuits. We also wished to reveal if feedforward pathways from V1 to different target areas refine with a similar rate. We injected the neuronal tracer CTb into V1 of juvenile ferrets, and visualized the distribution and pattern of orthogradely labeled axon terminals in extrastriate cortex. We then quantified the laminar and tangential extent of terminal fields in each area, as well as the density of labeled synaptic boutons and the interbouton interval along individual labeled axons. By 4 weeks postnatal (before eye opening) there are substantial numbers of orthogradely-labeled axons and terminals in areas 18, 19, 21, and the Suprasylvian cortex. As early as 4 weeks of age, orthogradely labeled terminals and retrogradely labeled cells were organized into essentially overlapped clusters, indicating reciprocal feedforward and feedback connections of each extrastriate area with V1. Bouton density of feedforward projections to all areas examined declines from six weeks to eight weeks postnatal (5.5 $x10^7$ to 2.1 $x10^7$ boutons per mm^3). Similarly, interbouton intervals along feedforward axons to all visual areas increase over the same postnatal period (6-8 weeks) from 0.85 um to 1.52 um. Furthermore, maximum tangential extent of individual feedforward terminals decrease in areas 18 and Ssy over the same postnatal period, while in areas 19 and 21 extent remains unchanged. Our results suggest while the basic organization of

feedforward projections from V1 to multiple visual areas is present before eye opening, these circuits remodel extensively in the weeks following eye opening. This postnatal period of refinement occurs at a similar rate in all visual cortical areas and appears to require early postnatal visual experience.

4.2 Introduction

The pattern of anatomical connections in the adult visual cortex is remarkably precise, and ultimately dictates receptive field properties of individual neurons and adult cortical function. However, during postnatal development, visual circuits undergo a period of extensive remodeling ultimately leading to the emergence of mature adult circuits. A common mechanism governing the refinement of many developing corticocortical and intracortical pathways is the initial overproduction of projections, followed by the removal of inappropriate connections to yield the mature adult pattern (Changeux and Danchin, 1976; Rakic et al., 1986; Innocenti and Price, 2005). Intracortical connections within primary visual cortex (V1) of several species (cat, ferret, human, monkey) undergo substantial postnatal refinement (Huttenlocher, 1979; Price, 1986; Callaway and Katz, 1990; Burkhalter et al., 1993; Coogan and Van Essen, 1996; Durack and Katz, 1996; Ruthazer and Stryker, 1996). Similarly, corticocortical connections between different mammalian visual cortical areas have been shown to refine and reorganize as well (Dehay et al., 1988; Price and Blakemore, 1989; Price and Zumbroich, 1989; Barone et al., 1995; Batardiere et al., 1998, 2002). The anatomical refinement of visual cortical circuits presumably underlies the maturation of neuronal physiological properties, and is therefore one indicator of functional maturity. We are

particularly interested in characterizing the postnatal refinement of interareal feedforward connections in the ferret visual cortex. Specifically we wish to reveal whether different aspects of feedforward projections from V1 to multiple extrastriate areas refine with a similar postnatal timecourse; we also wish to compare the postnatal maturation of interareal feedforward and feedback circuits between V1 and its cortical partners. Differential development of distinct cortical circuits could underlie the known differences in the rate at which various perceptual abilities mature (Harwerth et al., 1986; Lewis and Maurer, 2005; Braddick and Atkinson, 2011).

Feedforward projections from V1 to extrastriate visual areas refine during the postnatal period in a number of species. Price and Zumbroich (1989) examined the postnatal development of feedforward projections from cat V1 to extrastriate areas 18, 19, 12a, and Ssy. Their data suggested a hierarchical sequence of development of feedforward projections. At postnatal day 4, dense orthograde label at topographically appropriate regions was found only in area 18; areas 19, 21a and Ssy contained only sparse label. By postnatal day12, dense label was found in all areas. Carić and Price (1996) revealed an improvement in the accuracy with which corticocortical cells in V1 target appropriate regions in extrastriate cortex. Specifically, this change occurs primarily among those V1 neurons that innervate a wide region of the deep layers of extrastriate cortex at birth. Similarly, in a longitudinal study on the development of feedforward and feedback connections between V1 and V2 in human brains, Burkhalter et al. (1993) demonstrated that by 4 months of age feedforward connections from V1 to V2 have assumed the laminar features of mature connections. In contrast, at 4 months of age feedback connections to V1 are still relatively immature, showing terminations in

inappropriate layers. The findings suggest that feedforward connections from V1 to V2 attain their mature termination pattern before feedback connections from V2 to V1. Recent work in mouse visual cortex by Berezovskii et al. (2011) provides evidence for dissociation in the timing of axonal outgrowth of feedforward and feedback connections as well. The authors revealed that feedforward axon terminals from primary visual cortex to extrastriate cortex were present at the earliest age studied (P2). In Contrast, feedback neurons were first observed in the lateral medial area (LM) of extrastriate cortex nearly ten days later (P11). The results are in agreement with previous study in monkeys and humans (Batardiere et al., 2002; Burkhalter, 1993) suggesting that feedforward connections from primary visual cortex develop relatively early in postnatal development, while feedback connections are delayed in their timing of axonal outgrowth. Therefore, feedforward projections appear to refine in the postnatal period and attain maturity before feedback circuits. We are now poised to compare the refinement of feedforward projections from V1 to multiple visual areas with the refinement of feedback projections from these same areas we have previously described to determine if there is a dissociation in their timecourse of refinement.

There has been no detailed analysis of developmental changes in different aspects of feedforward projections from V1 to extrastriate visual areas in any species. In this study, we describe the developmental refinement of feedforward projections from V1 to multiple visual areas in ferret visual cortex from four weeks to eight weeks postnatal. We quantified the tangential extent of terminal fields in each area, as well as the density of labeled synaptic boutons and the interbouton interval along individual labeled axons. Specifically, we were interested in determining whether these different

anatomical features of feedforward circuitry refine simultaneously in all visual cortical areas. By 4 weeks postnatal (before eye opening), we find substantial numbers of orthogradely-labeled axons and terminals in areas 18, 19, 21, and the Suprasylvian cortex. In addition, orthogradely labeled terminals and retrogradely labeled cells were organized into essentially overlapped clusters, indicating reciprocal feedforward and feedback connections of each extrastriate area with V1. Bouton density of feedforward projections to all areas examined declines from six weeks to eight weeks postnatal. Similarly, interbouton interval of feedforward projections to all visual areas increase over this same postnatal period. This mirrors our finding that there is a greater density of retrogradely labeled cells providing feedback to area 17 in the juvenile ferret compared to the adult. Furthermore, our results suggest that feedforward circuitry from V1 to multiple cortical areas undergoes extensive refinement around the time of eye opening. This refinement process occurs at a similar rate in all visual cortical areas and requires early postnatal visual experience.

4.3 Materials and Methods

Protocol for anatomical tracer injections

We studied 6 female ferrets (Mustela putorius furo) at four postnatal ages: 4 weeks (n=2), 6 weeks (n=2), and 8 weeks (n=2). Animals were obtained from Marshall Farms (North Rose, NY); kits were housed with the jill under a 12 h light/dark cycle. All procedures conformed to National Institutes of Health guidelines. Prior to surgery, ferrets were sedated with an intramuscular injection of ketamine (25 mg/kg) and xylazine (2 mg/kg). The animal's head was fixed in a stereotaxic apparatus, and

secured with ear bars. The animals were respired using a pump, which delivered a mixture of 1%-2% isoflurane, in O_2. A small mask was placed on the nose and snout to administer isoflurane throughout the surgery. The EKG, pulse, tissue oxygenation, and rectal temperature were continuously monitored throughout the rest of the surgery, and maintained at appropriate levels. During a sterile surgery, Lidocaine HCL was injected into the scalp prior to incisions. The scalp was retracted and a craniotomy and durotomy were performed on either the left or right hemisphere. Cholera toxin B subunit (CTb: List Biological Laboratories, Campbell CA) was reconstituted in 0.1M potassium phosphate buffer (1%, pH.6), and either pressure injected or delivered with current into primary visual cortex. Iontophoretic injections using glass micropipettes (aperture 10-15 µm) were performed by passing anodal current at 2 µA for 10 minutes with a 7-second on-off cycle at two cortical depths to ensure that the extent of the injection site spanned both the upper and lower layers of the cortex. This method of injection typically yields an injection core with a diameter of 800-1000 µm. Pressure injections were delivered with a Picospritzer (Parker Hannifin, Fairfield, NJ), using glass micropipettes (aperture 30-40 µm) at two cortical depths with 2 X 10 msec pulses at each location. Both methods of injections applied iontophoretically or by pressure yielded comparable volumes of CTb in the brain.

Following the injections, craniotomies were filled with sterile Gelfoam. Lidocaine was injected into the wound margins before the scalp was sutured, and an intramuscular injection of a broad spectrum antibiotic (ampicillin: 25 mg/kg) and analgesic (buprenorphine: 0.05 mg/kg) was administered for 2 days postoperatively. After a survival period of five to seven days, the animals were sedated with ketamine

(25 mg/kg) + Xylazine (2 mg/kg), then euthanized with an intraperitoneal overdose of pentobarbital (100 mg/kg).

Protocol for tissue fixation and histological processing

Animals were transcardially perfused using saline solution followed by a 4% paraformaldehyde solution, then a 4% paraformaldehyde plus 10% sucrose solution. The brains were removed from the skull and the posterior portion was blocked, and placed in a postfix solution of 4% buffered paraformaldehyde plus 30% sucrose for 2-3 hours. The brains were then placed into a 0.1 M PB solution with 30% sucrose for 2 days until they were sunk.

Frozen tangential or sections were cut at 40 microns using a sliding microtome. The sections were separated into four numbered series. The first and the third series were processed to reveal the CTb label using a modified version of the CTb protocol described by Angelucci et al. (1996). All the procedures performed were done on free floating sections, and all solutions were made with 0.1 PBS PH (7.4). Sections were rinsed in PBS, incubated in a 1% H_2O_2 solution to eliminate endogenous peroxidase, and rinsed again in PBS. This was followed by a short incubation in 0.1M glycine solution, rinsed in PBS, then incubated overnight at 4° C in a blocking solution containing 4% normal rabbit serum (NRS), 2.5% bovine serum albumin (BSA), and 1% Triton-X solution to reduce non-specific staining. The sections were rinsed in PBS, then incubated for 48 hours in a solution containing a 1:5,000 dilution of goat anti-choleraganoid (primary antibody, List Biological Laboratories, Campbell CA), 2% NRS, 2.5% BSA, and 1% Triton-X. The sections were then rinsed in PBS, and incubated in a

1:200 dilution of biotinylated rabbit anti-goat IgG (secondary antibody, Vector Laboratories, Burlingame CA), 2% NRS, 2.5% BSA, and 2% Triton. After several rinses in PBS and a brief incubation in a blocking solution, the tissue sections were incubated in a solution containing Standard Elite ABC Kit (Vector Laboratories, Burlingame CA). Finally the tracer was developed with diaminobenzidine, and sections were mounted on subbed slides, dehydrated and cleared in xylene, and coverslipped in Permount.

Sections from the remaining series were processed for cytochrome oxidase (CO) (Wong-Riley, 1979), Nissl substance, or synaptic zinc following the protocol described in Khalil and Levitt (2012). Sections stained for CO and synaptic zinc were compared with adjacent CTb stained sections to assign cells to particular areas and layers.

Reconstruction of label

We relied on the following criteria to ensure that our injections were restricted to area 17 and did not intrude onto area 18 or white matter. The laminar location of the injection core was visually inspected using adjacent sections stained for Nissl or synaptic zinc to ensure that none of our cases intruded on white matter. Injection core was defined as the uniform, densely labeled region of CTb. We observed a typical pattern of label in all the layers (A, A1, and C) of the LGN following our area 17 injections. Consistent with previous reports (Baker et al., 1998), the density of labeled cells was greatest in the two A layers, but a small number of cells were also present in the C layers. In contrast, if the injection intruded on area 18, we would have found many more cells in the C-layers of the LGN. Furthermore, the lack of extensive label in ventral

cortex (which results from area 18 injections) was interpreted as further evidence that the location of our injections was indeed in Area 17.

Section outlines from every fourth semi-tangential section containing CTb labeled feedforward terminal clusters were traced, and axon terminals found within each visual area were plotted in the Neurolucida tracing and reconstruction program (MicroBrightField, Wiliston VT). Fiducial landmarks such as blood vessels were marked, and comparison of CTb tracings with adjacent CO, synaptic zinc, or Nissl stained sections was used for precise local alignment. Correct determination of laminar and areal boundaries was critical to our analysis. We have previously shown that visual cortical areas in juvenile ferrets may reliably be distinguished in sections stained for synaptic zinc (Khalil and Levitt, 2012); observed areal boundaries in zinc-stained sections were well correlated with adjacent CO sections and prior descriptions (Innocenti et al., 2002). Depending on the retinotopic location of our injection cores, one or several feedforward terminal clusters were found in each extrastriate area. Sections containing CTb-labeled terminal clusters or stained for CO, zinc, or Nissl were examined and photographed with bright field illumination using a Nikon Eclipse Ti inverted scope either at low power (4x), (10x) lens or high power (100x) oil immersion lens. Contrast and brightness of photomicrographs were enhanced in image processing software (Adobe Photoshop CS5, v.12) for display purposes, but were otherwise unaltered. All figures were assembled in (Adobe Photoshop CS5, v.12) and all line graphs and histograms were generated in Microsoft Excel.

Bouton density and interbouton interval

We analyzed the refinement of feedforward terminals by quantifying the density of labeled synaptic boutons and interbouton interval along individual labeled axons. In each target area, feedforward projections from V1 were analyzed by marking all reliably detectable synaptic boutons in a randomly placed 10 µm square at three different locations in the terminal cluster. We placed 3-4 sample boxes in the very center of the terminal field, at locations 50% of the distance from center to terminal edge (mid-periphery), and 95% of the distance from center to terminal edge (periphery). Samples were collected from at least 3 sections in each animal. Boutons were positively identified based on their staining intensity, which was much higher than adjacent portions of the axons. Boutons were typically round or oval shaped and are three times as thick as the adjacent axon portion. Boutons were counted through the depth of each box, with an exclusion zone of 1 µm at the top and bottom of the section. To minimize overcounting, boutons were counted if they fell entirely within the box, or touched the top and right sides; boutons touching the bottom and left sides of the counting box were excluded. Bouton density was calculated separately for each sample by dividing the number of boutons in a sample box by the volume of tissue. To assess developmental changes in bouton density of feedforward projections to each target area, we computed median values in each area at each developmental age. Similarly, boutons along individual axons in each target area were marked in the core of the terminal cluster as well in the periphery. The number of axons traced varied with age (6-10 axons). We subsequently pooled interbouton intervals to construct frequency histograms. To assess developmental changes in interbouton intervals of feedforward projections to each

target area, we computed median values in each area at each developmental age.

Tangential extent of terminal clusters

To reveal developmental changes in the territory occupied by feedforward projections from V1 to each target area, we quantified the tangential extent of terminal fields in each visual area throughout development. We tracked individual feedforward clusters through successive sections, and traced the maximum tangential extent of each cluster in any one section. In some cases, there were multiple terminal clusters in each area; therefore the maximum tangential extent of every individual cluster was measured. Terminal clusters were photographed with bright field illumination using a Nikon Eclipse Ti inverted scope or Olympus BX60 scope and imported into (Adobe Photoshop CS5, v.12). Contrast and brightness of photomicrographs were subsequently enhanced to reveal fine axonal details, but were otherwise unaltered.

Feedback cells in each area were typically superimposed upon feedforward terminal clusters, but spanned a wider region. To compare feedforward input to each target area with the amount of feedback provided to V1 throughout development, we computed a ratio of the maximum areal extent of all feedback clusters by the maximum areal extent of all feedforward clusters. We tracked successive sections to locate the section containing the maximum areal extent of the feedback cluster. We subsequently outlined the region that encompassed 90% of the areal extent of feedback clusters. Similarly, the section that contained the maximum extent of a feedforward cluster was chosen and a contour was drawn around the area that contained 90% of the feedforward terminals. We computed the ratio of the areal extent of the region

encompassing 90% of feedback cells to the areal extent of the region encompassing 90% of the feedforward terminals. To establish whether the area of overlap between feedback cells and feedforward terminals change throughout development we computed the ratio of the areal extent of feedforward terminal clusters by the areal extent of feedback cell cluster.

All statistical analyses were performed in MATLAB (The Mathworks, Natick, MA). We used the Kruskal–Wallis test to assess statistical differences in bouton density, interbouton interval, and spatial extent values among age groups and areas with a significance level of $p < 0.05$. Post hoc pair-wise comparisons between ages (in each area) and areas (at each age) were then computed using a Bonferroni correction.

4.4 Results

The characteristics of all our injection cases are summarized in Table 4.1. The injection core is defined as the uniformly dense region of CTb label typically ranging between 700 and 1500 μm in diameter. We confirmed that all injection sites were confined to area 17, and spanned all six layers without intruding on the white matter. This was verified by comparing tracings of the injection core with adjacent sections stained for CO, synaptic zinc, and Nissl substance to locate the areal borders between areas 17 and 18 in juvenile visual cortex based on prior descriptions (Innocenti et al., 2002; Khalil and Levitt, 2012). Correct identification of visual cortical areas in the juvenile was crucial to our analysis as one of our primary goals was to track

simultaneously the postnatal refinement of feedforward projections from primary visual cortex to multiple visual areas.

The pattern of feedforward labeling in extrastriate cortex of a 6 week old ferret is depicted in a representative photomicrograph of a semi-tangential section in Fig. 4.1A. The black arrowheads indicate feedforward terminal clusters in area 18. The black arrow indicates a small feedforward terminal cluster in area 19. The white arrowheads indicate feedforward clusters in area Ssy. We find that in all areas examined, feedforward terminal clusters are typically superimposed with feedback cells, reflecting the reciprocity of connections between primary visual cortex and these extrastriate visual areas. Typically, a single feedforward terminal cluster was observed in each target area. Multiple distinct feedforward clusters in a single area were observed in rare cases. Fig. 4.1B is a higher magnification image of the region indicated by the dashed rectangle in panel A encompassing a feedforward cluster in area 18. In Fig. 4.1B, feedforward axon terminals are observed in layer III, although feedforward terminals can generally be found throughout all laminae, but at much lower density. In Fig. 4.1C, a higher magnification image of an axon terminal in area 18 with multiple small and large boutons is shown. We find that axons formed both terminal boutons and boutons en passant, although the majority of boutons found at all ages were en passant. However, it was our impression that terminal boutons were found more frequently in the 8 week olds than in the younger animals.

Table 4.1. Characteristics of injection cases

Age	Case	Core diameter (µm)	Core volume (mm^3)	Mean Core volume (mm^3)	Max DV extent (µm)	Max ML extent (µm)	Laminar intrusion	# of labeled FF clusters 18/19/21/Ssy
4 wks	220	900	0.42	1.575	1000	800	More SG/little less IG	1 / 1 / 1 / 1
	247	1450	2.73		2300	1280	Equal uptake SG & IG	1 / 1 / 1 / 1
6 wks	255	1100	1.26	1.92	1500	800	Equal uptake SG & IG	4 / 2 / 2 / 2
	256	1500	2.58		2400	1280	Equal uptake SG & IG	1 / 1 / 1 / 1
8 wks	200	850	0.46	0.44	800	640	Mostly SG/ some IG	1 / 1 / 1 / 1
	235	700	0.42		1000	640	Mostly SG/ some IG	1 / 1 / 1 / 1

Age	Case	Total # of marked boutons in 18 (core) / (periphery)	Total # of marked boutons in 19 (core) / (periphery)	Total # of marked boutons in 21 (core) / (periphery)	Total # of marked boutons in Ssy (core) / (periphery)
4 wks	220	201 / 125	122 / 125	131 / 126	111 / 117
	247	110 / 115	132 / 133	140 / 106	151 / 126
6 wks	255	129 / 138	114 / 155	109 / 130	170 / 163
	256	120 / 125	119 / 133	180 / 129	174 / 112
8 wks	200	221 / 158	143 / 139	143 / 172	199 / 305
	235	158 / 300	180 / 228	178 / 220	243 / 194

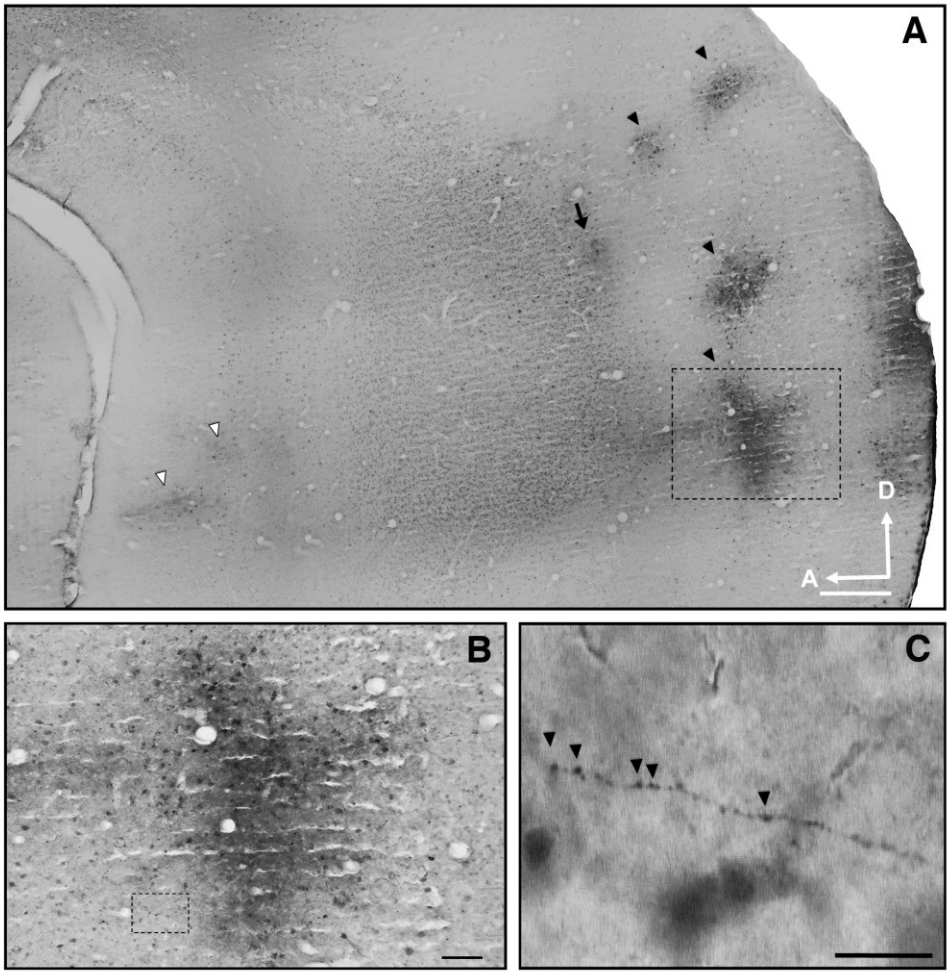

Figure 4.1. Representative area 17 injection in a 6 week old ferret with feedforward terminal clusters in extrastriate cortex. Photomicrographs of a semi-tangential brain section showing the typical pattern of feedforward labeling in extrastriate cortex after a CTb injection in area 17. A: Area 17 injection case with overlapping clusters of orthogradely labeled terminals and retrogradely labeled cells in areas 18, 19, 21, and Ssy. Black arrowheads point to clusters in area 18. Black arrow points to a cluster in area 19. White arrowheads point to clusters in Ssy. Dashed square indicates region shown at higher magnification in B. B: Feedforward terminal cluster in area 18. Dashed square indicates region shown at higher magnification in C. C: CTb labeled axon with en passant boutons appearing as tiny swellings. Arrowheads point to representative boutons. A: anterior, D: dorsal. Scale in A= 500 µm, scale in B= 50 µm, scale in C= 10 µm.

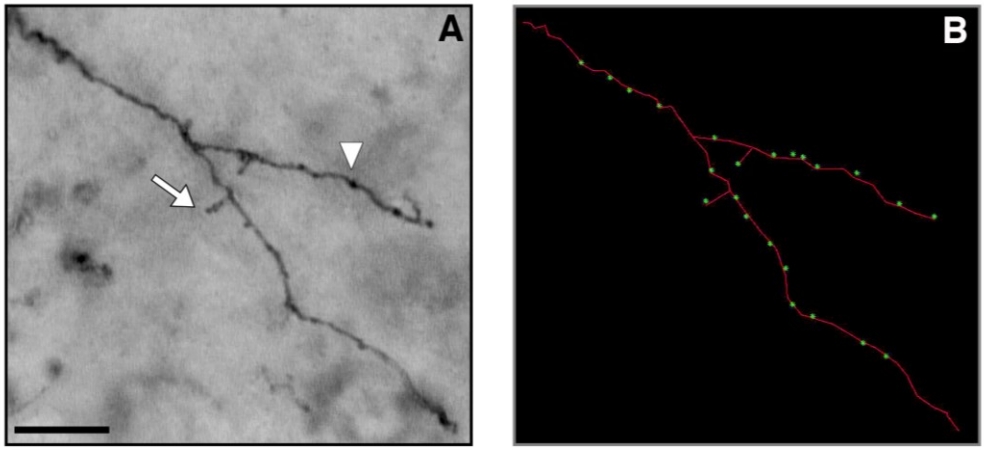

Figure 4.2. Reconstruction of boutons along an orthogradely labeled axon in area 19 of an 8 week old ferret. A: High power photomicrograph of a CTb labeled axon with a bifurcating node with en passant and terminal boutons. B: Neurolucida drawing of the axon shown in A with all the marked boutons shown in green. Arrow points to a terminal bouton and arrowhead points to en passant bouton. Scale bar = 10 µm. The image in A was captured in a focal plane to reveal the majority of labeled boutons. Therefore, the marked boutons shown in green in B may not all be visible in A.

Figure 4.2A shows a representative high power photomicrograph of an orthogradely labeled axon terminal in area 19 of an 8 week old with multiple boutons. The corresponding reconstruction is shown in Fig 4.2B with all boutons marked in green. Not all boutons were in the same focal plane and therefore may not be all be visible in the photomicrograph in Fig 4.2A. The white arrowhead points to an en passant bouton and the white arrow points to a terminal bouton.

To examine developmental changes in feedforward projections from V1 to extrastriate visual areas, we calculated bouton density in each target area at several different ages. We determined this value separately in the core, mid-periphery, as well as periphery of the terminal cluster because we wished to reveal if bouton density from

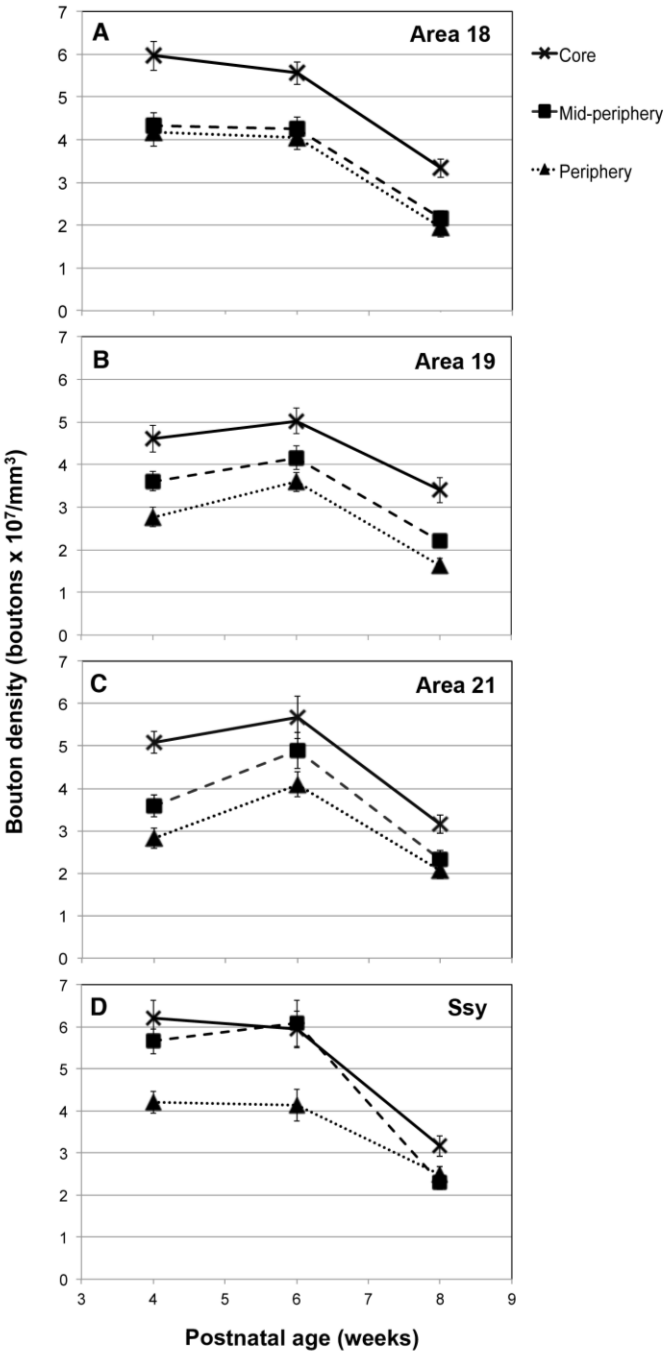

Figure 4.3. Developmental decrease in bouton density of feedforward projections to extrastriate cortex of juvenile ferrets. Bouton densities in the core (A), mid-periphery (B), and periphery (C) of feedforward terminal clusters in areas 18, 19, 21, and Ssy decline with age. Error bars represent ±SEM.

core to periphery was uniform, or if declined. We compared the decline with age of bouton density in each area. Figure 4.3 depicts the change in bouton density in the core, mid-periphery and periphery of each terminal cluster (solid, dashed, and dotted line respectively) as a function of age in areas 18, 19, 21, Ssy. Bouton density at 4 weeks was greatest and ranged from 5.64 x 107 boutons per mm3 in area 18 to 2.62 x 107 boutons per mm3 in area 21. In area 18, bouton density values in the mid-periphery and the periphery were comparable at all ages examined. The developmental changes in bouton density in area 18 and Ssy (Fig 4.3A and 4.3D) are broadly similar. In both areas, bouton density was greatest at 4 weeks of age and declined modestly from 4 to 6 weeks. Moreover, bouton density in the core, mid-periphery and periphery in both areas declines from 6 to 8 weeks of age (Kruskal-Wallis, $p<0.001$ in area 18 and Ssy). Similarly, bouton density in areas 19 and 21 (Fig 4.3B and 4.3C) change modestly from 4 to 6 weeks, but decline significantly from 6 to 8 weeks (Kruskal-Wallis, $p=0.001$ in area 19 and $p<0.001$ in 21). Throughout development, in areas 19 and 21, bouton density remained greatest in the core, followed by mid-periphery, and periphery. By 8 weeks postnatal, bouton density in the core, mid-periphery, and periphery of feedforward terminal clusters in all areas declines significantly (mean values ranged from 2.04 x 107 boutons per mm3 in Area 19 to 3.41 x 107 boutons per mm3 in area 21). Therefore, it appears that bouton density values between core and periphery are more pronounced early in development and are more similar in values by 8 weeks of age (except for area 19).

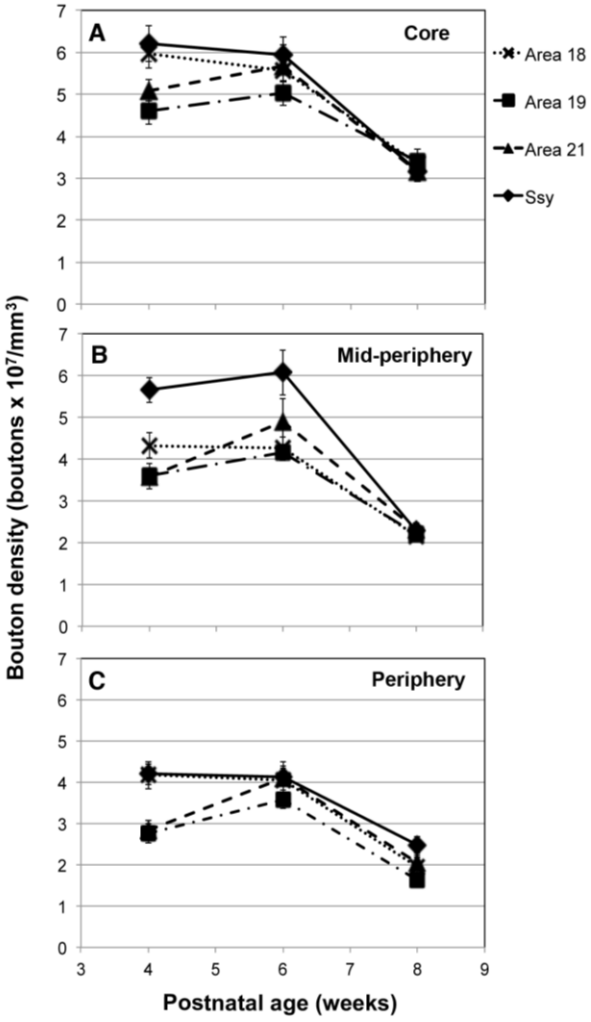

Figure 4.4. Developmental decrease in bouton density of feedforward projections to extrastriate cortex of juvenile ferrets. Bouton densities in the core, mid-periphery, and periphery of feedforward terminal clusters in area 18 (A), area 19 (B), area 21 (C), and Ssy (D) decline with age. Error bars represent ±SEM.

We replotted these data in Figure 4.4 to show more clearly if there is dissociation in the timecourse of refinement in bouton density among areas. Bouton density in the core of feedforward terminal clusters was greatest at 4 weeks of age in all areas examined with a mean value of 5.46 x 10^7 boutons per mm^3 (Figure 4.4A). Bouton density values in the core of both areas 18 and Ssy at 4 weeks were significantly greater than in area 19 (Kruskal-Wallis, p=0.01). Areas 18 and Ssy have the greatest bouton density with a mean value of 6.13 x 10^7

boutons per mm^3. Also, bouton density in the mid-periphery of Ssy was significantly higher than in other areas (Kruskal-Wallis, p=0.01). From 4 to 6 weeks, we observe little or no change in bouton density in the core, mid-periphery, and periphery in all areas. From 6 weeks to 8 weeks postnatal bouton density in the core of all areas declines significantly ($p<0.05$) and converges to a mean value of 3.2×10^7 boutons per mm^3. Similarly, bouton density in the mid-periphery (Figure 4.4B) of feedforward terminal clusters to all target areas declines significantly from 6 weeks to 8 weeks of age (Kruskal-Wallis, p=0.01 for all areas). Lastly, bouton density in the periphery of feedforward terminal clusters to all target areas shows minimal change from 4 to 6 weeks. However, from 6 weeks to 8 weeks we observe a significant decline in bouton density to a mean value of 2.03×10^7 boutons per mm^3 (Kruskal-Wallis, p=0.01 for all areas. Collectively, our data suggest that bouton density in all areas examined is greatest at 4 weeks of age and shows minimal change from 4 to 6 weeks postnatal. The period of major decline in bouton density in all areas appears to be from 6 weeks to 8 weeks postnatal. Furthermore, early on at 4 weeks of age, bouton density is greatest in the core, followed by mid-periphery and than periphery. However, by 8 weeks of age the bouton density in the core, mid-periphery, and periphery of feedforward terminal clusters in all target areas more comparable (mean in core 3.25×10^7 boutons per mm^3: mid-periphery= 2.25×10^7 boutons per mm^3: periphery= 2.03×10^7 boutons per mm^3).

To further assess developmental changes in characteristics of feedforward projections we determined interbouton interval along individual axons in the core and periphery of feedforward clusters. Decreasing bouton density could reflect either greater interbouton intervals along individual axons, or decreased density of feedforward axons

(or indeed both). We followed axons that were in the core or in the periphery of a feedforward terminal cluster and marked all reliably detectable boutons along the entire length of an individual axon. Figure 5 depicts individual frequency histograms of interbouton intervals for each visual area at all postnatal ages in the core (Fig 4.5A) and periphery (Fig 4.5B) of the feedforward cluster. The shape of the distributions can be described as positively skewed for all areas at all postnatal ages. Black arrowheads indicate the median interbouton interval in each area. At 4 weeks of age, the distribution of interbouton intervals in the core and periphery is more peaked with lower median values in all areas (mean interbouton interval among areas in core = 0.86 μm and periphery= 0.84 μm). By 8 weeks postnatal, the shape of the interbouton interval distribution in the core and periphery is dramatically different; the tail of the distribution becomes more prominent reflecting the increase of longer interbouton intervals with age. The mean interbouton interval among areas increases to a value of 1.41 μm in the core and 1.52 μm in the periphery. Thus, although bouton density in all areas examined declined from the core to the periphery, interbouton intervals along axons in the core and in the periphery are nearly identical. This suggests that the axons found in the core and in the periphery are of a similar nature, but it is the density of processes that directly influences the density of boutons throughout the feedforward terminal cluster.

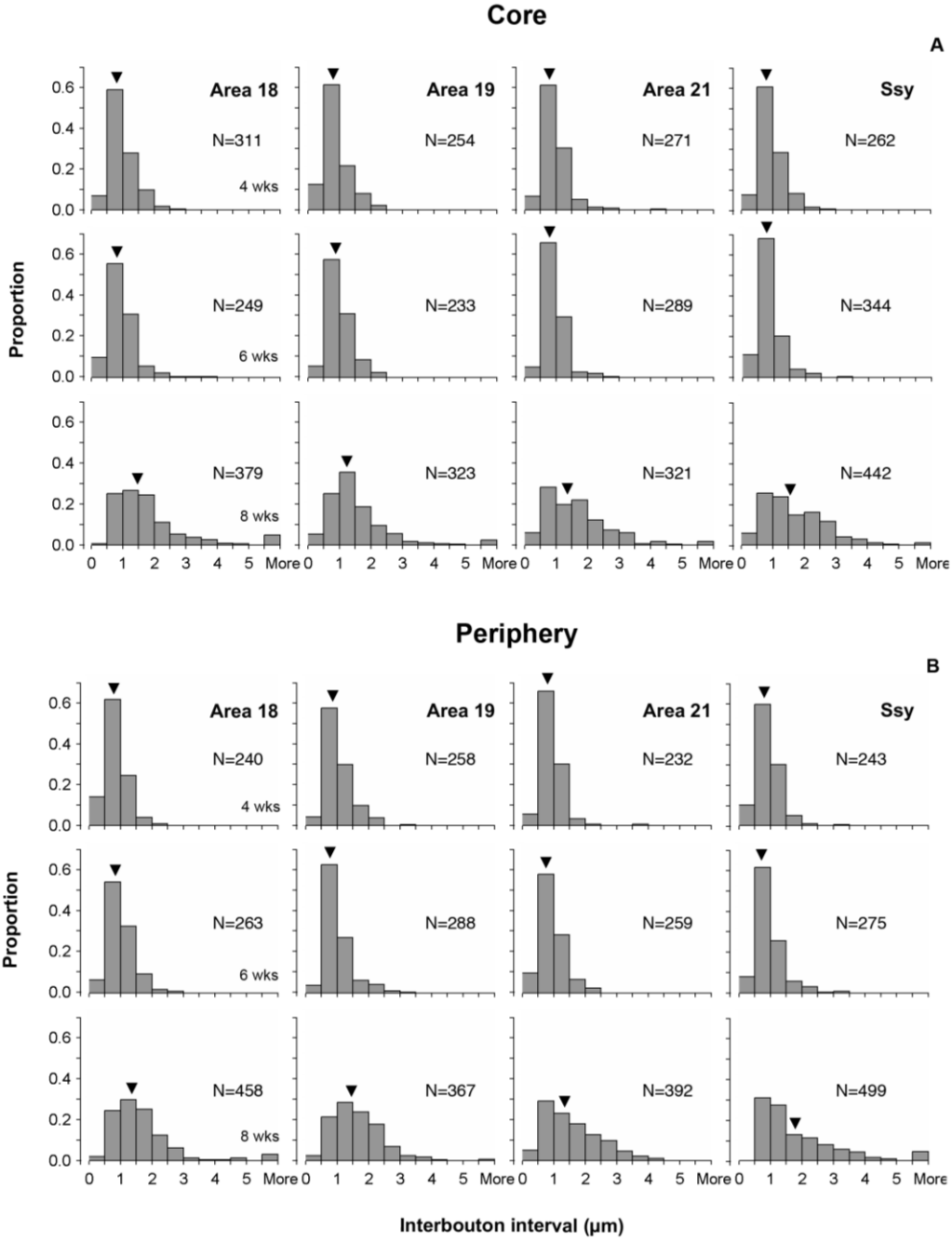

Figure 4.5. Developmental changes in the distribution of interbouton intervals along individual feedforward axons in extrastriate cortex of juvenile ferrets. Frequency distribution histograms of interbouton intervals in the core (A) and periphery (B) of feedforward terminal clusters from V1 to areas 18, 19, 21, and Ssy. Black arrowheads indicate median interbouton interval.

In Figure 4.6 the median interbouton interval values in the core (FIG 4.6A) and periphery (FIG 4.6B) of feedforward clusters in all target areas is plotted as a function of age. It is clear that median interbouton interval value among areas is comparable at all postnatal ages. This value does not change from 4 to 6 weeks postnatal (as we have seen from the interbouton interval frequency distributions in Figure 4.5A and 4.5B). However, there is substantial increase in this value in the core and periphery of all areas from 6 to 8 weeks postnatal that was not significant at the $p<0.05$ significance level. Therefore, it appears that the developmental decline in interbouton interval in the core and the periphery of feedforward terminal clusters of all target areas follows a similar timecourse, again suggesting a similar nature of axons throughout each terminal cluster.

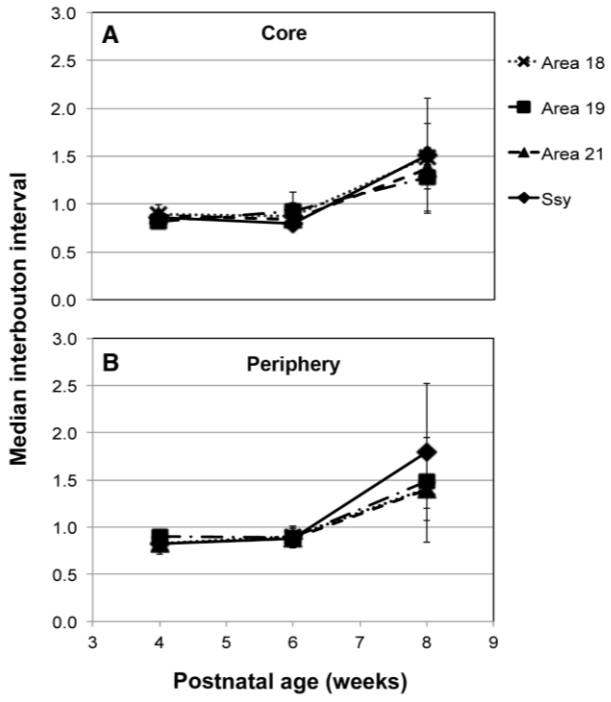

Figure 4.6. Age dependent increase in interbouton interval along individual axons of feedforward terminal clusters in extrastriate cortex of juvenile ferrets. Median interbouton interval in the core (A) and periphery (B) of feedforward terminal clusters from V1 to areas 18, 19, 21, and Ssy. Error bars represent ±SEM.

The cortical territory occupied by feedforward terminals from V1 to each target area could conceivably change in size with age. Therefore, we determined if maximum tangential extent of individual feedforward terminal clusters in each target area changes with age. Figure 4.7A depicts maximum tangential extent of each feedforward terminal cluster in each area as a function of age. The maximum areal extent in Ssy drops by 25% from 4 to 8 weeks postnatal (from 0.4 mm^2 to 0.29 mm^2). Similarly, the maximum areal extent in area 18 drops by 34% from 4 to 8 weeks postnatal (from 0.39 mm^2 to 0.13 mm^2). The maximum areal extent shows a modest increase from 0.18 mm^2 to 0.21 mm^2. In area 21, there is a 50% an increase in the maximum areal extent from 4 to 8 weeks postnatal (from 0.14 mm^2 to 0.29 mm^2). However, at the range of ages examined here, none of the changes we observe in maximum tangential extent with age in all areas examined were not significant at the $p<0.05$ level.

Lastly, we wished to compare the amount of overlap between the area of feedforward terminals with that of feedback cell label to reveal if this overlap region changes with age. Although feedforward terminals and feedback cells were organized into overlapped clusters at all ages examined, it is conceivable that the amount of overlap could change with age, reflecting the retinotopic refinement of either or both projections. The overlap ratios are plotted in Figure 4.7B. The total area innervated by feedforward terminals ranged from 0.24 mm^2 to 0.63 mm^2 at 4 weeks and from 0.28 mm^2 to 0.48 mm^2 at 8 weeks of age. Similarly, total area occupied by feedback cell label ranged from 0.34 mm^2 to 0.98 mm^2 at 4 weeks and from 0.52 mm^2 to 0.95 mm^2 at 8 weeks. Figure 7B shows the overlap ratio of the area of feedforward terminals to the area of feedback cell label. The overlap ratio in Ssy appears to decrease from 4 to 8 weeks from a value of 0.54 to 0.33. In

contrast, the overlap ratio in area 18 appears to decrease from 4 to 8 weeks postnatal from 0.26 to 0.47. Areas 21 shows a modest decrease from 4 to 8 weeks postnatal from 0.38 to 0.34, while area 19 shows a modest increase from 0.37 to 0.46 over the same postnatal period. Similar to maximum tangential extent, the changes we observe in the overlap ratio with age in all areas were not significant at the $p<0.05$ level.

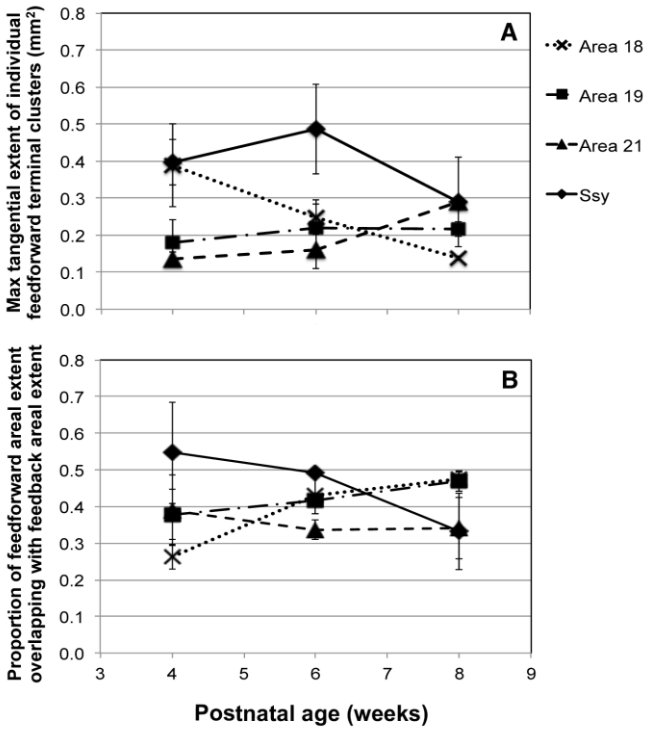

Figure 4.7. Age dependent changes in the spatial extent of feedforward terminals. A: Maximum tangential extent of individual feedforward terminal clusters in each area as a function of age. B: The relative overlap of the area of feedforward terminals with that of the area of feedback cell label. Error bars represent ±SEM.

4.5 Discussion

This is the first study to simultaneously examine multiple aspects of refinement of feedforward projections from V1 to multiple target visual cortical areas. Corticocortical feedforward projections from V1 to extrastriate areas are presumed to provide an excitatory drive endowing neurons in these respective areas with distinctive physiological properties. Therefore, the anatomical refinement of each feedforward pathway from V1 to target visual areas is undoubtedly involved in the maturation of response properties of neurons in extrastriate visual areas. We examined the anatomical refinement of feedforward projections from ferret V1 to extrastriate visual areas. As early as 4 weeks postnatal, feedforward terminals and feedback cells were organized into overlapped clusters, reflecting the reciprocity of connections between V1 and each extrastriate area. We found that bouton density, a measure reflecting the relative contribution of input from primary visual cortex to individual visual areas is very high before the time of eye-opening (4 weeks postnatal). Similarly, interbouton interval along individual axons of feedforward terminals to different target areas is quite low (median= 0.86) at 4 weeks of age. From 6 to 8 weeks postnatal, interbouton interval increases, and bouton density decreases. The maximum tangential extent of individual feedforward terminals decreases in areas 18 and Ssy over the same postnatal period, while in areas 19 and 21 extent remains fairly similar. Moreover, the region of overlap between the area of feedforward terminals and the area of feedback cell label appears to decrease in Ssy and increase in area 18. Our results are broadly consistent with previous studies documenting the refinement of feedforward projections from V1 to

extrastriate visual areas (Burkhalter, 1993; Batardiere et al., 2002; Caric and Price, 1996; Price and Zumbroich, 1989).

We demonstrated that the refinement in bouton density and interbouton interval of feedforward projections to multiple visual areas from 6 to 8 weeks postnatal follows an essentially similar timecourse. However, the maximum tangential extent of individual feedforward terminals, and the amount of overlap of feedforward terminals and feedback cell label in each target area appear to have a unique developmental trajectory. Our results indicate that bouton density declines in all areas at a broadly similar rate. Bouton density values in extrastriate cortex (3.9-5.5 x 10^7 boutons/mm^3) are comparable to bouton density in thalamocortical axons to layer IV of mouse barrel cortex (4.8 x 10^7 thalamocortical synapses/ mm^3: Wimmer et al., 2012). In area 18, bouton density was greatest in the core throughout development, and on average was one and a half times greater than density in the mid-periphery and periphery. This implies that exuberant synapses formed early in development are subsequently decreased in number after eye opening. A critical question remains whether the decline in bouton density is due solely to the elimination of boutons on a given branch, or if it is elimination of boutons and axon branches. Friedlander and Martin (1989) showed similar developmental changes in the development of geniculocortical axons. The authors observed that several aspects of geniculocortical Y-axons that project to area 18 of 4 week old kittens refine during development; a reduction in bouton density, an increase in bouton size, and an increase in the surface area of cortex that is innervated by geniculocortical afferents. Increased spacing of boutons reflected in our interbouton interval measures is likely due to elimination of boutons driven by visual experience.

Since spines are known to be sites of synaptic contacts, it is important to relate the changes we observe in bouton density to potential changes in spine density on postsynaptic targets. Spine density in the visual cortex of the monkey has been shown to undergo dramatic changes during development. Lund et al. (1977) examined the development of neurons in (area 17) of Macaca nemestrina and observed that the dendrites of these neurons show a marked increase in the number of spines on their surface during the first eight weeks of postnatal life. The authors also revealed that spine numbers on these neurons decrease into adulthood. In a subsequent study, Boothe et al. (1979) examined how spine development in spiny stellate cells in layer IVCα and IVCβ, as well as pyramidal neurons in layer IIIB of monkey area 17 proceeds during development. It was found that spine numbers decrease on all neurons between nine months of age and adult (5-7 years), suggesting a protracted period of maturational changes. The normal development and refinement of spines on visual cortical neurons in the ferret has been yet been investigated. Nontheless, it would be intriguing to reveal whether the timecourse of spine refinement parallels the timecourse over which we observe the decline in bouton density.

A reduction in the maximum tangential extent of individual feedforward terminals in areas 18 and Ssy was observed from 4 to 8 weeks of age. One possible explanation for the decrease in maximum tangential extent in areas 18 and Ssy may be due to elimination of inappropriate axons from nontopographically linked neurons in V1. This restriction in the cortical territory occupied by feedforward terminals may well be related to the refinement of the topographic map in these areas. Furthermore, the overlap ratio of feedforward to feedback appears to decline in Ssy and increase in area 18. In Ssy,

this decline implies that the territory occupied by feedforward terminals is decreasing. As we have shown previously, the maximum tangential extent of feedback cell label does not change appreciably throughout development (Khalil and Levitt, 2013). Therefore, the only way for the overlap ratio to decline is for the territory occupied by feedforward terminals in Ssy to decline. This is in accord with the decline in the maximum tangential extent in Ssy that we also observed.

A biologically plausible strategy for the refinement of feedforward projections to multiple visual areas is one described by the hierarchical model of cortical maturation. Feedforward projections from V1 to area 18 would mature first, followed by areas 19, 21, and Ssy. Evidence for cortical maturation that follows a sequential scheme comes from Price and Zumbroich (1989). The authors followed the development of feedforward projections from cat V1 to areas 19, 19, 21a, and Ssy and show that the pathway from V1 to area 18 matures ahead of the pathway from V1 to more higher order visual areas (19, 21a, and Ssy). However, these authors were merely documenting the density of feedforward terminals in each area, and that is only one measure of refinement. It is conceivable that the outgrowth of feedforward terminals and innervation of particular target visual areas ensues in a sequential fashion. However, the fine spatial refinement (i.e. change in bouton density or interbouton interval) of feedforward projections from V1 to multiple target areas can in fact occur simultaneously, as we have shown here.

Batardiere et al. (2002) suggested a difference in the development of different types of cortical connections of primate area V4; the laminar distribution of the feedforward pathway from area V2 to V4 is adultlike early in prenatal life, while feedback projections from V4 to V2 undergo extensive remodeling. Burkhalter (1993)

demonstrated a similar developmental sequence of events in human infants; the laminar termination pattern of feedforward connections matures before that of feedback connections. Likewise, Berezovski et al. (2011) examined the development of feedforward and feedback connections in mouse visual cortex between V1, anterolateral area (AL), and lateromedial area (LM). Feedforward connections were present at the earliest time point examined (postnatal day 2), while feedback connections were not detectable until postnatal day 11. Collectively, these studies focused on the early phase of cortical development that includes outgrowth of feedforward terminals and innervation of target visual areas. However, in this study we were interested in the later phase of cortical maturation and refinement in an attempt to understand how normal visual experience affects the refinement of these pathways.

Visual functions mature at different rates because the underlying visual pathways have different developmental timecourses. Therefore, understanding the timing of when individual feedforward pathways are adultlike will help us attribute particular neural substrates to particular functions. We can not claim that because bouton density and interbouton interval are changing at a similar rate in all areas that a common developmental mechanism is operating to refine them. We did not classify our boutons, but it was our impression that bouton size varied from 4 to 8 weeks postnatal and terminal boutons were more prevalent in the 8 week old than in the 4 week old. Thus, our data do not reveal whether different subclasses of boutons mature differentially. Fish et al. (2013) examined the developmental trajectories of two distinct classes of GABA neurons (Parvalbumin-containing chandelier cells and basket cells) in monkey prefrontal cortex to show that bouton density formed by each class has a different

developmental trajectory. Thus, their findings suggest that different kinds or sources of boutons may mature at different rates. Furthermore, this study provides evidence for cell type specific mechanisms of maturation. In another study, Smith and Thompson (1999) examined developmental changes in the expression of different glutamate receptors (NMDA and AMPA) in ferret V1. The authors revealed very different temporal profiles whereby AMPA receptor density is very high at birth and declines by the second postnatal month, while NMDA receptor density is initially low and increases over the same postnatal period. Therefore, it seems that even if a given anatomical pathway to multiple areas refines with a similar rate, other aspects (i.e. types of receptors or boutons) of the pathway can in fact mature at different rates.

It is unclear whether the postnatal refinement of interareal feedforward connections parallels that of feedback projections. The prevailing model of visual cortical development points to a hierarchical sequence such that the formation of basic anatomical connections between lower order areas precedes that of successively higher order areas. We have shown earlier that feedback connections to ferret V1 undergo a period of extensive remodeling in the weeks following eye opening. The areal and laminar proportion of feedback refine immediately after eye opening and are essentially adultlike by 6 weeks postnatal. That fact that the proportion of feedback arising from Ssy is decreasing while the proportion arising from area 18 is increasing is functionally relevant and may be related to the relative contribution from Ssy and area 18 to the surround of V1 neurons. In contrast, peak density, and nearest neighbor distance between feedback cells show a monotonic rate of refinement that continues to about 10 weeks postnatal. Our feedforward data are partly consistent with these results in that

refinement ensues from 6 to 8 weeks postnatal. It is temping to speculate that because feedforward projections are refining at a similar rate in multiple areas, it implies that perhaps a particular receptive field property of neurons in these areas is similarly refining with the same timecourse. To clarify, future studies investigating the development of receptive field properties of neurons in multiple visual areas are needed. It seems more likely that the functional maturity of neurons in the visual cortex proceeds in a hierarchical manner. Zhang et al. (2013) showed that the spatial organization of the subfields within the receptive field of V2 neurons is immature in young monkeys, but mostly adult-like by 4 weeks of age. Moreover, Zhang et al. (2005) demonstrated that at 2 weeks of age, receptive field properties of V2 neurons were considerably immature relative to receptive field properties of V1 neurons. Their results suggest that the feedforward input underlying the receptive field center of V2 neurons were not as well developed as those in V1 neurons at 14 days of age. This is consistent with the notion that neuronal responses mature later in higher-order visual areas than in V1 (Kiorpes and Bassin, 2003; Kiorpes and Movshon, 2004).

Several other aspects of cortical connections appear to refine in the month after eye opening. Horizontal projections in layers II/III of ferret visual cortex begin to refine around P22 and continues until distinct adult-like terminal clusters are observed at P45 (Durack and Katz, 1996; Ruthazer and Stryker, 1996). Around the time of eye opening, these long-range horizontal connections are limited in spatial extent, and are less clustered than in the adult. While ocular dominance columns are established early in the ferret (P16: Crowley and Katz, 2000), the critical period for ocular dominance plasticity roughly coincides with the period of major reorganization of feedback circuitry, and

continues until the end of the second postnatal month (Issa et al., 1999). Furthermore, we have previously described (Khalil and Levitt, 2012) the developmental trajectory of zinc staining in five visual cortical areas of the ferret brain in the month after eye opening. Similar to the simultaneous refinement of feedforward projections to multiple visual areas, zinc levels decline in these same areas with a similar timecourse.

The transformation of immature cortical circuits into precise patterns of connections subserving adult brain function is thought to involve the elimination of inappropriate connections as well as selective loss of synapses. We have shown that feedforward projections from ferret primary visual cortex to multiple visual areas undergo substantial refinement that includes a decrease in bouton density of their terminals, increase in interbouton interval, and change with age in the maximum tangential extent of individual feedforward terminal clusters. The changes observed occur largely synchronously in all visual areas and add further evidence to the notion that some features of cortical maturation occur simultaneously in multiple areas. Visual experience likely plays a critical role in mediating these maturational processes to refine visual circuits.

References:

Barone P, Dehay C, Berland M, Bullier J, Kennedy H. 1995. Developmental remodeling of primate visual cortical pathways. Cereb Cortex.5(1):22-38.

Batardiere A, Barone P, Dehay C, Kennedy H. 1998. Area-specific laminar distribution of cortical feedback neurons projecting to cat area 17: quantitative analysis in the adult and during ontogeny. J Comp Neurol. 396(4): 493-510.

Batardière A, Barone P, Knoblauch K, Giroud P, Berland M, Dumas AM, Kennedy H. 2002. Early specification of the hierarchical organization of visual cortical areas in the macaque monkey. Cereb Cortex.12(5):453-65.

Berezovskii VK, Nassi JJ, Born RT. 2011. Segregation of feedforward and feedback projections in mouse visual cortex. J Comp Neurol. 519(18):3672-83.

Boothe RG, Greenough WT, Lund JS, Wrege K. 1979. A quantitative investigation of spine and dendrite development of neurons in visual cortex (area 17) of Macaca nemestrina monkeys. J Comp Neurol. 186(3):473-89.

Braddick OJ, Atkinson J. 2011. Development of human visual function. Vision Res. 51(13):1588-609.

Burkhalter A. 1993. Development of forward and feedback connections between areas V1 and V2 of human visual cortex. Cereb Cortex. 3(5):476-87.

Caric D, Pice DJ. 1996. The organization of visual corticocortical connections in early postnatal kittens. J Neurosci. 73(3):817-29

Changeux JP, Danchin A. 1976. Selective stabilisation of developing synapses as a mechanism for the specification of neuronal networks. Nature. 264(5588):705-12

Chapman B, Stryker MP. 1993. Development of orientation selectivity in ferret visual cortex and effects of deprivation. J Neurosci. 13(12):5251-62.

Chapman B, Stryker MP, Bonhoeffer T. 1996. Development of orientation preference maps in ferret primary visual cortex. J Neurosci. 16(20):6443-53.

Coogan TA, Van Essen DC. 1996. Development of connections within and between areas V1 and V2 of macaque monkeys. J Comp Neurol. (3):327-42.

Crowley JC, Katz LC. 2000. Early development of ocular dominance columns. Science. 290(5495):1321-4.

Durack JC, Katz LC. 1996. Development of horizontal projections in layer 2/3 of ferret visual cortex. Cereb. Cortex. 6: 178-183.

Fish KN, Hoftman GD, Sheikh W, Kitchens M, Lewis DA. 2013. Parvalbumin-Containing Chandelier and Basket Cell Boutons Have Distinctive Modes of Maturation in Monkey Prefrontal Cortex. J Neurosci. 33(19):8352-8358.

Friedlander MJ, Martin KA. 1989. Development of Y-axon innervation of cortical area 18 in the cat. J Neurophys. 416:183-213.

Harwerth RS, Smith EL 3rd, Duncan GC, Crawford ML, von Noorden GK. 1986. Multiple sensitive periods in the development of the primate visual system. Science. 232(4747):235-8.

Huttenlocher PR. 1979. Synaptic density in human frontal cortex - developmental changes and effects of aging. Brain Res. 163(2):195-205

Innocenti GM, Price DJ. 2005. Exuberance in the development of cortical networks. Nat Rev Neurosci. 6(12):955-65.

Issa NP, Trachtenberg JT, Chapman B, Zahs KR, Stryker MP. 1999. The critical period for ocular dominance plasticity in the ferret's visual cortex. J Neurosci. 19(16):6965-78.

Khalil R, Levitt JB. 2013. Zinc histochemistry reveals circuit refinement and distinguishes visual areas in the developing ferret cerebral cortex. Brain Struct Funct. 218:1293-1306.

Kiorpes L, Bassin SA. 2003. Development of contour integration in macaque monkeys. Vis Neurosci. 20(5):567-75.

Kiorpes L, Movshon JA. 2004. Development of sensitivity to visual motion in macaque monkeys. Visual Neuroscience, 21, 851–859.

Lewis TL, Maurer D. 2005. Multiple sensitive periods in human visual development: evidence from visually deprived children. Dev Psychobiol.46(3):163-83.

Li Y, Fitzpatrick D, White LE. 2006. The development of direction selectivity in ferret visual cortex requires early visual experience. Nat Neurosci. 9(5):676-81.

Lund JS, Boothe RG, Lund RD. 1977. Development of neurons in the visual cortex (area 17) of the monkey (Macaca nemestrina): a Golgi study from fetal day 127 to postnatal maturity. J Comp Neurol. 176(2):149-88.

Price DJ. 1986. The postnatal development of clustered intrinsic connections in area 18 of the visual cortex in kittens. Brain Res. 389(1-2):31-8.

Price DJ, Blakemore C. 1985. Regressive events in the postnatal development of association projections in the visual cortex. Nature. 316(22)721-724.

Price DJ, Ferrer JM, Blakemore C, Kato N. 1994. Postnatal development and plasticity of corticocortical projections from area 17 to area 18 in the cat's visual cortex. J Neurosci. 14:2747-62.

Price DJ, Zumbroich TJ. 1989.Postnatal development of corticocortical efferents from area 17 in the cat's visual cortex. J Neurosci. 9(2):600-13.

Rakic P, Bourgeois JP, Eckenhoff MF, Zecevic N, Goldman-Rakic PS. 1986. Concurrent overproduction of synapses in diverse regions of the primate cerebral cortex. Science. 232(4747):232-5.

Ruthazer ES, Stryker MP.1996. The role of activity in the development of long-range horizontal connections in area 17 of the ferret. J. Neurosci. 15(22): 7253-69.

Smith AL, Thompson ID. 1999. Spatiotemporal patterning of glutamate receptors in developing ferret striate cortex. Eur J Neurosci. 2:923-934.

Wimmer VC, Broser PJ, Kunar T, Bruno RM. 2010. Experience-induced plasticity of thalamocortical axons in both juveniles and adults. JCN. 518:4629-4648.

Wong-Riley M.1979. Changes in the visual system of monocularly sutured or enucleated cats demonstrable with cytochrome oxidase histochemistry. Brain Res 171(1):11–28

Zhang B, Zheng J, Watanabe I, Maruko I, Bi H, Smith EL 3rd, Chino Y. 2005. Delayed maturation of receptive field center/surround mechanisms in V2. Proc Natl Acad Sci 102(16):5862-7.

CHAPTER 5

GENERAL DISCUSSION

The broad goal of this work was to investigate the postnatal anatomical development of interareal feedforward and feedback projections linking ferret primary visual cortex (V1) and extrastriate visual areas. We were particularly interested in establishing whether the developmental timecourses of feedforward and feedback cortical circuits are similar. Secondarily, we wished to determine whether individual feedback and feedforward pathways refine at comparable rates. Visual cortical areas are presumed to subserve different perceptual functions as a result of their rich network of interareal anatomical circuits. Therefore, differential development of distinct cortical circuits could underlie the known differences in the rate at which various receptive field properties such as center/surround interactions mature (Zhang et al., 2005: 2013), as well as various perceptual abilities mature (Harwerth et al., 1986; Lewis and Maurer, 2005; Braddick and Atkinson, 2011).

Here we presented research using both anatomical tracer injections of neuronal tracers as well as the use of zinc histochemistry. Ferrets (Mustela putorius furo) are ideal for use in developmental connectional studies because of their protracted postnatal period of brain development, and their relatively smooth cerebral cortex that facilitates access to all visual cortical areas. These ages were chosen to span the period just after eye opening, during which emergent visual responses undergo much of their refinement to the adultlike state.

In chapter 2, we quantified synaptic zinc density (reflecting specific glutamatergic inputs) in multiple visual areas of ferret visual cortex over the course of development. We found that by 6 weeks of age there was a significant decline in visual cortical synaptic zinc; this decline was most pronounced in layer IV of areas 17 and 18, with

much less change in higher-order extrastriate areas. Synaptic zinc has been shown to act as a potent modulator of excitatory neurotransmission by acting at zinc-specific binding sites on the N-methyl-D-aspartate (NMDA) subtype of glutamate receptors (Westbrook and Mayer, 1987; Christine and Choi, 1990; Hollmann et al., 1993). In the developing cat visual cortex, Dyck et al. (1993) have suggested that the transient patchy staining of zinc in layer IV of cat V1, which declines during the period of ocular dominance column formation, may contribute to the mechanisms of column formation in the visual cortex during the critical period. However, we note that geniculocortical afferents in layer IV of primary visual cortex make up the minority of synapses in this layer.

Synaptic zinc is sequestered in a subset of interareal feedforward and feedback projections. It is important to compare the developmental refinement of zinc circuits in ferret visual cortex to the general network of feedforward and feedback connections. A relavent question is what proportion of the total labeled boutons from feedforward projections to each target visual area contain zinc. This can be accomplished through colocalization of synaptic zinc with VGlut1, as this glutamate transporter is preferentially used by corticocortical connections. A further question arises concerning the proportion of feedback cells in extrastriate cortex that are zinc positive. This can be revealed by making focal injections of sodium selenite into V1 of ferret visual cortex and tracking developmental changes in the distribution of zinc-positive feedback cells in extrastriate cortex.

Furthermore, we show that zinc histochemistry can be used to reliably distinguish visual areas in juvenile and adult ferret cerebral cortex, and that the postnatal decline in

levels of synaptic zinc follows a broadly similar developmental trajectory in multiple areas of ferret visual cortex. Consistent with other studies in different species (Dyck et al. 1993; Garrett and Slomianka 1992; Valente et al. 2002) we found that synaptic zinc was developmentally regulated. However, unlike other studies, we directly show a dramatic decline in synaptic zinc in layer IV of areas 17 and 18 in the period immediately after eye-opening. This finding suggests that visual experience in the postnatal period is critical for the refinement of visual cortical circuits and provides further evidence that some aspects of cortical maturation follows a similar developmental timecourse in multiple visual areas.

Interestingly, the period of major decline in zinc levels in layer IV of V1 is coincident with the maturation of orientation and direction selective responses of V1 neurons that occurs after eye opening. In the ferret, both orientation and direction selective responses become adult like by 6 weeks of age (Chapman and Stryker, 1993; Li et al., 2006). This finding suggests that the decline in zinc levels in layer IV of ferret V1 may be involved in the maturation of orientation and direction selectivity responses of V1 neurons. Furthermore, the decline in zinc levels in layer IV may also contribute to the formation of orientation selective columns. It is difficult to conclude whether synaptic zinc is simply an indicator of the maturity of a region, or plays a key role in mediating the maturation process. Perhaps future experiments can resolve this issue by raising animals in complete darkness and subsequently examine changes in zinc levels. Complete darkness has been shown to cause abnormal direction selectivity tuning in ferrets (Li et al., 2006).

In chapter 3, we assessed the postnatal refinement of feedback projections

arising from multiple visual areas to ferret primary visual cortex to determine whether different features of the spatial organization of these pathways mature at similar rates. We showed that there is substantial refinement in the spatial organization of feedback projections arising from multiple visual areas to primary visual cortex of the ferret during the period after eye opening. Our results are in broad agreement with previous studies showing that feedback projections undergo a period of prolonged remodeling (Barone et al. 1995; Batardiere et al. 1998, 2002; Burkhalter 1993). Our results also indicate that much of the overall pattern of feedback label in extrastriate cortex is present as early as four weeks postnatal. Baldwin et al. (2012) recently demonstrated that the adultlike pattern of cortical connections between V1 and V2 is also present in early postnatal monkeys. However, they also show refinement of connections between 2 to 8 weeks postnatal.

In the course of our analysis we find a greater number of feedback cells from contralateral visual areas to primary visual cortex at 5 weeks of age. In addition, we find that the proportions of contralateral feedback from multiple visual areas in the 5 week old are very similar to the areal proportions from the ipsilateral side. At 5 weeks of age, Ssy provides the greatest proportion of callosal feedback to primary visual cortex. By 8 weeks of age, area 18 provides the greatest proportion of callosal feedback. Our results are consistent with previous studies revealing refinement and pruning of visual callosal circuits (Innocenti and Frost, 1979,1980: Innocenti and Price, 2005).

While much is known about the developmental refinement of the laminar distribution of feedback projections in cat and monkey visual cortex (Barone et al. 1995; Batardiere et al. 1998, 2002), little is known about the rate of refinement of the fine

spatial scale of feedback projections in multiple visual areas. We therefore quantified different anatomical aspects related to the topography of feedback projections and found that the fine scale refinement of the spatial layout of feedback connections in multiple visual areas occurs largely synchronously. This implies that perhaps feedback from these visual areas to V1 have a similar kind of contribution to the receptive field surround of V1 neurons, albeit with differing spatial extents.

Feedback projections from extrastriate visual areas have been shown to influence the response properties of V1 neurons as they provide a modulatory influence. In the monkey, Zhang et al. (2005) showed that at the time that certain receptive field properties are mature in V1 and V2, the modulatory surround effects are not. Therefore, it is likely that feedback projections to V1 and V2 from other extrastriate visual areas have not yet assumed their adultlike organization. Taken together, their results suggest that the spatial extent of both the RF center and surround refine throughout the course of development. This is presumably due to the refinement of the spatial organization of feedback cells in extrastriate visual areas that project to V1 and V2. The anatomical refinement of feedback circuits presumably parallels the maturation of neuronal physiological properties and more broadly visual perceptual abilities. As such, the different developmental trajectories of different aspects of feedback connections we observe (drastic change in areal and laminar proportion from 4-6 weeks versus the slow monotonic rate of refinement in peak density, median NND and Q3 values) mirrors the multiple developmental trajectories of different visual functions. Having revealed the ages at which feedback connections are adultlike in ferret visual cortex, we can next characterize the functional properties of neurons in these areas at different postnatal

ages to determine if there is a functional correlation.

The decline in the proportion of feedback arising from the supragranular layers during development could conceivably result in the maturation of V1 RF properties. Feedback projections arising from different layers presumably provide different types of input and consequently may have different influence in how they shape RF properties of their targets. For example, inactivating layer V cells in area 18 of the cat affects response magnitude and selectivity to stimulus velocity and orientation in layer IV cells of area 17 (Alonso et al., 1993). However, inactivating area 18 cells in layers II/III affects response magnitude only, without affecting the selectivity of neuronal responses of area 17 cells (Martinez-Conde et al., 1999).

The functional properties of V1 neurons are also determined by their intrinsic properties such as the composition of their voltage-gated channels as well as their transmitter receptor complement. Both of these features that are inherent to visual cortical neurons have been shown to undergo changes during development. These changes in turn play a role in the maturation and refinement of anatomical circuits. For example, Smith and Thompson (1999) showed that different glutamate receptors (NMDA and AMPA) in ferret V1 have very different temporal profiles during development. AMPA receptor density is very high at birth and declines by the second postnatal month, while NMDA receptor density is initially low and increases over the same postnatal period. In addition, Catalano et al. (1997) monitored immunohistochemical changes in the distribution of NMDA receptors in the development of the cat and ferret visual cortex and revealed that levels of NMDAR1 change in development with a laminar-specific time course. Importantly, the authors

showed that within layer 4, the transient increase in NMDAR1 immunostaining in cat visal cortex occurs during the period of ocular dominance column formation (P21–42) (LeVay et al., 1978). The electrophysiologcal properties of visual cortical neurons also undergo marked changes during development. For example, McCormick and Price (1987) investigated the electrophysiologcal properties of cortical pyramidal neurons in layer V in the rat and revealed considerable changes during development. As pyramidal neurons mature, their action potentials become faster in both their rate of rise and fall, briefer in duration, and larger in amplitude. Collectively, these studies provide evidence for marked changes during development in the intrinsic properties of cortical neurons; these changes in turn may be involved in the refinement of anatomical circuits.

In chapter 4, we examined the maturation of feedforward projections from V1 to multiple visual areas in ferret visual cortex from four weeks to eight weeks postnatal. We quantified the tangential extent of terminal fields in each area, as well as the density of labeled synaptic boutons and the interbouton interval along individual labeled axons. Specifically, we were interested in determining whether different anatomical features of feedforward circuitry refine simultaneously in all visual cortical areas. Simultaneous refinement of different features could in turn affect receptive field properties in the respective in a similar way. By 4 weeks postnatal (before eye opening), we find substantial numbers of orthogradely-labeled axons and terminals in areas 18, 19, 21, and the Suprasylvian cortex. In addition, orthogradely labeled terminals and retrogradely labeled cells were organized into essentially overlapped clusters, indicating reciprocal feedforward and feedback connections of each extrastriate area with V1. Bouton density of feedforward projections to all areas examined declines from six

weeks to eight weeks postnatal. Similarly, interbouton interval of feedforward projections to all visual areas increase over this same postnatal period.

Other studies have shown that the maturation of feedforward projections from cat V1 to extrastriate areas occurs in a sequential fashion (Price and Zumbroich, 1989). We document here that different other aspects (fine-scale) of feedforward projections from ferret V1 to multiple visual areas refine with a similar timecourse. Declining bouton density of feedforward projections could in part reflect the amount of drive a particular area is receiving from V1. Therefore, the decline in bouton density and the increase in interbouton interval we observe could represent a decrease in excitatory synaptic drive, which would ultimately refine receptive field properties in the target areas. The fact that bouton density and interbouton intervals are changing at a similar rate in all areas does not necessarily mean that a single developmental mechanism is governing this maturation process. We have seen that even if a given anatomical pathway to multiple areas refines with a similar rate, other aspects (i.e. types of receptors or boutons) of the pathway can in fact mature at different rates (Fish el al., 2013 ; Smith and Thompson, 1999). Future studies should certainly focus on elucidating different developmental profiles of various aspects of these feedforward connections (i.e. receptor type, bouton type). Lastly, we propose to extend this study to older aged ferrets to reveal a possible protracted period of refinement in feedforward projections from V1 to extrastriate visual areas.

Finally, understanding how visual cortical circuits develop and mature is central to our understanding of visual perception. Since other sensory areas have cortical connections similar to that found in visual cortex, elucidating the developmental

trajectory of feedback projections to V1 and of feedforward connections from V1 to extrastriate visual areas may illuminate how other sensory cortices develop. Corticocoritcal feedforward and feedback projections are also a prominent feature in the auditory cortex in monkeys and humans (Pandya, 1995), as well as in monkey somatosensory cortex (Cerkevich et al., 2013). Our results will motivate future studies to determine if the development of the physiological properties of the receptive field surrounds of V1 neurons (which are presumably shaped by modulatory influences from feedback in extrastriate visual areas) parallels the anatomical development of feedback connections we have documented here. Furthermore, our feedforward data will be useful for future studies documenting the development of receptive field properties of neurons in extrastriate visual areas.

LITERATURE CITED

Adams DL, Zeki S. 2001. Functional organization of macaque V3 for stereoscopic depth. J. Neurophysiol. 86:2195–2203.

Albright TD. 1984. Direction and orientation selectivity of neurons in visual area MT of the macaque. J Neurophysiol. 52(6):1106-30.

Albright TD, Desimone R. 1987. Local precision of visuotopic organization in the middle temporal area (MT) of the macaque.Exp Brain Res. 65(3):582-92.

Albus K, Wolf W. 1984. Early postnatal development of neuronal function in the kitten's visual cortex: a laminar analysis. J Physiol. 348:153-85.

Albus K. 1980. The detection of movement direction and effects of contrast reversal in the cat's striate cortex. Vision Res. 20(4):289-93.

Allman JM, Kaas JH. 1971a. Representation of the visual field in striate and adjoining cortex of the owl monkey (Aotus trivirgatus). Brain Res. 35(1):89-106.

Allman JM, Kaas JH. 1971b. A representation of the visual field in the caudal third of the middle tempral gyrus of the owl monkey (Aotus trivirgatus). Brain Res. 31(1):85-105.

Allman JM, Kaas JH. 1974a. The organization of the second visual area (V II) in the owl monkey: a second order transformation of the visual hemifield.Brain Res. 76(2): 247- 65.

Allman JM, Kaas JH. 1975. The dorsomedial cortical visual area: a third tier area in the occipital lobe of the owl monkey (Aotus trivirgatus). Brain Res. 100(3): 473-87.

Allman JM, Kaas JH. 1976. Representation of the visual field on the medical wall of occipital-parietal cortex in the owl monkey. Science.191(4227): 572-5.

Amirikian B, Georgopoulos AP. 2003. Modular organization of directionally tuned cells in the motor cortex: is there a short-range order? Proc. Natl Acad. Sci. USA. 100:12 474–12 479.

Andjelic S, Gallopin T, Cauli B, Hill EL, Roux L, Badr S, Hu E, Tamás G, Lambolez B. 2009. Glutamatergic nonpyramidal neurons from neocortical layer VI and their comparison with pyramidal and spiny stellate neurons. J Neurophysiol. 101(2):641-54.

Angelucci A, Levitt JB, Lund JS. 2002. Anatomical origins of the classical receptive field and modulatory surround field of single neurons in macaque visual cortical area V1. Prog Brain Res.136:373-88.

Angelucci A, Bullier J. 2003. Reaching beyond the classical receptive field of V1 neurons: horizontal or feedback axons? J Physiol Paris. 97(2-3):141-54. Review.

Atkinson J, Braddick OJ, Moar K. 1977. Development of contrast sensitivity over the first 3 months of life in the human infant. Vision Res. 17(9):1037-44

Atkinson J, Braddick OJ. 2003. Neurobiological models of normal and abnormal visual development. In: de Haan, M. & Johnson, M. (eds.) The Cognitive Neuroscience of Development. Hove: Psychology Press, pp. 43-72.

Atkinson J, Hood B, Wattam-Bell J, Anker S, Tricklebank J. 1988. Development of orientation discrimination in infancy. Perception.17(5):587-95.

Atkinson J, Braddick O. 1992. Visual segmentation of oriented textures by infants. Behav Brain Res. 49(1):123-31.

Bair W. 2005. Visual receptive field organization. Curr Opin Neurobiol. 15(4) 459-64. Review.

Banks MS, Salapatek P. 1978. Acuity and contrast sensitivity in 1-, 2-, and 3-month-old human infants. Invest Ophthalmol Vis Sci.17(4):361-5.

Banks M, Bennett P. 1988. Optical and photoreceptor immaturities limit the spatial and chromatic vision of human neonates. OptSoc Am A. 5:2059-2079.

Barlow HB, Blakemore C, Pettigrew JD. 1967. The neuronal basis of binocular depth discrimination. J. Physiol. Lond. 193: 327-42.

Barone P, Dehay C, Berland M, Bullier J, Kennedy H. 1995. Developmental remodeling of primate visual cortical pathways. Cereb Cortex.5(1):22-38.

Barone P, Batardiere A, Knoblauch K, Kennedy H. 2000, Laminar distribution of neurons in extrastriate areas projecting to visual areas V1 and V4 correlates with the hierarchical rank and indicates the operation of a distance rule. J Neurosci. 20(9): 3263-3281.

Batardiere A, Barone P, Dehay C, Kennedy H. 1998. Area-specific laminar distribution of cortical feedback neurons projecting to cat area 17: quantitative analysis in the adult and during ontogeny. J Comp Neurol. 396(4): 493-510.

Batardière A, Barone P, Knoblauch K, Giroud P, Berland M, Dumas AM, Kennedy H. 2002. Early specification of the hierarchical organization of visual cortical areas in the macaque monkey. Cereb Cortex.12(5):453-65.

Benedek G, Benedek K, Kéri S, Janáky M. 2003. The scotopic low-frequency spatial contrast sensitivity develops in children between the ages of 5 and 14 years. Neurosci Lett. 24;345(3):161-4.

Berezovskii VK, Nassi JJ, Born RT. 2011. Segregation of feedforward and feedback projections in mouse visual cortex. J Comp Neurol. 519(18):3672-83.

Birch EE, Gwiazda J, Held R. Stereoacuity development for crossed and uncrossed disparities in human infants. Vision Res. 22(5):507-13.

Blakemore C, Tobin EA. 1972. Lateral inhibition between orientation detectors in the cat visual cortex. Exp. Brain Res. 15: 439-40.

Blasdel GG, Salama G. 1986. Voltage-sensitive dyes reveal a modular organization in monkey striate cortex. Nature 321:579–85.

Blasdel GG. 1992. Orientation selectivity, preference, and continuity in monkey striate cortex. J Neurosci. 12(8):3139-61.

Bonhoeffer T, Grinvald A. 1991. Iso-orientation domains in cat visual cortex are arranged in pinwheel-like patterns. Nature. 353(6343):429-31.

Bosking WH, Zhang Y, Schofield B, Fitzpatrick D. 1997. Orientation selectivity and the arrangement of horizontal connections in tree shrew striate cortex. J Neurosci. 17(6):2112-27.

Bourgeois JP, Jastreboff PJ, Rakic P. 1989. Synaptogenesis in visual cortex of normal and preterm monkeys: evidence for intrinsic regulation of synaptic overproduction. Proc Natl Acad Sci. 86(11): 4297–4301.

Bourgeois, JP, Patricia S, Goldman-Rakic, Rakic P. 1994. Synaptogenesis in the Prefrontal Cortex of Rhesus Monkeys. Cerebral Cortex. 4:78-96.

Bourne JA, Rosa MG. 2006. Hierarchical development of the primate visual cortex, as revealed by neurofilament immunoreactivity: early maturation of the middle temporal area (MT). Cereb Cortex. (3):405-14.

Braddick OJ. 1993. Orientation- and motion-selective mechanisms in infants. In K. Simons (Ed.), Early visual development: Normal and abnormal (pp. 163–177). New York: Oxford University Press.

Braddick O, Wattam-Bell J, Day J, Atkinson J. 1983. The onset of binocular function in human infants. Hum Neurobiol. 2(2):65-9.

Braddick O, Atkinson J, Julesz B, Kropfl W, Bodis-Wollner I, Raab E. 1980. Cortical binocularity in infants. Nature. 288(5789):363-5.

Braddick OJ, Atkinson J. 1983. Some recent findings on the development of human binocularity: a review. Behav Brain Res. 10(1):141-50. Review.

Braddick O, Atkinson J. 2011. Development of human visual function. Vision Res. 51(13):1588-609.

Braddick OJ, Wattam-Bell J, Atkinson J. 1986a. Orientation specific cortical responses develop in early infancy. Nature. 320:617-619.

Brown AM, Yamamoto M. 1986. Visual acuity in newborn and preterm infants measured with grating acuity cards. Am J Ophthalmol. 102(2):245-53.

Bucher K, Dietrich T, Marcar VL, Brem S, Halder P, Boujraf S. 2006. Maturation of luminance- and motion-defined form perception beyond adolescence: A combined ERP and fMRI study. Neuroimage, 31(4):1625–1636.

Burkhalter A, Bernardo KL, Charles V. 1993. Development of local circuits in human visual cortex. J Neurosci. 13(5):1916-31.

Burkhalter A. 1993. Development of forward and feedback connections between areas V1 and V2 of human visual cortex. Cereb Cortex. 3(5):476-87.

Buzas P, Eysel UT, Adorjan P, Kisavaray ZF. 2001. Axonal topography of cortical basket cells in relation to orientation, direction, and ocular dominance maps. J. Comp. Neurol. 437: 259-85.

Callawy EM, Katz LC. 1990. Emergence and refinement of clustered horizontal connections in cat striate cortex. J. Neurosci. 10(4):1134-53.

Callaway EM. 2004. Feedforward, feedback and inhibitory connections in primate visual cortex. Neural Netw.17(5-6):625-32. Review.

Callaway EM, Katz LC. 1991. Effects of binocular deprivation on the development of clustered horizontal connections in cat striate cortex. Proc Natl Acad Sci U S A. 88(3):745-9.

Callaway EM, Katz LC. 1992. Development of axonal arbors of layer 4 spiny neurons in cat striate cortex. J Neurosci. 12(2):570-82.

Carandini M, Heeger DJ, Movshon JA. 1997. Linearity and normalization in simple cells of the macaque primary visual cortex. J Neurosci. 17(21) 8621-44.

Cantone G, Xiao J, McFarlane N, Levitt JB. 2005. Feedback connections to ferret straite cortex: Direct evidence for visuotopic convergence of feedback inputs. JCN. 487:312-331.

Carić D, Price DJ. 1996. The organization of visual corticocortical connections in early postnatal kittens. Neuroscience. 73(3):817-29.

Catalano SM, Chang CK, Shatz CJ. 1997. Activity-dependent regulation of NMDAR1 immunoreactivity in the developing visual cortex. J Neurosci. 17(21):8376-8390.

Cerkevich CM, Qi Hui-Xin, Kaas JH. 2013. Corticocortical projections to representations of the teeth, tongue, and face in somatosensory area 3b of macaque monkeys. DOI 10.1002/cne.23426. JCN

Changeux JP, Danchin A. 1976. Selective stabilisation of developing synapses as a mechanism for the specification of neuronal networks. Nature. 264(5588):705-12

Chapman B, Stryker MP. 1993. Development of orientation selectivity in ferret visual cortex and effects of deprivation. J Neurosci.13(12):5251-62.

Chapman B, Stryker MP, Bonhoeffer T. 1996. Development of Orientation Preference Maps in Ferret Primary Visual Cortex. J Neurosci. 16(20)6443-6453.

Chen B, Boukamel K, Kao JP, Roerig B. 2005. Spatial distribution of inhibitory synaptic connections during development of ferret primary visual cortex. Exp Brain Res160(4):496-509.

Chino YM, Smith EL 3rd, Hatta S, Cheng H. 1997. Postnatal development of binocular disparity sensitivity in neurons of the primate visual cortex. J Neurosci. 17(1):296-307.

Chino YM, Smith EL 3rd, Yoshida K, Cheng H, Hamamoto J . 1994. Binocular Interactions in Striate Cortical Neurons of Cats Reared with Discordant Visual Inputs. J Neurosci. 14(8): 5050-5067.

Chiron C, Raynaud C, Mazière B, Zilbovicius M, Laflamme L, Masure MC, Dulac O, Bourguignon M, Syrota A. 1992. Changes in regional cerebral blood flow during brain maturation in children and adolescents. J Nucl Med. 33(5):696-703.

Jared M. Clemens, Neil J. Ritter, Arani Roy, Julie M. Miller, and Stephen D. Van Hooser. 2012. The Laminar Development of Direction Selectivity in Ferret Visual Cortex. J Neurosci. 32(50):18177–18185.

Condé F, Lund JS, Lewis DA. 1996. The hierarchical development of monkey visual cortical regions as revealed by the maturation of parvalbumin-immunoreactive neurons. Brain Res Dev Brain Res. 96(1-2):261-76.

Coppola DM, White LE, Fitzpatrick D, Purves D. 1998a. Unequal representation of cardinal and oblique contours in ferret visual cortex. Proc Natl Acad Sci USA. 95(5): 2621-3.

Courage ML, Adams RJ. 1990. Visual acuity assessment from birth to three years using the acuity card procedure: cross-sectional and longitudinal samples. Optom Vis Sci. 67(9):713-8.

Crair MC, Gillespie DC, Stryker MP. 1998. The role of visual experience in the development of columns in cat visual cortex. Science. 279(5350):566-70.

Crawford MLJ, Blake R, Cool SJ, Von Noorden GK. 1975. Physiological consequences of unilateral and bilateral eye closure in macaque monkeys: some further observations. Brain Res. 84:150.

Daniel PM, Whitteridge D. 1961. The representation of the visual field on cerebral cortex in monkeys. J. Physiol. 159: 203-1.

DeAngelis GC, Robson JG, Ohzawa I, Freeman RD. 1992. Organization of suppression in receptive fields of neurons in cat visual cortex. J Neurophysiol. 68(1):144-63.

DeAngelis GC, Ohzawa I, Freeman RD. 1993A. Spatiotemporal organization of simple-cell receptive fields in the cat's striate cortex. I. General characteristics and postnatal development. J Neurophysiol. 69(4):1091-117.

DeAngelis GC, Freeman RD, Ohzawa I. 1994. Length and width tuning of neruons in the cat’s primary visual cortex. J. Neurophysiology 71:347-374.

Dehay C, Kennedy H, Bullier J. 1988. Characterization of transient cortical projections from auditory, somatosensory, and motor cortices to visual areas 17, 18, and 19 in the kitten. J Comp Neurol. 272(1):68-89.
Derrington AM, Fuchs AF. 1981. The development of spatial-frequency selectivity in kitten striate cortex. J Physiol. 316:1-10.
Derrington AM. 1984. Development of spatial frequency selectivity in striate cortex of vision-deprived cats. Exp Brain Res. 55(3):431-7.
De Valois RL, Yund EW, Hepler N. 1982. The orientation and direction selectivity of cells in macaque visual cortex. Vision Res. 22(5):531-44.
De Valois RL, Albrecht DG, Thorell LG. 1982. Spatial frequency selectivity of cells in macaque visual cortex. Vision Res. 22(5):545-59.
Dobson V, Schwartz TL, Sandstrom DJ, Michel L. 1987. Binocular visual acuity of neonates: the acuity card procedure. Dev Med Child Neurol. 29(2):199-206.
Douglas RJ, Martin KA. 2004. Neuronal circuits of the neocortex. Annu Rev Neurosci. 27:419-51. Review.
Drager UC. 1975. Receptive fields of single cells and topography in mouse visual cortex. J Comp Neurol. 160:269–290
Durack JC, Katz LC. 1996. Development of horizontal projections in layer 2/3 of ferret visual cortex. Cereb. Cortex. 6: 178-183.
Ellemberg D, Lewis TL, Liu CH, Maurer D. 1999. Development of spatial and temporal vision during childhood. Vision Res. 39(14):2325-33.
Ellemberg D, Lewis TL, Meghji KS, Maurer D, Guillemot JP, Lepore F. 2003. Comparison of sensitivity to first- and second-order local motion in 5-year-olds and adults. Spat Vis. 16(5):419-28.
El-Shamayleh Y, Movshon JA, Kiorpes L. 2010. Development of sensitivity to visual texture modulation in macaque monkeys. J Vis. 10(11):11.
Everson RM, Prashanth AK, Gabbay M, Knight BW, Sirovich L, Kaplan E. 1998. Representation of spatial frequency and orientation in the visual cortex. Proc Natl Acad Sci U S A. 95(14):8334-8.
Fantz RL. 1961. The origin of form perception. Scientific American. 204 (May), 61-72.
Felleman DJ, Van Essen DC. 1991. Distributed Hierarchical Processing in the Primate. Cerebral Cortex. 1:1-47.
Felleman DJ, Burkhalter A, Van Essen DC. 1997. Cortical connections of areas V3 and VP of macaque monkey extrastriate visual cortex. JCN. 379:21–47.
Fitzpatrick D. 2000. Seeing beyond the receptive field in primary visual cortex. Curr Opin Neurobiol. 10(4): 438-43.
Fitzpatrick D. The functional organization of local circuits in visual cortex: insights from the study of tree shrew striate cortex. Cereb Cortex. 6(3):329-41. Review.
Flechsig P. 1901. Developmental (myelogenetic) localisation of the cerebral cortex in the human subject. Lancet, 2:1027-1029.
Fox R, Aslin RN, Shea SL, Dumais ST. 1980. Stereopsis in human infants. Science. 207: 323–4.
Freeman RD, Ohzawa I. 1992. Development of binocular vision in the kitten's striate cortex. J Neurosci. 12(12):4721-36.
Frégnac Y, Imbert M. 1984. Development of neuronal selectivity in primary visual cortex of cat. Physiol Rev. 64(1):325-434. Review.

Fujita I, Tanaka K, Ito M, Cheng K. 1992. Columns for visual features of objects in monkey inferotemporal cortex. Nature. 360:343–346.
Galuske RA, Schlote W, Bratzke H, Singer W. 2000. Interhemispheric asymmetries of the modular structure in human temporal cortex. Science. 289:1946–1949.
Garey LJ, de Courten C.1983. Structural development of the lateral geniculate nucleus and visual cortex in monkey and man. Behav Brain Res. 10(1):3-13.
Gary-Bobo E, Przybyslawski J, Saillour P. 1995. Experience-dependent maturation of the spatial and temporal characteristics of the cell receptive fields in the kitten visual cortex. Neurosci Lett. 189(3):147-50.
Gattas R, Gross CG, Sandell JH. 1981. Visual topography of V2 in the macaque. J Comp Neurol. 201(4):519-39.
Gattas R, Sousa AP, Gross CG. 1988. Visuotopic organization and extent of V3 and V4 of the macaque. J. Neurosci. 8(6): 1831-45.
Gilbert CD, Wiesel TN. 1979. Morphology and intracrotical projections of functionally characterised neurones in the cat visual cortex. Nature. 280: 120-25.
Gilbert CD, Wiesel TN. 1983. Clustered intrinsic connections in cat visual cortex. J Neurosci. 3(5): 1116-33.
Gilbert CD, Wiesel TN. 1989. Columnar specificity of intrinsic horizontal and corticocortical connections in cat visual cortex. J Neurosci. 9(7):2432-42.
Gilbert CD, Wiesel TN. 1990. The influence of contextual stimuli on the orientation selectivity of cells in primary visual cortex of the cat. Vision Res. 30(11): 1689-701.
Gilbert CD. 1992. Horizontal integration and cortical dynamics. Neuron. 9(1): 1-13.
Girard P, Salin P, Bullier A. 1991. Visual activity in areas V3a and V3 during reversible inactivation of area V1 in the macaque monkey. J Neurophysiol. 66;(5)1493-1503.
Girard N, Raybaud C, du Lac P. 1991. MRI study of brain myelination. J Neuroradiol. 18(4):291-307.
Gödecke I, Kim DS, Bonhoeffer T, Singer W. 1997. Development of orientation preference maps in area 18 of kitten visual cortex. Eur J Neurosci. 9(8):1754-62.
Gödecke L, Dae-Shik K, Bonhoeffer T, Singer W. 2006. Development of Orientation Preference Maps in Area 18 of Kitten Visual Cortex. European Journal of Neuroscience. 9;(8)1754-1762.
Hartline HK. 1938. The receptive fields of optic nerve fibers. Am. J. Physiol. 130: 690-699.
Harwerth RS, Smith EL 3rd, Duncan GC, Crawford ML, von Noorden GK. 1986. Multiple sensitive periods in the development of the primate visual system. Science. 232(4747):235-8.
Hatta S, Kumagami T, Qian J, Thornton M, Smith EL 3rd, Chino YM. 1998. Nasotemporal directional bias of V1 neurons in young infant monkeys. Invest Ophthalmol Vis Sci 39:2259 –2267.
Held R, Birch E, Gwiazda J.1980. Stereoacuity of human infants. Proc Natl Acad Sci U S A. 77(9):5572-4.
Hendrickson AE, Wilson JR, Ogren MP. 1978. The neuroanatomical organization of pathways between the dorsal lateral geniculate nucleus and visual cortex in Old World and New World primates. J Comp Neurol. 182:123–136.

Hendry SH, Schwark HD, Jones EG, Yan J. 1987. Numbers and proportions of GABA-immunoreactive neurons in different areas of monkey cerebral cortex. J Neurosci. 7(5):1503-19.

Henry GH, Salin PA, Bullier J. 1991. Projections from areas 18 and 19 to cat striate cortex: divergence and laminar specificity. Eur J Neurosci. 3: 186-200.

Hirsch J, Gilbert CD. 1991. Synaptic Physiology of horizontal connections in the cat's visual cortex. J. Neurosci. 11(6): 1800-09.

Horton JC, Adams DL. 2005. The cortical column: a structure without a function. Philos Trans R Soc Lond B Biol Sci. 360(1456):837-62. Review.

Huang JY, Wang C, Dreher B. 2007. The effects of reversible inactivation of postero-temporal visual cortex on neuronal activities in cat's area 17. Brain Res 23; 1138:111-28

Hubel DH, Wiesel TN. 1961. Integrative action in the cat's lateral geniculate body. J Physiol (Lond) 155:385–398.

Hubel DH, Wiesel TN. 1962. Receptive fields, binocular interaction and functional architecture in the cat's visual cortex. J. Physiol. Lond. 160: 106-154.

Hubel DH, Wiesel TN.1963. Shape and arrangement of columns in cat's striate cortex. J. Physiol. 1965: 559-68.

Hubel DH, Wiesel TN. 1965. Receptive fields and functional architecture in 2 nonstriate visual areas (18 and 19) of cat. J Neurophysiol. 28(2):229-89.

Hubel DH, Wiesel TN. 1968. Receptive fields and functional architecture of monkey striate cortex. J. Physiol 195: 215-43.

Hubel DH, Wiesel TN. 1969. Anatomical demonstration of columns in the monkey striate cortex. Nature. 221(5182):747-50.

Hubel DH, Wiesel TN. 1970. The period of susceptibility to the physiological effects of unilateral eye closure in kittens. J Physiol. 206:419-36.

Hubel DH, Wiesel TN. 1974a. Sequence regularity and geometry of orientation columns in monkey striate cortex. 158: 267-94.

Hubel DH, Wiesel TN. 1974b. Uniformity of monkey striate cortex: a parallel relationship between field size, scatter, and magnification factor. J Comp Neurol.158: 295-306.

Hubel DH, Wiesel TN. 1977. The Ferrier lecture: functional architecture of macaque monkey visual cortex. Proc. R. Soc. B. 198:1–59.

Hubener M, Shoham D, Grinvald A, Bonhoeffer T. 1997. Spatial relationships among three columnar systems in cat area 17. J. Neurosci. 17(23):9270-84.

Hupe JM, James AC, Payne BR, Lomber SG, Girard P, Bullier J. 1998. Cortical feedback can improve discrimination between figure and background by V1, V2, and V3 neurons. Nature. 394: 784-87.

Huttenlocher PR. 1984. Synapse elimination and plasticity in developing human cerebral cortex. Am J Ment Defic. 88(5):488-96.

Huttenlocher PR, de Courten C, Garey LJ, Van der Loos H. 1982. Synaptogenesis in human visual cortex--evidence for synapse elimination during normal development. Neurosci Lett. 33(3):247-52.

Innocenti GM, Clarke S. 1984. Bilateral transitory projection to visual areas from auditory cortex in kittens. Brain Res. 316(1):143-8.

Innocenti GM, Frost DO. 1979. Effects of visual experience on the maturation of the efferent system to the corpus callosum. 280:231-234. Nature.

Innocenti GM, Frost DO. 1980. The postnatal development of visual callosal connections in the absence of visual experience or of the eyes. 39:365-375.
Innocenti GM, Price DJ. 2005. Exuberance in the development of cortical networks. Nat Rev Neurosci. 6(12):955-65.
Issa NP, Trepel C, Stryker MP. 2000. Spatial frequency maps in cat visual cortex. J Neurosci. 20(22):8504-14.
Jones HE, Andolina IM, Oakely NM, Murphy PC, Sillito AM. 2000. Spatial summation in lateral geniculate nucleus and visual cortex. Exp Brain Res 135: 279-284.
Julesz B, Kropfl W, Petrig B. 1980. Large evoked potentials to dynamic random-dot correlograms and stereograms permit quick determination of stereopsis. Proc Natl Acad Sci U S A. 77(4):2348-51.
Kapadia MK, Westheimer G, Gilbert CD. 1999. Dynamics of spatial summation in primary visual cortex of alert monkeys. Proc. Natl. Acad. S. 96:12073-78.
Kato N, Ferrer JM, Price DJ. 1991. Regressive changes among corticocortical neurons projecting from the lateral suprasylvian cortex to area 18 of the kitten's visual cortex. Neuroscience. 43(2-3):291-306.
Kennedy H, Bullier J, Dehay C. 1989. Transient projection from the superior temporal sulcus to area 17 in the newborn macaque monkey. Proc Natl Acad Sci U S A. 86(20):8093-7.
Kennedy H, Dehay C, Bullier J. 1986. Organization of the callosal connections of visual areas V1 and V2 in the macaque monkey. J Comp Nerol. 247:398-415.
Kennedy H, Bullier J. 1985. A double-labeling investigation of the afferent connectivity to cortical areas V1 and V2 of the macaque monkey. J Neurosci. 5(10):2815-30.
Kiorpes L. 1992a. Development of vernier acuity and grating acuity in normally reared monkeys. Vis Neurosci. 9(3-4):243-51.
Kiorpes L. 1992b. Effect of strabismus on the development of vernier acuity and grating acuity in monkeys. Vis Neurosci. 9(3-4):253-9.
Kiorpes L, Bassin SA. 2003. Development of contour integration in macaque monkeys. Vis Neurosci. 20(5):567-75.
Kiorpes L, Price T, Hall-Haro C, Movshon JA. 2012. Development of sensitivity to global form and motion in macaque monkeys (Macaca nemestrina). Vision Res. 63:34-42.
Kiorpes L, Movshon JA. 2004.Development of sensitivity to visual motion in macaque monkeys.Vis Neurosci. 21(6):851-9.
Kovács I, Kozma P, Fehér Á, Benedek G. 1999. Late maturation of visual spatial integration in humans. Proceedings of the National Academy of Sciences USA, 96, 12204–12209.
Kritzer MF, Cowey A, Somogyi PJ. 1992. Patterns of inter- and intralaminar GABAergic connections distinguish striate (V1) and extrastriate (V2, V4) visual cortices and their functionally specialized subdivisions in the rhesus monkey. Neurosci. 12(11):4545-64.
Krug K, Akerman CJ, Thompson ID. 2001. Responses of neurons in neonatal cortex and thalamus to patterned visual stimulation through the naturally closed lids. J Neurophysiol. 85(4):1436-43.
Kuffler SW. 1953. Discharge patterns and functional organization of mammalian retina. J. Nuerophysiol. 16: 37-68.

Lamme VAF, Super H, Spekreijse H. 1998. Feedforward, horizonatal, and feedback processing in the visual cortex. Curr. Opin. In Neurobiol. 8: 529-35.
Landisman CE, Ts'o DY. 2002b. Color processing in macaque striate cortex: electrophysiological properties. J Neurophysiol. 87(6):3138-51.
Law MI, Zahs KR, Stryker MP. 1988. Organization of Primary Visual cortex (area 17) in the Ferret. J Comp Neurol. 278: 157-80.
Leat SJ, Yadav NK, Irving EL. 2009. Development of Visual Acuity and Contrast Sensitivity in Children. J Optom, Vol. 2, No. 1.
Lennie P. 2003. Receptive fields. Curr Biol. 13(6): R216-9.
LeVay S, Hubel DH, Wiesel TN. 1975. The pattern of ocular dominance columns in macaque visual cortex revealed by a reduced silver stain. J Comp Neurol 159:559–576.
LeVay S, Stryker MP, Shatz CJ. 1978. Ocular dominance columns and their development in layer IV of the cat's visual cortex: a quantitative study. J Comp Neurol 179:223–244.
LeVay S, Connolly M, Houde J, Van Essen DC. 1985. The complete pattern of ocular dominance stripes in the striate cortex and visual field of the macaque monkey. J Neurosci 5:486–501.
LeVay S, Nelson SB. 1991. Columnar organization of the visual cortex. In: Leventhal A.G, editor. The neural basis of visual function. CRC Press; Boston. pp. 266–315.
Levick WR, Cleland BG, Dubin MW. 1972. Lateral geniculate neurons of cat: retinal inputs and physiology. Invest Ophthalmol Vis Sci. 11:302–311.
Levitt JB. 2009. "Receptive fields", In Encyclopedia of Perception (Goldstein EB ed., Sage Publications), in press.
Levitt JB, Lund JS. 2002. The spatial extent over which neurons in macaque striate cortex pool visual signals. Vis Neurosci. (4):439-52
Levitt JB, Lund JS. 1997. Contrast dependence of contextual effects in primate visual cortex. Nature. 387(6628): 73-6.
Lewis TL, Maurer D. 2005. Multiple sensitive periods in human visual development: evidence from visually deprived children. Dev Psychobiol.46(3):163-83.
Lewis TL, Ellemberg D, Maurer D, Dirks M, Wilkinson F, Wilson HR. 2004. A window on the normal development of sensitivity to global form in Glass patterns. Perception. 33(4):409-18.
Li C, Li W. 1994. Extensive Integration field beyond the classic receptive field of cat's striate cortical neurons-classification and tuning properties. Vision Research. 34(18):2337-2355.
Li Y, Fitzpatrick D, White LE. 2006. The development of direction selectivity in ferret visual cortex requires early visual experience. Nat Neurosci 9:676 – 681.
Li Y, Van Hooser SD, Mazurek M, White LE, Fitzpatrick D. 2008.Experience with moving visual stimuli drives the early development of cortical direction selectivity. Nature 456:952–956.
Livingston MS, Hubel DH. 1984b. Specificity of intrinsic connections in primate primary visual cortex. J. Neurosci. 4(11):2830-5.
Löwel S, Singer W. 1992. Selection of intrinsic horizontal connections in the visual cortex by correlated neuronal activity. Science. 255(5041):209-12.

Lübke J, Albus K. 1992. Lack of Exuberance in Clustered Intrinsic Connections in the Striate Cortex of One-month-old Kitten. Eur J Neurosci. 4(2):189-192.

Luhmann HJ, Martínez Millán L, Singer W. 1986. Development of horizontal intrinsic connections in cat striate cortex. Exp Brain Res. 63(2):443-8.

Lund JS. 1973. Organization of neurons in the Visual Cortex, Area 17, of Monkey Macaca mulatta) J. Comp Neuorl. 147; 455-96.

Lund JS. 1987. Local circuit neurons of macaque monkey striate cortex: I. Neurons of laminae 4C and 5A. J. Comp. Neurol. 257(1):60-92.

Lund JS. 1988. Anatomical organization of macaque monkey striate visual cortex. Annu. Rev Neurosci. 1: 253-88.

Lund JS, Henry GH, MacQueen CL, Harvey AR. 1979. Anatomical organization of the primary visual cortex (area 17) of the cat. A comparison with area 17 of the macaque monkey. J Comp Neurol. 184(4):559-618.

Lund JS, Yoshioka T. 1991. Local circuit neurons of macaque monkey striate cortex: III. Neurons of laminae 4B, 4A, and 3B. J. Comp. Neurol. 311(2):234-58.

Lund JS, Wu CQ. 1997. Local circuit neurons of macaque monkey striate cortex: IV. Neurons of laminae 1-3A. J Comp Neurol. 384(1):109-26.

Lund JS Wu CQ, Hadingham PT, Levitt JB. 1995. Cells and circuits contributing to functional properties in area V1 of macaque monkey cerebral cortex: bases for neuroanatomically realistic models. J. Anat. 187: 563-81.

Maffei L, Campbell FW. 1970. Neurophysiological localization of the vertical and horizontal visual coordinates in man. Science. 167(3917):386-7.

Maffei R, Fiorentini A. 1976. The unresponsive regions of visual cortical receptive fields.Vision Res. 16: 1131-39.

Maffei L, Fiorentini A. 1973.The visual cortex as a spatial frequency analyzer. Vision Res. 13(7):1255-67

Maffei L, Fiorentini A. 1977. Spatial frequency rows in the striate visual cortex. Vision Res. 17(2):257-64

Malach R, Amir Y, Harel M, Grinvald A. 1993. Relationship between intrinsic connections and functional architecture revealed by optical imaging and in vivo targeted biocytin injections in primate striate cortex. Proc. Natl. Acad. Sci. 90:10469-10473.

Malach R, Schirman TD, Harel M, Tootell RB, Malonek D. 1997. Organization of intrinsic connections in owl monkey area MT. Cereb. Cortex. 7:386–393.

Manny RE, Klein SA. 1984. The development of vernier acuity in infants. Curr Eye Res. 3(3):453-62.

Mansfield RJ. 1974. Neural basis of orientation perception in primate vision. Science. 186(4169):1133-5.

Martinez LM, Wang Q, Reid RC, Pillai C, Alonso JM, Sommer FT, Hirsch JA. 2005. Receptive field structure varies with layer in the primary visual cortex. Nat Neurosci. 8(3):372-9. Epub 2005 Feb 13.

Mata ML, Ringach DL. 2005. Spatial overlap of ON and OFF subregions and its relation to response modulation ratio in macaque primary visual cortex. J Neurophysiol. 93(2): 919-28. Epub 2004 Sep 15.

McCormick DA, Prince DA. 1987. Post-natal development of electrophysiological properties of rat cerebral cortical pyramidal neurons. J Physiol. 393:743-762.

Maunsell JHR, Newsome WT. 1987. Visual processing in monkey extrastriate cortex. Ann. Rev. of Neurosci. 10:363-401.

Maunsell JH, Van Essen DC. 1983. The connections of the middle temporal visual area (MT) and their relationship to a cortical hierarchy in the macaque monkey. J Neurosci. 3(12):2563-86.

Mayer DL, Dobson V. 1982. Visual acuity development in infants and young children, as assessed by operant preferential looking. Vision Res. 22(9):1141-51.

Mizobe K, Polat U, Pettet MW, Kasamatsu T. 2001. Facilitation and suppression of single-cell activity by spatially discrete pattern stimuli presented beyond the receptive field. Vis Neurosci. 18(3):377-91.

Morrone MC, Burr DC. 1986. Evidence for the existence and development of visual inhibition in humans. Nature. 321(6067):235-7.

Movshon JA. 1974. Velocity preferences of simple and complex cells in the cat's striate cortex. J. Physiol. 242: 121-23.

Movshon JA, Kiorpes L. 1988. Analysis of the development of spatial contrast sensitivity in monkey and human infants. J Opt Soc Am A. 5(12):2166-72.

Movshon JA, Thompson ID, Tolhurst DJ. 1978a. Spatial Summation in Receptive-Fields of Simple Cells in Cats Striate Cortex. Journal of Physiology- London 283: 53–77.

Movshon JA, Thompson ID, Tolhurst DJ. 1978b. Receptive field organization of complex cells in the cat's striate cortex. Journal of Physiology- London 283: 79–99.

Movshon JA, Thompson ID, Tolhurst DJ. 1978C. Spatial and temporal contrast sensitivity of neurones in areas 17 and 18 of the cat's visual cortex. J Physiol. 283:101-20.

Movshon JA, Van Sluyters RC. 1981. Visual neural development. Annu Rev Psychol. 32:477-522.

Mountcastle VB, Berman AL, Davies PW. 1955 .Topographic organization and modality representation in first somatic area of cat's cerebral cortex by method of single unit analysis. Am. J. Physiol. 183:464.

Murphy P, Sillito AM. 1987. Corticofugal feedback influences the generation of length tuning in the visual pathway. Nature 329:727–729

Nelson JI, Frost BJ. 1978. Orientation-selective inhibition from beyond the classic receptive field. Brain Res. 139: 359-65.

Nelson JL, Frost BJ. 1985. Intracortical facilitation among co-oriented, co-axial aligned simple cells in cat striate cortex. Exp. Brain Res. 61: 54-61.

Norcia AM, Tyler CW. 1985. Spatial frequency sweep VEP: Visual acuity during the first year of life. Vision Res. 25:1399-1408.

Norcia AM, Pei F, Bonneh Y, Hou C, Sampath V, Pettet MW. 2005. Development of sensitivity to texture and contour information in the human infant. J Cogn Neurosci.17(4):569-79.

O'Dell C, Boothe RG. 1997. The development of stereoacuity in infant rhesus monkeys. Vision Res. 37(19):2675-2684.

Palmer LA, Davis TL. 1981. Receptive-field structure in cat striate cortex. J Neurophysiol. 46(2) 260-76.

Palmer LA, Rosenquist AC, Tusa RJ. 1978. The retinotopic organization of lateral suprasylvian visual areas in the cat. J Comp Neurol. 177(2): 237-56.

Palomares M, Pettet M, Vildavski V, Hou C, Norcia A. 2010. Connecting the dots: How local structure affects global integration in infants. Journal of Cognitive Neuroscience, 22, 1557–1569.
Pandya DN. 1995. Anatomy of the auditory cortex. 151(8-9):486-494. Rev.Neurol. (Paris).
Parrish EE, Giaschi DE, Boden C, Dougherty R. 2005. The maturation of form and motion perception in school age children. Vision Research. 45:827-837.
Paus T, Collins DL, Evans AC, Leonard G, Pike B, Zijdenbos A. 2001. Maturation of white matter in the human brain: a review of magnetic resonance studies. Brain Res Bull. 54(3):255-66. Review.
Payne BR, Berman N, Murphy EH. 1981. Organization of direction preferences in cat visual cortex. Brain Res. 211(2):445-50.
Perkel DH, Bullier J, Kennedy H. 1986. Topography of the afferent connectivity of area 17 of the macaque monkey: double-labeling study. J Comp Neurol. 253: 374-402.
Pettigrew JD. 1974. The effect of visual experience on the development of stimulus specificity by kitten cortical neurones. J Physiol. 237(1):49-74.
Pinon MC, Gattass R, Sousa AP. 1998. Area V4 in Cebus monkey: extent and visuotopic organization. Cereb Cortex. 8: 685-701.
Polat U, Mizobe K, Pettet MW, Kasamatsu T, Norcia AM. 1998. Nature (London) 391:580–584.
Price DJ, Zumbroich TJ. 1989.Postnatal development of corticocortical efferents from area 17 in the cat's visual cortex. J Neurosci. 9(2):600-13.
Rakic P, Bourgeois JP, Eckenhoff MF, Zecevic N, Goldman-Rakic PS. 1986. Concurrent overproduction of synapses in diverse regions of the primate cerebral cortex. Science. 232(4747):232-5.
Read HL, Winer JA, Schreiner CE. 2001. Modular organization of intrinsic connections associated with spectral tuning in cat auditory cortex. Proc. Natl Acad. Sci. USA. 98:8042–8047.
Ringach DL. 2004. Mapping receptive fields in primary visual cortex. J Physiol. 5558(Pt 3): 717-28. Epub 2004 May 21. Review
Rockland KS, Lund JS. 1982. Wide spread periodic intrinsic connections in the tree shrew visual cortex. Brain Res. 169: 19-40.
Rockland KS, Lund JS, Humphrey AL. 1982. Anatomical binding of intrinsic connections in striate cortex of tree shrews (Tupaia glis). J Comp Neurol. 209(1):41-58.
Rockland KS, Lund JS. 1983. Intrinsic laminar lattice connections in primate visual cortex. J. Comp. Neurol. 216: 303-318.
Rockland KS. 1985. A reticular pattern of intrinsic connections in primate area V2 (area 18). J Comp Neurol. 235(4):467-78.
Rockland KS, Pandya DN. 1979. Laminar origins and terminations of cortical connections of the occipital lobe in rhesus monkey. Brain Research, 179: 3-20.
Ruthazer, ES, Stryker MP.1996. The role of activity in the development of long-range horizontal connections in area 17 of the ferret. J. Neurosci. 15(22): 7253-69.
Salin PA, Bullier J, Kennedy H. 1989.Convergence and divergence in the afferent projections to cat area 17. J. Comp. Neurol. 283(4):486-512
Salin PA, Bullier J. 1995. Corticocortical connections in the visual system: structure and function. Physiol Rev. 75(1):107-54. Review

Salin PA, Girard P, Kennedy H, Bullier JV. 1992. Visuotopic organization of corticocortical connections in the visual system of the cat. J. Comp. Neurol. 320(4): 415-34.
Salin PA, Girard P, Bullier J. 1993. Visuotopic organization of corticocortical connections in the visual system. Prog Brain Res. 95: 169-178.
Sandell JH, Schiller PH. Effect of cooling area 18 on striate cortex cells in the squirrel monkey. J Neurophysiol. 48(1):38-48.
Saul AB, Feidler JC. 2002. Development of response timing and direction selectivity in cat visual thalamus and cortex. J Neurosci. 22(7):2945-55.
Sceniak MP, Hawken MJ, Shapley R. 2001.Visual spatial characterization of macaque V1 neurons. J Neurophysiol. 85(5): 1873-87.
Sceniak MP, Ringach DL, Hawken MJ, Shapley R. 1999. Contrast's effect on spatial summation by macaque V1 neurons. Nat Neurosci. 2(8):733-9.
Schiller PH, Malpeli JG. 1977. The effect of striate cortex cooling on area 18 cells in the monkey. Brain Res. 126(2):366-9.
Schiller PH, Finlay BL, Volman SF. 1976C. Quantitative studies of single-cell properties in monkey striate cortex. III. Spatial frequency. J Neurophysiol. 39(6):1334-51.
Segraves MA, Rosenquist AC. 1982. The distribution of the cells of origin of callosal projections in cat visual cortex. J Neurosci. 2: 1079-1089.
Sengpiel F, Sen A, Blakemore C. 1997. Characteristics of surround inhibition in the cat. Exp. Brian Res. 116: 216-228.
Shaw C, Yinon U, Auerbach E. Receptive fields and response properties of neurons in the rat visual cortex. Vision Res. 1975;15:203–208.
Sherk H. 1978. Area 18 cell responses in cat during reversible inactivation of area 17. J Neurophysiol 41: 204-215.
Sherman MS, Guillery RW. 1998. On the actions that one nerve cell can have on anther: Distinguishing “drivers” from “modulators”. Proc.Natl.Acad.Sci.USA. 95:7121-7126.
Shimojo S, Birch EE, Gwiazda J, Held R. 1984. Development of vernier acuity in infants. Vision Res. 24(7):721-8.
Shimojo S, Held R. 1987. Vernier acuity is less than grating acuity in 2- and 3-month-olds. Vision Res. 27(1):77-86.
Shushruth S, Nurminen L, Bijanzadeh M, Ichida JM, Vani S, Angelucci A. 2013. Different orientation tuning of near- and far- surround suppression in macaque primary visual cortex mirrors their tuning in human perception. J Neurosci. 33(1):106-119.
Sillito AM, Cudeiro J, Murphy PC. 1993. Orientation sensitive elements in the corticofugal influence on centre-surround interactions in the dorsal lateral geniculate nucleus. Exp Brain Res 93:6–16.
Silverman MS, Grosof DH, De Valois RL, Elfar SD. 1989. Spatial-frequency organization in primate striate cortex. Proc Natl Acad Sci U S A. 86(2):711-5.
Sincich LC, Horton JC. 2003a. An albino-like decussation error in the optic chiasm revealed by anomalous ocular dominance columns. Vis. Neurosci. 19:541–545.
Singer W, Creutzfeldt OD. 1970. Reciprocal lateral inhibition of on and off-centre neurones in the lateral geniculate body of the cat. Exp Brain Res

10:311–330.
Slater A, Morison V, Somers M. 1988. Orientation discrimination and cortical function in the human newborn. Perception. 17(5):597-602.
Skoczenski AM, Norcia AM. 1999. Development of VEP Vernier acuity and grating acuity in human infants. Invest Ophthalmol Vis Sci. 40(10):2411-7.
Skottun BC, De Valois RL, Grosof DH, Movshon JA, Albrecht DG, Bonds AB. 1991. Classifying simple and complex cells on the basis of response modulation. Vision Res. 31:1079-1086.
Smith J, Atkinson J, Braddick OJ, Wattam-Bell J. 1988. Development of sensitivity to binocular correlation and disparity in infancy. Perception. 17: 365.
Solomon SG, White AJ, Martin PR. 2002. Extraclassical receptive field properties of parvocellular, magnocellular, and koniocellular cells in the primate lateral geniculate nucleus. J Neurosci. 22: 338-349.
Stavros KA, Kiorpes L. 2008. Behavioral measurement of temporal contrast sensitivity development in macaque monkeys (Macaca nemestrina). Vision Res. 48(11):1335-44.
Symonds LL, Rosenquist AC. 1984.Corticocortical connections among visual Areas in the cat. J Comp Neurol. 229(1):1-38.
Talbot SA, Marshall WH. 1941. Physiological studies on neural mechanisms of visual localization and discrimination. Am. J. Opthamol. 24: 1255-63.
Tani T, Ribot J, O'Hashi K, Tanaka S. 2012. Parallel development of orientation maps and spatial frequency selectivity in cat visual cortex. Eur J Neurosci. 35(1):44-55.
Teller DY. 1997. First glances: the vision of infants. the Friedenwald lecture. Invest Ophthalmol Vis Sci. 38(11):2183-203. Review.
Teller DY, Morse R, Borton R, Regal D. 1974. Visual acuity for vertical and diagonal gratings in human infants. Vision Res. 14(12):1433-9.
Tiao YC, Blakemore C. 1976. Functional organization in the visual cortex of the golden hamster. J. Comp. Neurol. 168:459–481.
Tolhurst DJ, Dean AF. 1987. Spatial summation by simple cells in the striate cortex of the cat. Exp Brain Res. 66(3) 607-20.
Tolhurst DJ, Dean AF, Thompson ID. 1981. Preferred direction of movement as an element in the organization of cat visual cortex. Exp Brain Res. 44(3):340-2.
Tolhurst DJ, Thompson ID. 1982. Organization of neurons preferring similar spatial frequencies in cat striate cortex. Exp Brain Res. 48(2):217-27.
Tootell RB, Silverman MS, De Valois RL. 1981. Spatial frequency columns in primary visual cortex. Science. 214(4522):813-5.
Tootell RB, Silverman MS, Hamilton SL, Switkes E, De Valois RL. 1988. Functional anatomy of macaque striate cortex. V. Spatial frequency. J Neurosci. 8(5):1610-24.
Ts'o DY, Gilbert CD, Wiesel TN. 1986. Relationships between horizontal interactions and functional architecture in cat striate cortex as revealed by cross-correlation analysis. J. Neurosci. 6(4): 1160-70.
Ts'o DY, Roe AW, Gilbert CD. 2001b. A hierarchy of the functional organization for color, form and disparity in primate visual area V2. Vision Res. 41(10-11):1333-49.
Tusa RJ, Rosenquist AC, Palmer LA. 1979. Retinotopic organization of areas 18 and 19 in the cat. J Comp Neurol. 185(4):657-78.

Tusa RJ, Palmer LA. 1980. Retinotopic organization of areas 20 and 21 in the cat. J. Comp. Neurol. 193(1): 147-64.
Tusa RJ, Palmer LA, Rosenquist AC. 1978. The retinotopic organization of area 17 (striate cortex) in the cat. J. Comp. Neurol. 177(2): 213-35.
Van Essen DC, Zeki SM. 1978. The topographical organization of rhesus monkey prestriate cortex. J. Physiol. 277: 193-226.
Van Essen DC, Newsome WT, Maunsell JHR. 1984. The visual field representation in striate cortex of the macaque monkey: asymmetries, anisotropies, and individual variability. Vision Res. 24(5):429-48.
Wang G, Tanifuji M, Tanaka K. 1998. Functional architecture in monkey inferotemporal cortex revealed by in vivo optical imaging. Neurosci. Res. 32:33–46.
Wattam-Bell J. 1991. The development of motion-specific cortical responses in infants. Vision Research. 31:287-297.
Wattam-Bell J. 1992. The development of maximum displacement limits for discrimination of motion direction in infancy. Vision Res. 32(4):621-30.
Wattam-Bell J. 1996a. Visual motion processing in one-month-old infants: preferential looking experiments. Vision Res. 36(11):1671-7.
Wattam-Bell J, Birtles D, Nyström P, von Hofsten C, Rosander K, Anker S, Atkinson J, Braddick O. 2010. Reorganization of global form and motion processing during human visual development. Curr Biol. 20(5):411-5.
Weliky M, Bosking WH, Fitzpatrick D. 1996. A systematic map of direction preference in primary visual cortex. Nature 379(6567): 725-8.
White LH, Bosking WH, Fitzpatrick D. 2001. Consistent mapping of orientation preference across irregular functional domains in ferret visual cortex. Vis. Neurosci. 18: 65-78.
Wilkinson F, Crotogino J. 1995. The late onset of visual texture segmentation in kittens. Behav Brain Res. 68(2):201-17.
Wilson HR. 1988. Development of spatiotemporal mechanisms in infant vision. Vision Res. 28:611-628.
Wilson HR. 1993. Theories of infant visual development. In: Simons K, ed. Early Visual Development, Normal and Abnormal. New York: Oxford University Press; 560-572.
Wong-Riley M. 1979. Changes in the visual system of monocularly sutured or enucleated cats demonstrable with cytochrome oxidase histochemistry. Brain Res 171(1):11–28
Xiao Y, Wang Y, Felleman DJ. 2003. A spatially organized representation of color in macaque cortical area V2. Nature. 421(6922):535-9.
Yoshioka T, Blasdel GG, Levitt JB, Lund JS. 1996. Relation between patterns of intrinsic lateral connectivity, ocular dominance, and cytochrome oxidase-reactive regions in macaque monkey striate cortex. Cereb. Cortex. 6(2):297-310.
Yuodelis C, Hendrickson A. 1986. A qualitative and quantitative analysis of the human fovea during development. Vision Res. 26(6):847-55.
Zheng J, Zhang B, Bi H, Maruko I, Watanabe I, Nakatsuka C, Smith 3rd E L, and Chino Y M. 2007. Development of Temporal Response Properties and Contrast Sensitivity of V1 and V2 Neurons in Macaque Monkeys. J Neurophysiol 97: 3905–3916.
Zeki S, Shipp S. 1988. The functional logic of cortical connections. Nature 335(6188):311-7.

Zeki S, Shipp S. 1989. Modular connections between areas V2 and V4 of macaque monkey visual cortex. Eur J Neurosci. 1:494-506.

Zemon V, Gutowski W, Horton T. 1983. Orientational anisotropy in the human visual system: an evoked potential and psychophysical study. Int J Neurosci. 19(1-4):259-86.

Zipser K, Lamme VAF, Schiller PH. 1996. Contextual modulation in primary visual cortex. J. Neurosci. 16(22): 7376-89.